AD-A047 503 HUGHES AIRCRAFT CO TORRANCE CALIF ELECTRON DYNAMICS DIV F/G 9/5
20 WATT SOLID STATE X-BAND POWER AMPLIFIER.(U)
JUN 76 W LOCKYEAR DAAB07-75-C-0023
UNCLASSIFIED EDD-W-41146-F ECOM-75-0023-F NL

1 OF 2
AD A047503

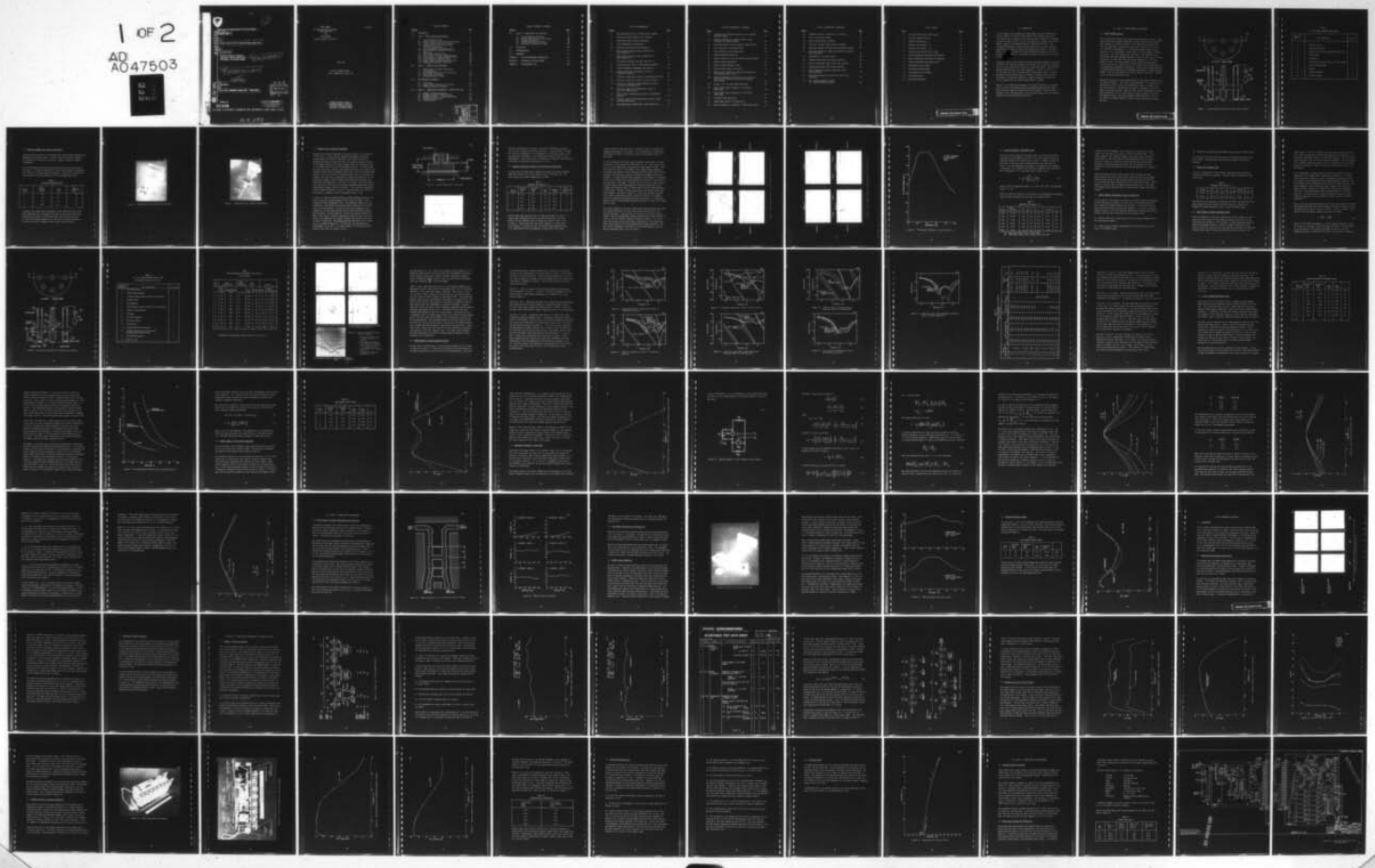

Research and Development Technical Report

(18) (19) ECOM-75-0023-F

(6) 20 WATT SOLID STATE X-BAND POWER AMPLIFIER.

(10) W. LOCKYEAR

HUGHES AIRCRAFT COMPANY
3100 WEST LOMITA BOULEVARD
TORRANCE, CALIFORNIA 90509

(14) EDD-W-H1146-F

(15) DAABQ7-75-C-QQ23

(12) 185p.

(11) June 1976

(9) Final Report, for Period January 1975 – March 1976

Prepared for

ECOM

US ARMY ELECTRONICS COMMAND FORT MONMOUTH, NEW JERSEY 07703

FINAL REPORT

W-41146

20 WATT SOLID STATE X-BAND POWER AMPLIFIER

FOR

USA SATCOMA

Contract DAAB07-75-C-0023 new

JUNE 1976

Project Manager W14R3P

Attn: AMCPM-SC-4D, Bldg. 209

HUGHES AIRCRAFT COMPANY
ELECTRON DYNAMICS DIVISION
3100 WEST LOMITA BOULEVARD
TORRANCE, CALIFORNIA 90509

TABLE OF CONTENTS

TABLE OF CONTENTS CONTINUED

LIST OF ILLUSTRATIONS

LIST OF ILLUSTRATIONS CONTINUED

LIST OF ILLUSTRATIONS CONTINUED

LIST OF TABLES

1.0 INTRODUCTION

In this report we will summarize in some detail the work accomplished on Contract DAAB07-75-C-0023 for USA SATCOMA. The original objective of this program was to develop a solid state amplifier capable of delivering 20 watts of power in the 7.9 to 8.4 GHz band with 14 dB gain and a 20 dB dynamic range per USA SATCOMA Technical Guidelines, SCA-2161. This included development of four and eight diode circular cavity combiners, development of a hybrid-coupled driver amplifier, design of a dc power supply, packaging and electrical and environmental testing of the final version of the amplifier. Two amplifiers were to be delivered at the end of the program.

During the course of the program, the objectives were changed to build one amplifier with a nominal saturated output power of 10 watts but optimized for use at much lower power levels as a linear TWT driver. The specified maximum operating power level was changed to 1.5 watts over the 7.9 to 8.4 GHz band with 38 to 40 dB gain and a 20 dB dynamic range. An intermodulation product specification of 30 dBc at 200 mW output was added. The number of stages was increased to eight including two four-diode cavity combiners and two hybrid-coupled pairs of stages.

Results of the amplifier development work ~~will~~ be discussed including RF and dc circuitry and thermal design. Problems encountered with IMPATT diode and power combiner bandwidth will be discussed. Electrical performance of the final amplifier will be presented along with its schematic diagram and outline and mounting details.

2.0 TASK I - POWER COMBINER DEVELOPMENT

2.1 POWER COMBINER SCALING

The output stage design for this program was initially based on an eight diode X-band power combiner developed by Hughes Research Laboratories.[1,2] When operated as a stable amplifier, this combiner using single drift silicon diodes gave 9 watts output power near 10 GHz with 4.8 dB gain and a 400 MHz 1 dB bandwidth. It incorporated eight coaxial modules spaced on a 0.6 inch diameter circle within a 0.9 inch diameter cylindrical cavity. The cavity height was 0.125 inch. This combiner, which yielded the best gain bandwidth measured to date for this type of circuit, was scaled to 1.108 inches with the coaxial modules on a 0.739 inch diameter circle. The cavity height was not scaled but maintained at 0.125 inch in order to lower the Q of the coax-to-cavity transition with a corresponding improvement in bandwidth. Several other changes designed to improve tuning flexibility and bandwidth were made. A cross-sectional sketch of the 8.15 GHz combiner is shown in Figure 1 and Table 1 contains a list of the most important parts.

Mechanical details of the RF coupling probe for the power combiner circuit are shown in Figure 1. The "split collet/retainer", 7, is split near its tapered end so that it grips the "input/output coax", 6, tightly near the cavity surface. Good electrical contact is necessary as this is a region of high RF currents. When the split collet is loosened, the probe may be moved into or out of the cavity in order to adjust the gain of the amplifier stage. The tuning plunger may be moved into or out of the cavity in a similar manner in order to adjust the center frequency and gain.

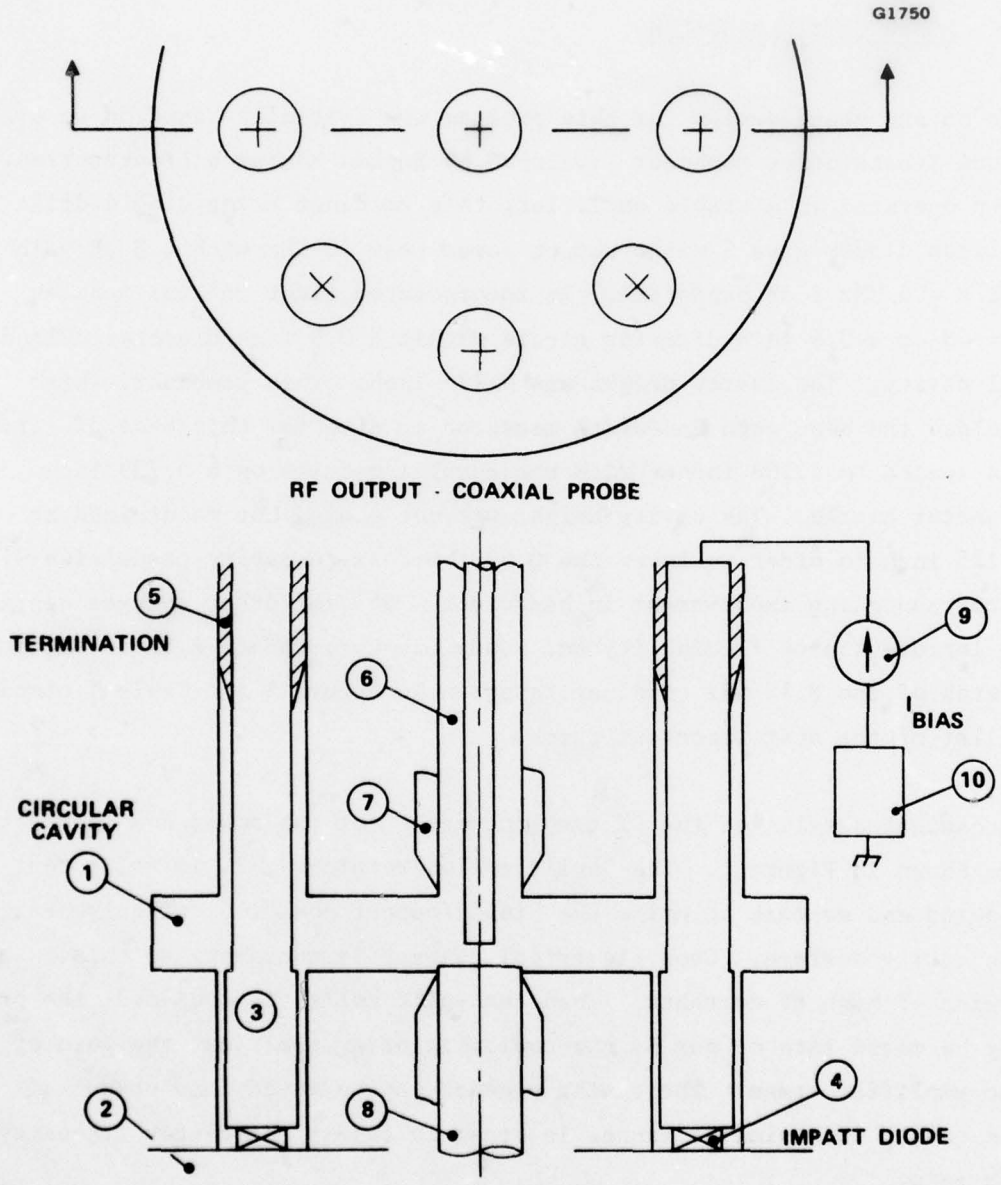

Figure 1 Cross-sectional sketch of 8-diode power combiner.

TABLE 1

8.15 GHz POWER COMBINER PARTS INDEX

Find No., Figure 1	Part Description	No. Req.
1.	Circular Cavity	1
2.	Diode Mounting Base	1
3.	Coaxial Branch Center Conductor/Transformer	8
4.	IMPATT Diode	8
5.	Termination	8
6.	Input/Output Coaxial Probe (.141 Coax Cable)	1
7.	Split Collet/Retainer	2
8.	Plunger	1
9.	Current Regulator	8
10.	DC Power Supply	1

2.2 COMBINER ASSEMBLY AND INITIAL TEST RESULTS

During the second quarter of the program, the scaled 8-diode combiner was assembled and evaluation begun. Figure 2 shows the combiner assembled and connected to a four-port circulator. Figure 3 shows the combiner disassembled.

For the preliminary testing some low power double drift silicon diodes were used. In a single diode coaxial circuit, these diodes will generate only 100 mW in saturated amplifier operation. The results obtained with these diodes in the power combiner at 8 GHz are summarized below:

TABLE 2

LOW POWER COMBINER RESULTS

No. of Diodes	Power Output (Watts)	Gain (dB)	1 dB Bandwidth (GHz)
1	.20	4.0	.06
2	.39	3.9	.12
4	.84	4.2	.18
8	1.33	3.3	.20

In general the results were encouraging in that stable gain and proper power combination were obtainable from each of the various multi-diode configurations tried. In the 8-diode case, less than the expected 1.6 watts was obtained because two of the last four diodes installed in the circuit were of somewhat lower quality than the others.

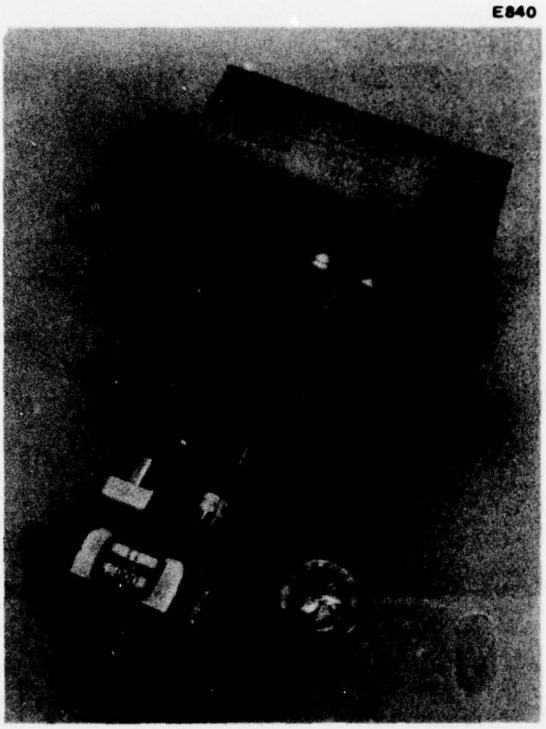

Figure 2 Eight-diode power combiner and circulator.

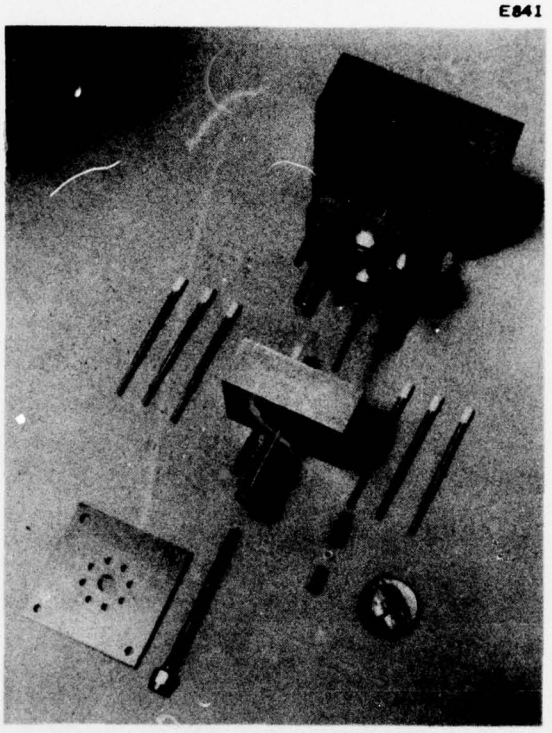

Figure 3 Eight-diode power combiner disassembled.

2.3 PROBE-TO-CAVITY TRANSITION MATCHING

Because of the narrow bandwidths of the above results, it was decided at this point to pursue certain bandwidth improvement techniques. Although gain and frequency adjustments may be made by probe and plunger adjustments as described above, the gain and frequency should be determined primarily by circuit elements which are physically close to the IMPATT diodes for best gain-bandwidth product. For this reason an effort was made to achieve a good match between the input/output coax TEM wave and the cavity's dominant radial mode. That is, any reactances present in the coax-to-cavity transition region were to be reduced to a minimum. This was done by adjusting the length and penetration of the probe and by adding a metal matching bead (whose size and shape was determined experimentally) to the end of the probe. This would require that nearly all of the gain and frequency determining matching be done on the coaxial modules close to the diodes. The circuit was designed to provide enough flexibility to allow for this matching and to allow for differences in impedance between individual diodes, if any.

A series of tests was conducted wherein tapered absorbent material was placed around the outside diameter of the cavity in order to form a terminated radial transmission line. The impedance looking into this transmission line through the probe-to-cavity transition was measured using a network analyzer. In this way the probe configuration and dimensions could be varied and the effect on the transition impedance match measured. It was found that a nearly non-reactive match with a VSWR of less than 1.3 could be achieved over the 7.9 to 8.4 GHz band using a disc soldered to the center conductor of the 0.141 coax probe as shown in Figure 4a. The maximum measured VSWR from 7.0 to 9.0 GHz was 1.6 as shown by Figure 4b. It was found that the dimensional relationship of the disc to the outer conductor of the probe and the bottom of the cavity is rather critical.

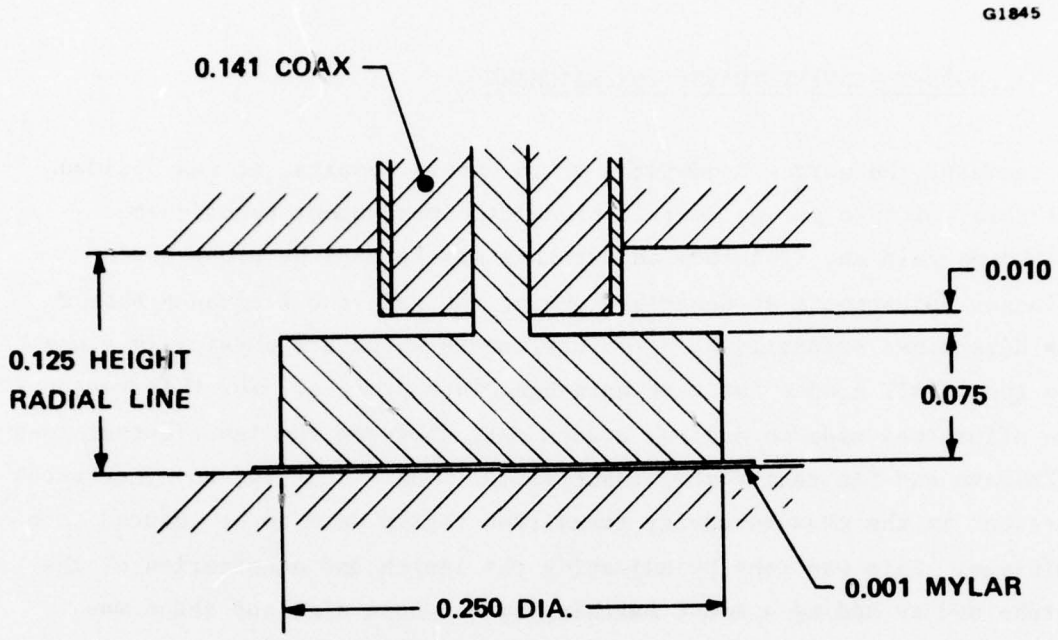

Figure 4a Coax-to-Radial-Line Transitions.

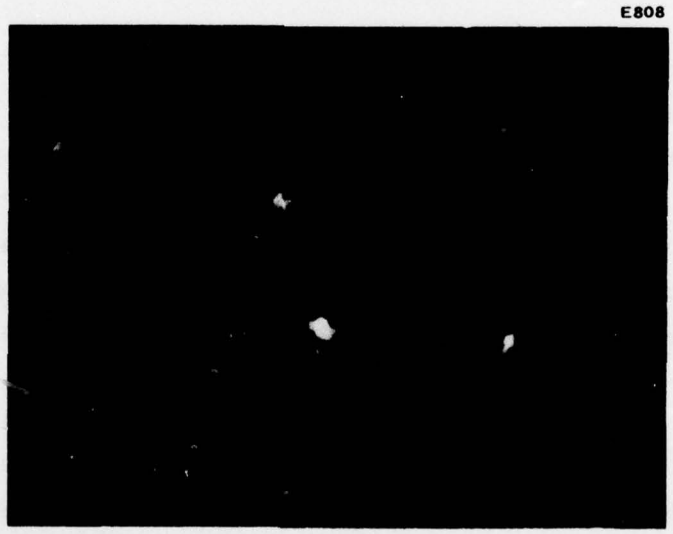

Figure 4b Matched Coax-to-Radial-Line Transition.

The probe configuration of Figure 4 was tested in amplifier operation and only very low gain results were obtained. It was necessary to change the probe disc dimensions to 0.100 diameter by 0.50 long in order to get good amplifier performance. This necessitated further studies of the relationship of probe-cavity-coax configuration to amplifier gain-bandwidth performance as discussed in Sections 2.5 to 2.10.

2.4 COMBINER EVALUATION; INITIAL TESTS WITH HIGH POWER DIODES

At this point, the eight-diode combiner was tested with vendor-supplied high power double drift silicon diodes in sets of two and four. The tests results are briefly summarized as follows:

TABLE 3

COMBINER TEST RESULTS - I

	No. of Diodes	RF Input Power (W)	RF Output Power (W)	Gain (dB)	Frequency (GHz)	1 dB Bandwidth (GHz)
1.	2	1.59	3.55	3.5	8.13	.16
2.	2	1.59	3.44	3.4	8.12	--
3.	4	3.16	6.99	3.5	8.09	--
4.	4	3.22	4.94	1.9	8.19	--
5.	4	3.57	7.49	3.2	8.11	.24

Initial tests were done with pairs of high power diodes in order to assure proper combinatorial action and stable operation. The test results for two different pairs of diodes are shown on lines 1 and 2 of Table 3. These pairs were then tested together to product test result number 3. During this test, two diodes failed apparently due to a tuning mismatch while attempting to obtain more output power.

Further tests were done with pairs of diodes in order to optimize the impedances presented to the diodes. Two of these pairs of diodes were then tested as a set of four with the results indicated by line 4 of the table.

It can be seen that the power output obtained in test result 4 is well below that of the previous four diode test (no. 3). The cause was that not all of the diodes were contributing an equal amount of power. This was verified by plots of the diodes' bias voltages versus frequency. The diodes are biased by current regulators which hold the bias current constant as the RF input is swept in frequency throughout the band of interest. A slight variation with frequency in the diodes' dc characteristics occurs because they are generating more RF power in the center of the band than at the edges. This and the fact that the current is held constant causes a small (approximately 3 percent) variation in bias voltage with frequency which is proportional to the RF power generation of the diodes. The bias voltage variations of each diode used in test result number 4 are shown in Figure 5. These plots indicate that the four diodes are generating unequal amounts of RF power; for example, diode #1 is generating substantially more than diode #4. In addition, diodes #1 and #3 are generating substantial amounts of power out of band above 8.4 GHz.

The coaxial modules of the three diodes which were generating less power were adjusted slightly in order to more nearly equalize their bias voltage variations. This was done in two steps to yield test result number 5 and the corresponding voltage variation plots shown in Figure 6. A plot of the RF frequency response is shown in Figure 7. It can be seen from the plots that the RF power contributions of the diodes are nearly equal and that out-of-band generation has been minimized. This has caused a substantial improvement in the RF performance as can be seen by comparing lines 4 and 5 of Table 3.

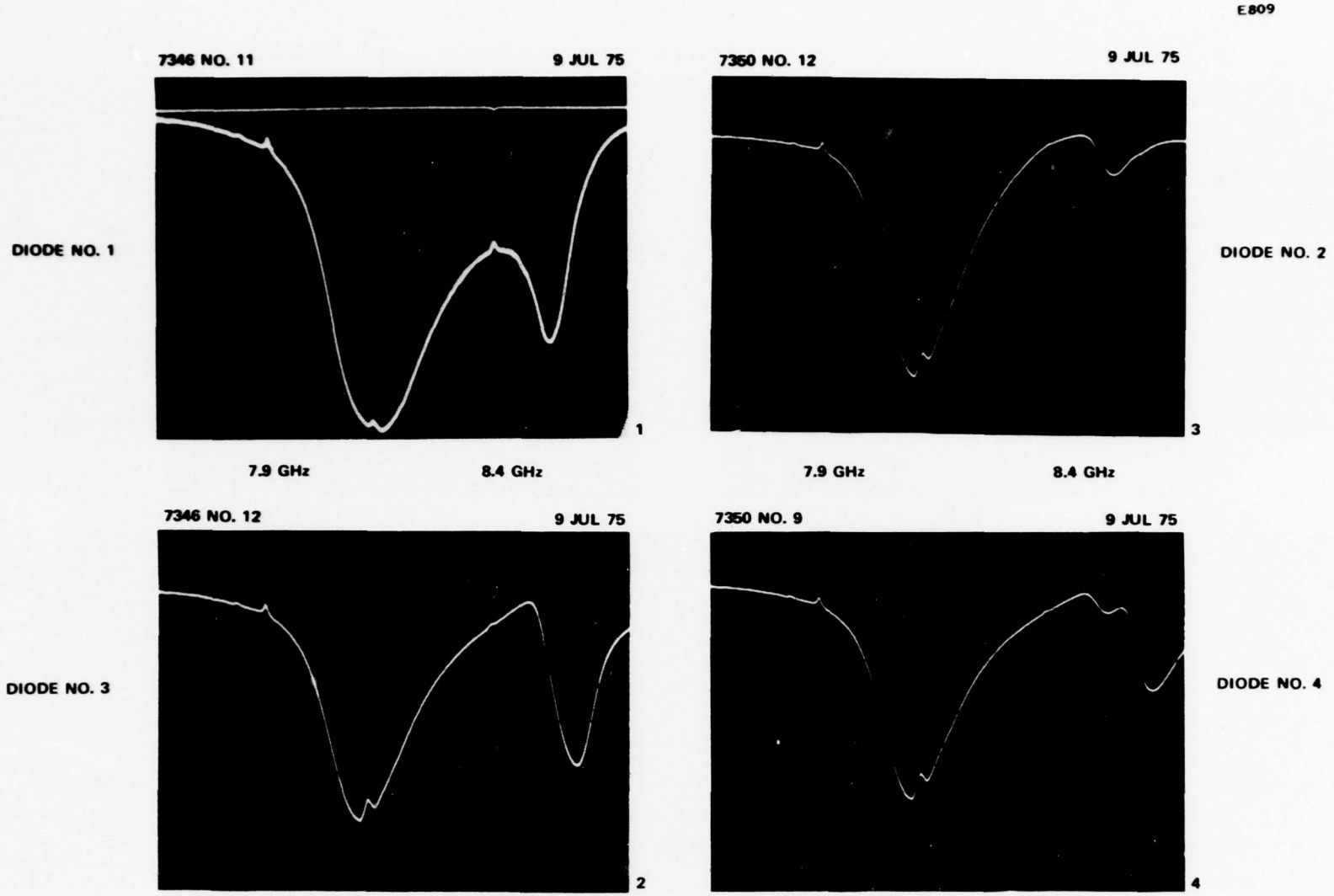

Figure 5 Bias voltage variation versus frequency for test result No. 4.

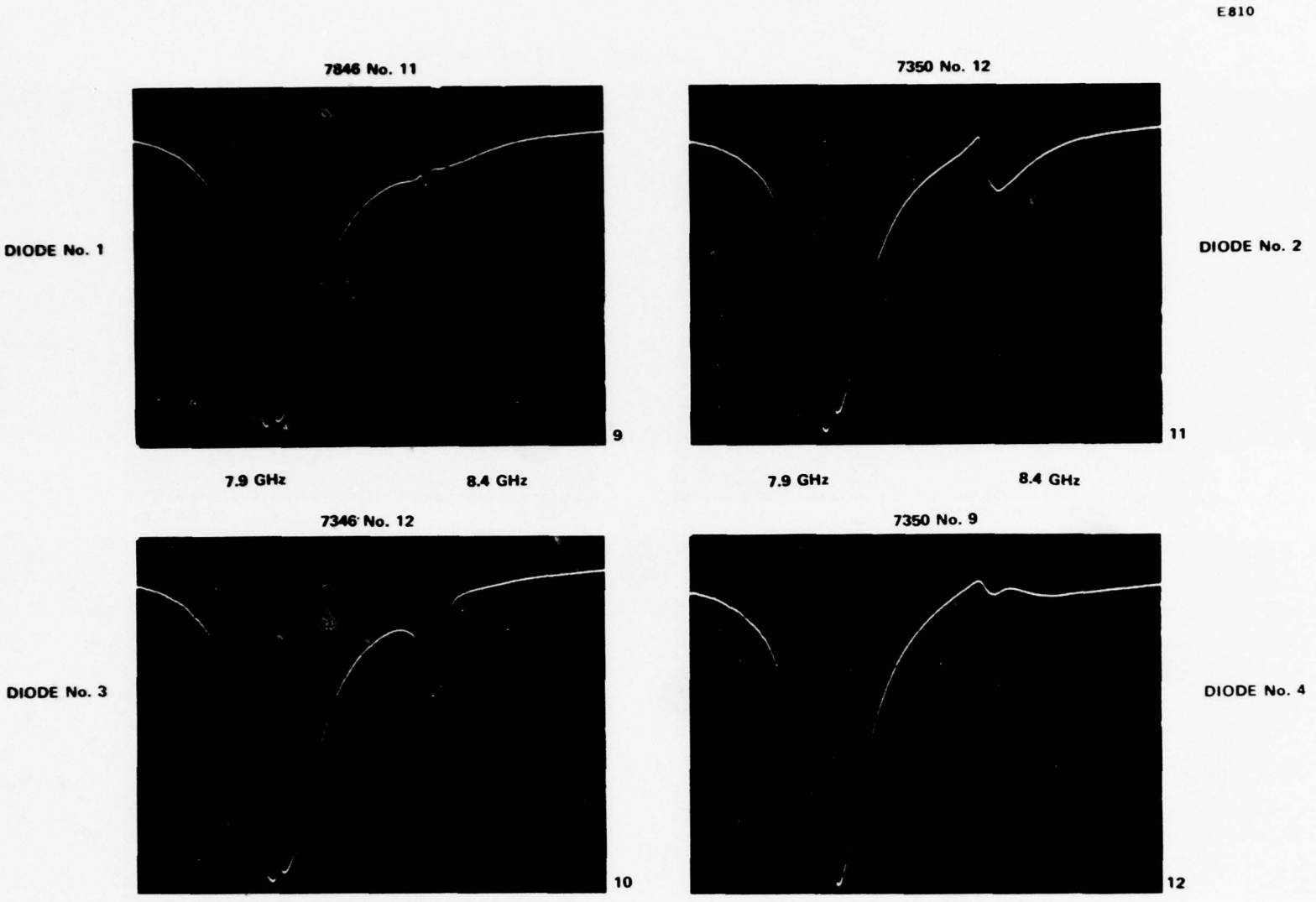

Figure 6 Bias voltage variation versus frequency for test result No. 5.

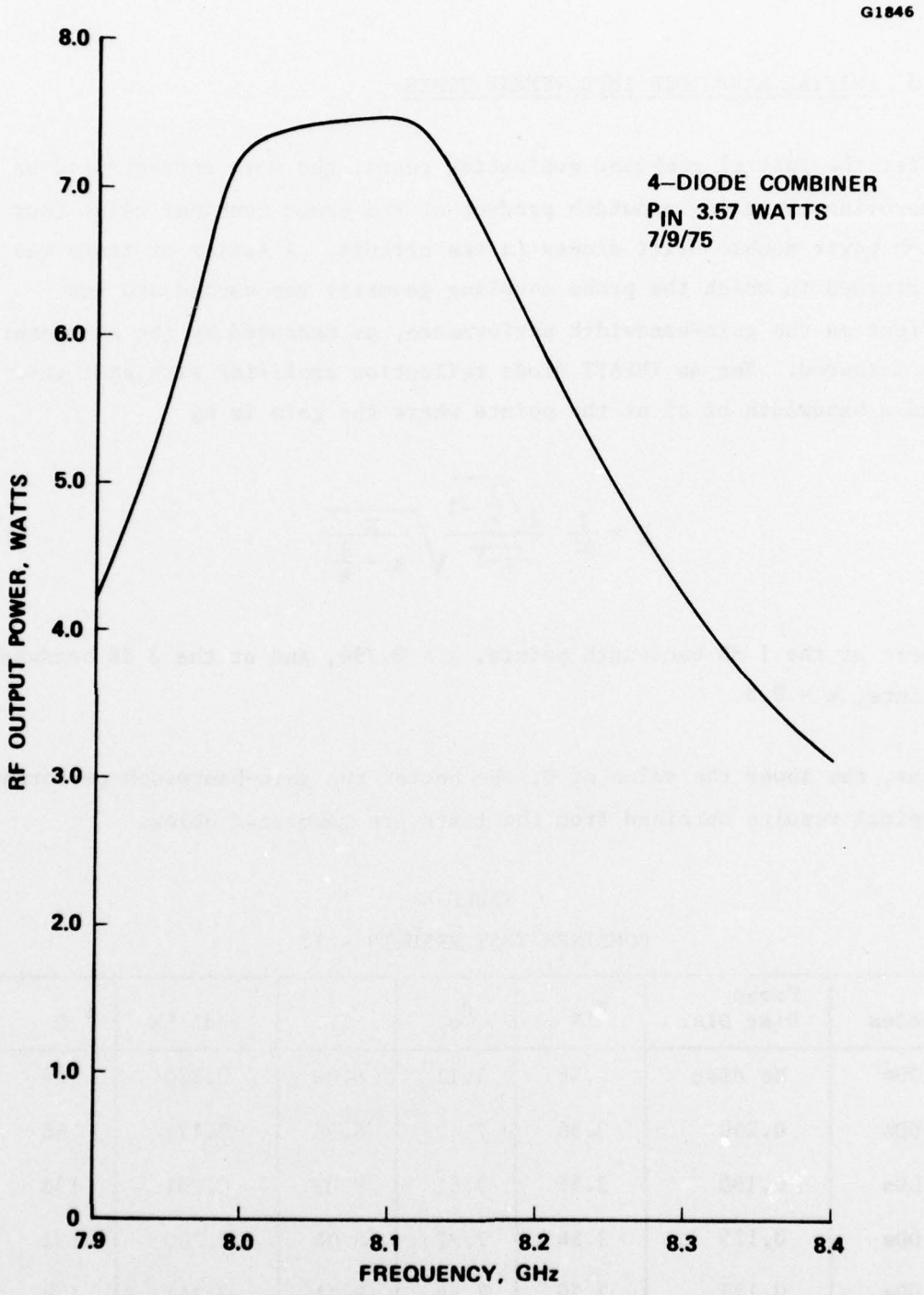

Figure 7 RF frequency response for test result No. 5.

2.5 INITIAL BANDWIDTH IMPROVEMENT TESTS

After the initial combiner evaluation tests, the work concentrated on improving the gain-bandwidth product of the power combiner using four high power double drift diodes in the circuit. A series of tests was performed in which the probe coupling geometry was varied and its effect on the gain-bandwidth performance, as measured by the parameter Q, measured. For an IMPATT diode reflection amplifier with peak gain g and a bandwidth of Δf at the points where the gain is kg

$$Q = \frac{f}{\Delta f} \frac{2\sqrt{\frac{1}{k} - 1}}{\sqrt{g-1}} \sqrt{\frac{g}{g - \frac{1}{k}}} \quad , \qquad (1)$$

where at the 1 dB bandwidth points, k = 0.794, and at the 3 dB bandwidth points, k = 0.5.

Thus, the lower the value of Q, the better the gain-bandwidth performance. Typical results obtained from the tests are tabulated below.

TABLE 4

COMBINER TEST RESULTS - II

Diodes	Probe Disc Dia.	P_{IN}	P_o	f	1 dB BW	Q
4 DDs	No disc	3.56	5.11	8.00	0.220	528
4 DDs	0.250	3.56	7.49	8.06	0.171	168
4 DDs	0.180	3.56	7.61	8.03	0.201	138
4 DDs	0.125	3.56	7.77	8.04	0.200	132
4 DDs	0.125	3.56	7.49	8.11	0.241	120
2 SDs	0.125	1.58	2.86	8.05	0.268	161

DD: high power double drift silicon diode
SD: high power single drift, diamond heat sink diode

A large (0.250 inch diameter) disc on the end of the probe was tried because this disc gave good results in previous passive tests. It was found, however, that a smaller diameter disc gives a lower amplifier Q. Additionally, it was found that the probe penetration into the cavity should be as deep as is possible without reducing the gain available. Shallower probe penetrations may be used and the desired gain level obtained by tuning the plunger but the resulting amplifier Q is slightly higher.

Some testing was done with silicon single drift, diamond heat sink diodes because they have a lower device Q than the double drift diodes. These were more prone to have spurious outputs and were more difficult to tune under high power conditions than the double drift diodes. Their amplifier Q was no lower in combiner operation than that of the double drift diodes which indicates that the Q was circuit (rather than device) limited.

2.6 POWER COMBINER DEVELOPMENT STATUS AND DIRECTION

At this point in the program, the status of the power combiner development and the experimental results of the two sets of four diodes which have been tested in the power combiner were reviewed. It was noted that the most significant technical problem was bandwidth. A plan was formulated whereby actions to solve the bandwidth problem and to demonstrate 8-diode combiner operation would take place in the following order.

(1) Perform tests with 8 diodes until parts for passive bandwidth tests were delivered to Hughes.

(2) Perform passive bandwidth improvement tests using 50 ohm loads in place of the IMPATT diodes.

(3) Perform active bandwidth improvement tests using four IMPATT diodes.

(4) Procure four sets of machined parts for the deliverable power combiner stages. Simultaneously, perform further eight diode tests as required.

2.7 EIGHT DIODE COMBINER TESTS

In order to demonstrate 8 diode combiner operating, some preliminary tests were performed as scheduled. The best results obtained are tabulated below.

TABLE 5

COMBINER TEST RESULTS - III

Diodes	P_{IN}	P_o	f	1 dB BW	Q
8 DDs	3.16 W	8.99 W	8.20	0.153	107
8 DDs	4.99 W	10.65 W	8.18	0.187	151

Some difficulty was obtained in equalizing the power contributions of all eight diodes indicating further work was necessary to optimize the impedance and power matching circuitry of the individual diodes.

2.8 FIRST SERIES OF PASSIVE BANDWIDTH TESTS

Since the bandwidth of the power combiner was circuit limited, the work during the third quarter of the program (outlined in section 2.6) concentrated on the solution to this problem. A rather extensive series of passive experiments was done in order to optimize simultaneously the probe-to-cavity and cavity-to-coax coupling values (section 2.6, item (2)). In these tests, small 50 ohm rod resistors were used in place of the

IMPATT diodes. Two sets of eight coax module center conductors (20 ohm and 35 ohm) were made which incorporated quarter-wave transformers of an appropriate impedance to match to the 50 ohm resistors. Rings of various sizes were made to vary the cavity height and diameter. The configuration of the combiner during the passive tests is compared with that of active operation in Figure 8. Table 6 is a list of the key parts of both configurations.

In the experiments, a network analyzer was used to measure the input impedance of the 50-ohm-resistor-loaded power combiner at the coaxial probe input/output connector. First, the combiner configuration used in previous four and eight-diode active measurements was analyzed. Then the parameters probe configuration and position, plunger position, coax module impedance, cavity height and cavity diameter were varied and tested in order to obtain a low VSWR, low Q, match at the combiner's input port. This would imply a good, broadband match to the 50 ohm resistors. At that point it is merely necessary to match the IMPATT diodes to a resistive, coax load which is readily done by well known techniques.[3,4]

Some of the more significant results of the tests are presented in Table 7. Photographs taken from the network analyzer are shown in Figure 9 for the configurations of lines 1, 2 and 7 of Table 7. The Q's of Table 7 were obtained from the network analyzer data using the formula

$$Q = \frac{S^2-1}{S} \quad \frac{\omega_o}{2} \frac{d\psi}{\omega} \tag{2}$$

where S is the VSWR at resonance, ω_o is the resonant frequency, and ψ is one-half of the angle of the reflection coefficient. It was assumed in the derivation of this formula that $\frac{dS}{d\omega} \cong 0$, that is, that the impedance plotted on a Smith Chart is nearly circular with a radius, S,

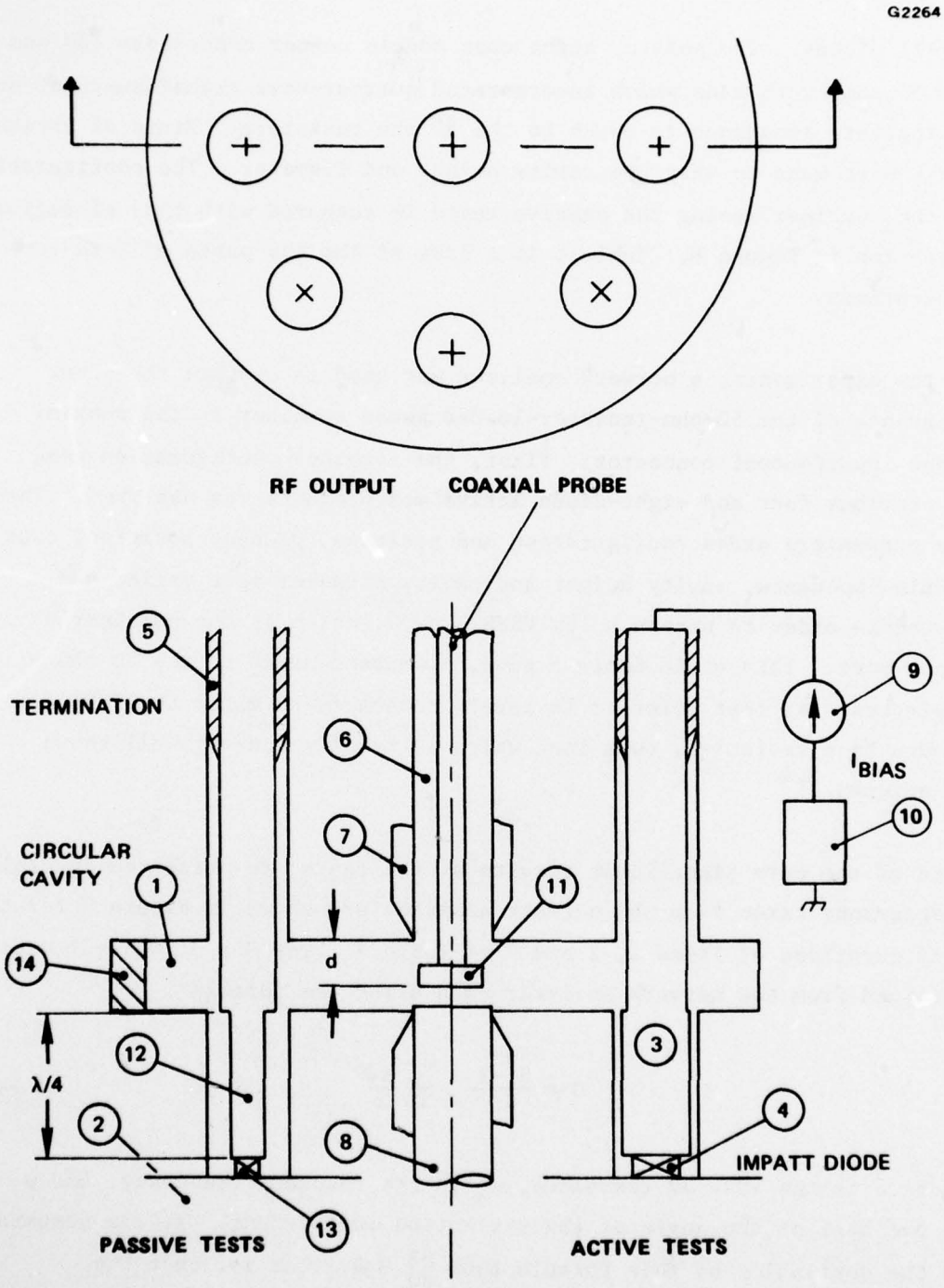

Figure 8 Cross-sectional sketch of 8-diode power combiner.

TABLE 6

8.15 GHz POWER COMBINER PARTS INDEX

(Including Passive Test Parts)

Find No., Figure 8	Part Description	No. Req.
1.	Circular Cavity	1
2.	Diode Mounting Base	1
3.	Coaxial Branch Center Conductor/Transformer	8
4.	IMPATT Diode	8
5.	Termination	8
6.	Input/Output Coaxial Probe (0.141 Coax Cable)	1
7.	Split collet/Retainer	2
8.	Plunger	1
9.	Current Regulator	8
10.	DC Power Supply	1
11.	Probe Disc	1
d.	Probe Penetration Distance	-
12.	Center Conductor With Transformer Modified For Passive Tests	8
13.	50 Ohm Rod Resistor	8
14.	Cavity Ring	1

TABLE 7

PASSIVE BANDWIDTH IMPROVEMENT TEST RESULTS

(FIRST SERIES)

Test No.	Probe Configuration		Coax Module Impedance	Size Cavity		Results		
	Disc. Dia.	Penetration		Dia.	Height	Freq.	Best VSWR	Q
1*	.125"	.075"	20 ohm	1.108	.125	8.1	2.83	28.8
2	.125	.075	20	1.108	.125	8.1	1.74	14.8
3	.250	.075	20	1.108	.125	8.1	2.18	20.7
4	.125	.075	20	1.108	.200	8.1	1.85	19.1
5	.125	.055	20	1.108	.125	8.1	1.80	17.1
6	.125	.095	20	1.108	.125	8.1	1.87	17.7
7	.125	.075	35	1.108	.125	8.35	1.12	2.1
8	.125	.095	35	1.108	.125	8.4	1.11	2.2
9	.125	.075	35	.952	.125	8.85	1.11	9.6
10	.125	.075	35	.893	.125	9.59	1.12	7.1
11	.125	.075	20	.893	.125	9.98	1.19	11.3

* Amplifier configuration used in previous active tests.

a. Polar Display, Normal Smith Chart

b. Polar Display, Normal Smith Chart

c. Polar Display, Normal Smith Chart

d. Polar Display, Expanded Smith Chart (14 dB Return Loss Min.)

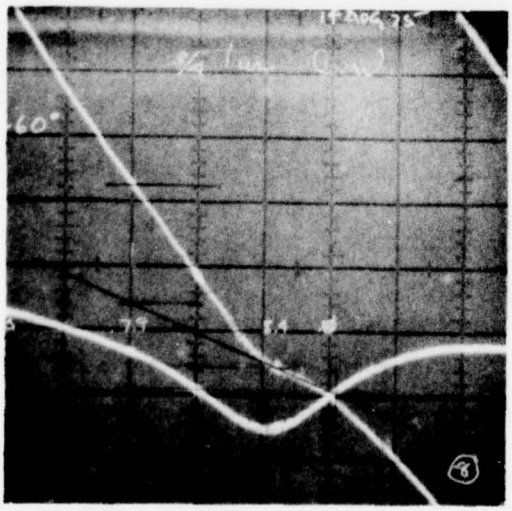

e. Rectangular Display - Amplitude: 10 dB/Div.
Phase: 45 Deg./Div.

Figure 9 Passive Bandwidth Improvement Test Results

a. Original Amplifier Configuration (Table I, Line 1).
b. Best Match Obtainable From Original Configuration (Table I, Line 2).
c., d. Circuit with improved VSWR and Q (Table I, Line 7).
e. Rectangular Display of Circuit of c., d.

and the center at 1 + j0. From a polar display, such as Figure 9, S is displayed directly and it can be verified that the impedance plot has a nearly constant radius over a limited frequency range near resonance. From a rectangular display, such as Figure 9e, that value of the phase slope near resonance, $\frac{2d\psi}{d\omega}$, can be determined.

Table 7, line 1 shows that the circuit Q of the original amplifier configuration is 28.8. This circuit, using diodes with a Q of 21, gives an amplifier Q of 60 under small signal conditions. The circuit of line 2 is like that of line 1 except that the plunger has been inserted deeper into the cavity in order to obtain a better match and Q. This condition, however, does not give good amplifier performance - the gain is very low. The circuits of lines 7 and 8 gave very low values of measured circuit Q which should lead to an improvement in amplifier bandwidth. However, when this circuit was tried in active amplifier operation and the expected bandwidth improvement did not occur. The amplifier Q's of the best obtained were similar to those of previous tests. The reason for this is apparently due to a double tuning effect in the passive circuit wherein part of the input power was absorbed by the rod resistor loads and part by the terminations. This was demonstrated in the active tests by the fact that the circuit could be tuned so that plots of the IMPATT diodes' bias voltages indicated broadband, double-tuned power generation. The RF power output covered only about one-half of this bandwidth and generally corresponded to the lower frequency peak of the double tuned response. The power generated in the higher frequency peak was apparently being absorbed by the terminations.

2.9 SECOND SERIES OF PASSIVE BANDWIDTH TESTS

At this point it was necessary to perform further passive tests in order to lower the circuit Q. In these tests particular attention was paid to the double tuning effects and absorption by the terminations. The tests

were conducted using a network analyzer and a resistively loaded power combiner in the same manner as the first series of tests. An X-Y plotter was used to record the results. Some of the most significant test plots are shown in Figures 10 through 16 and the quantitative data reduced from these plots is presented in Table 8. The test data and plots are discussed briefly below.

Test No. 5: This is a repeat of the original amplifier configuration and corresponds to Test No. 1 of Table 7. The cavity diameter is 1.108 inches and the coaxial module impedances are 20 ohms for all of the tests in Table 8.

Test Nos. 1 and 3: These are like Test No. 5 except that the plunger has been inserted into the cavity slightly to obtain lower VSWR's and Q's. In active tests these yielded low amplifier gains. Test No. 3 gave the flattest return loss versus frequency response in the 7.9 to 8.5 GHz band.

Test Nos. 2, 3 and 4: During the above tests (1, 3 and 5) the coaxial termination positions remained fixed at one-quarter wavelength from the cavity (0.360 inches). For Test Nos. 2, 3 and 4 the termination positions were varied from 0.180 inches to 0.450 inches from the top of the cavity and the results are shown in Figure 10. It can be seen that increasing the termination's distance from the cavity tends to lower the VSWR and Q of the circuit with the major effect being at the higher frequency peak. This peak represents power absorption by the terminations. It was the goal of these tests to minimize this absorption by finding a circuit whose response does not vary nearly as much with termination position. Additionally, since the magnitude of the termination impedance is low (0.4 times the coaxial line impedance) replacing them with shorts should not greatly affect the passive circuit if the terminations are not absorbing power.

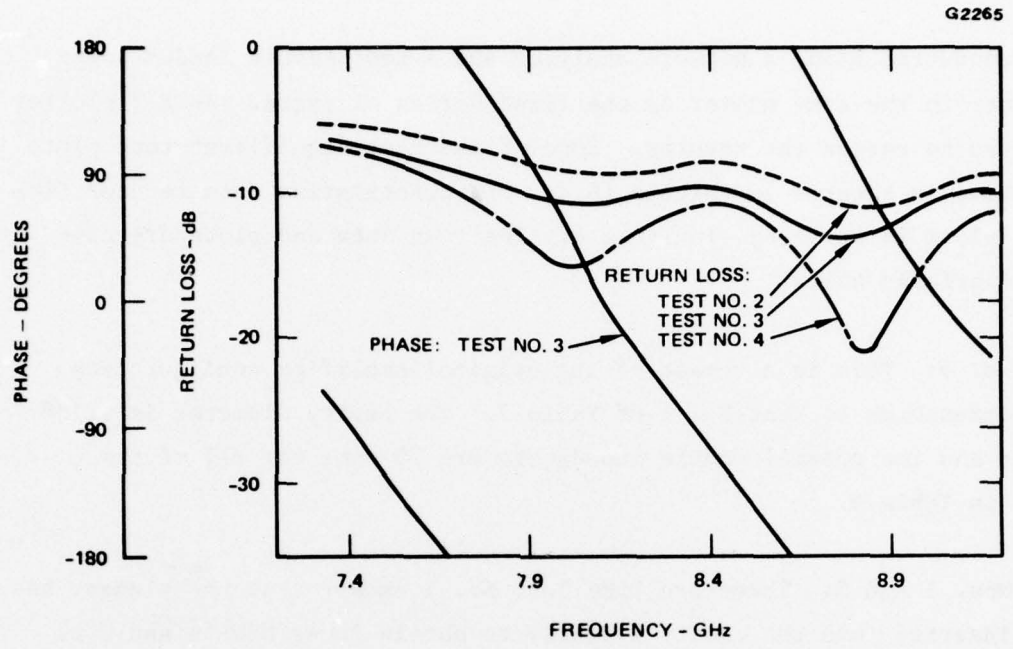

Figure 10 *Original amplifier configuration, effect of termination position.*

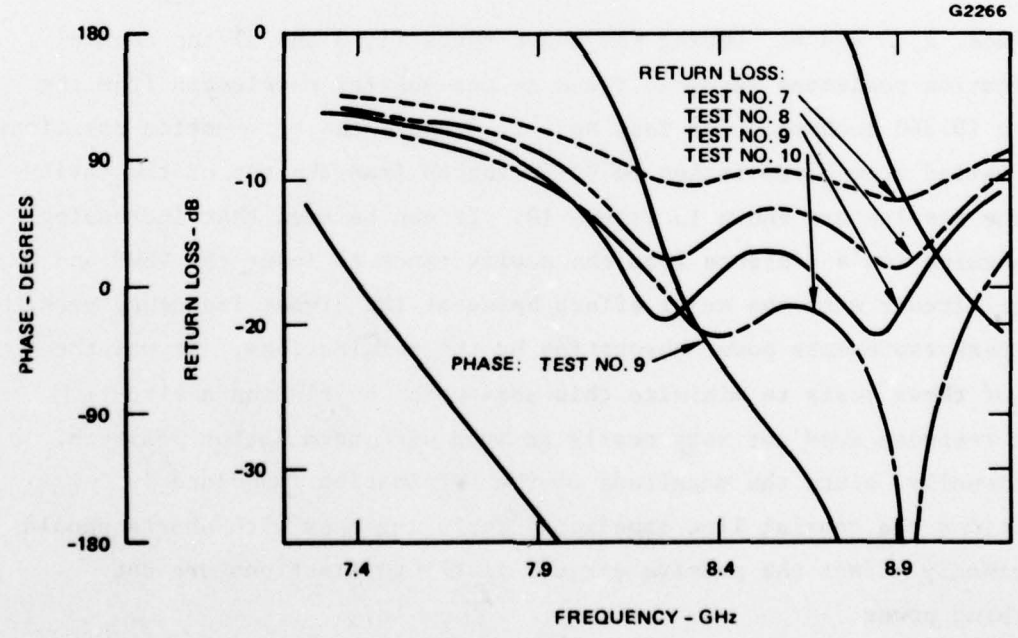

Figure 11 0.072 dia. probe disc, effect of termination position.

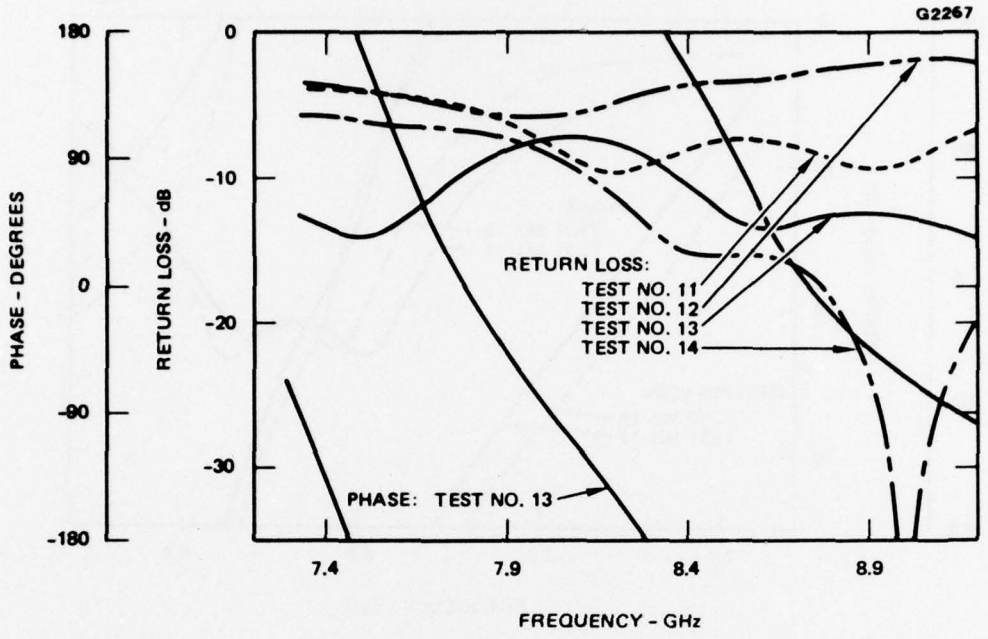

Figure 12 0.072 dia. probe disc, effect of short position.

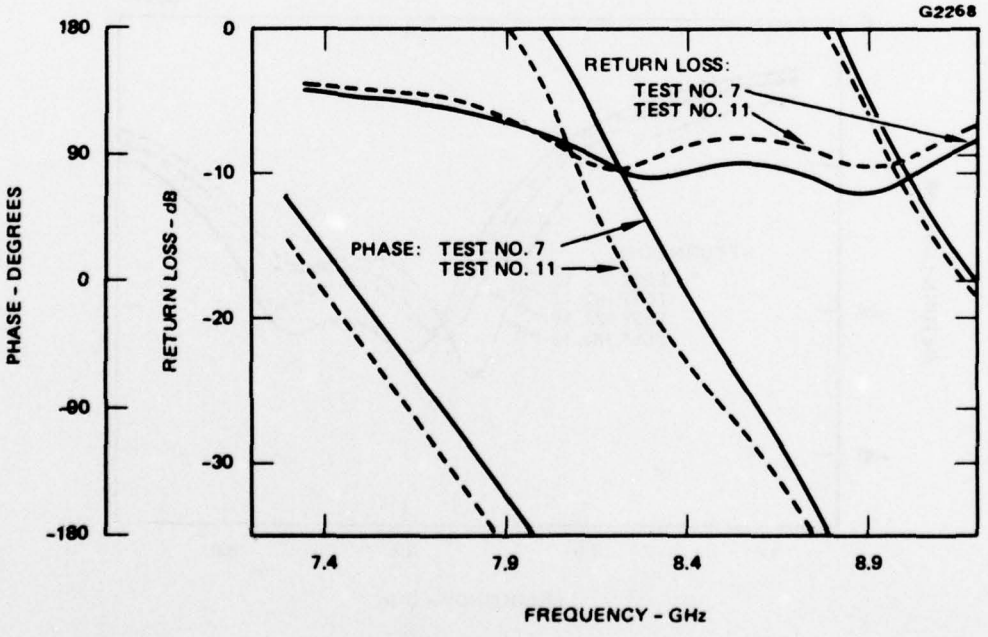

Figure 13 0.072 dia. probe disc, 0.085 penetration, effect of short at 0.180 position.

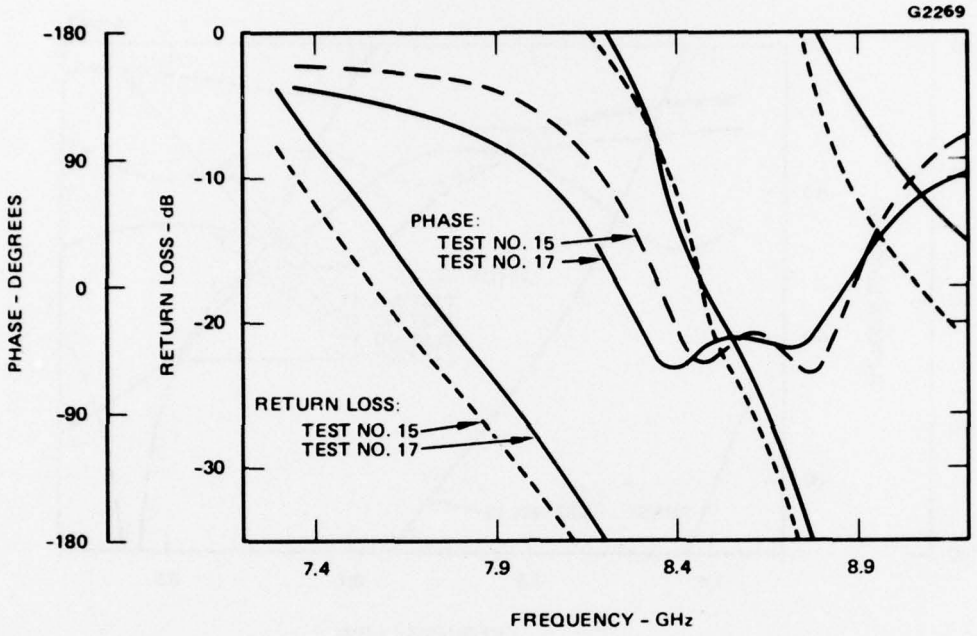

Figure 14 0.072 dia. disc, 0.115 penetration, effect of short at 0.180 position.

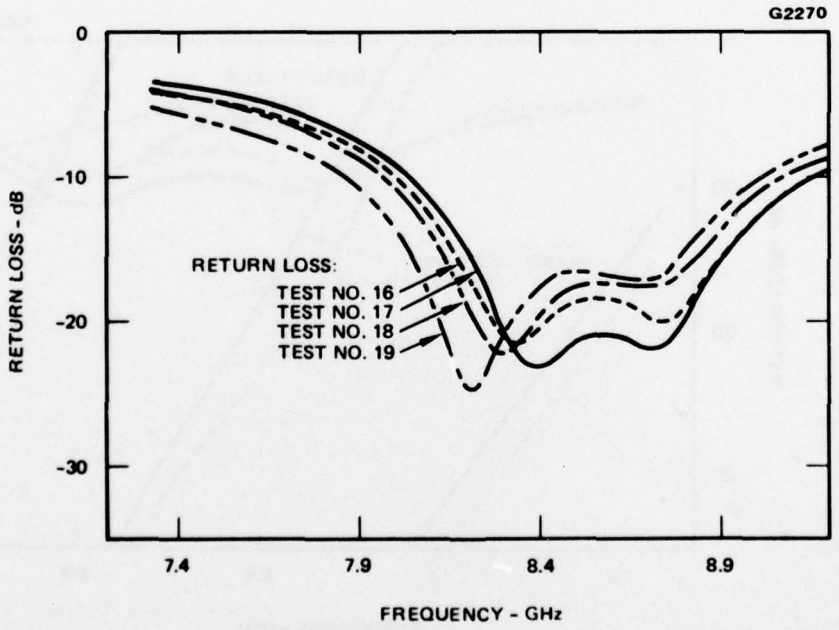

Figure 15 Final circuit configuration, effect of termination position.

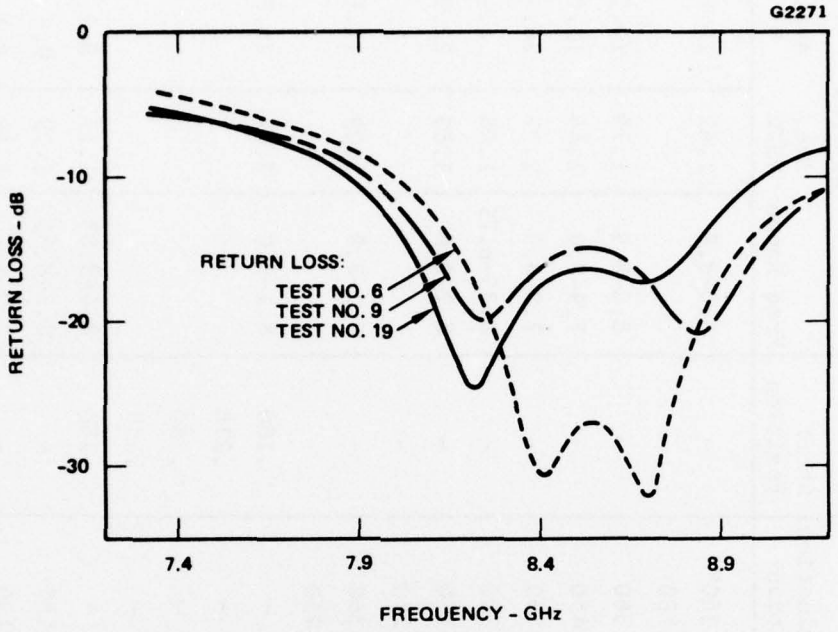

Figure 16 0.072 dia. disc, 0.360 termination position, effect of probe penetration.

TABLE 8

PASSIVE BANDWIDTH IMPROVEMENT TEST RESULTS
(Second Series)

Test #	Plot: Figure #	Probe Configuration			Termination Position	Short Position	Results		
		Disc Dia.	Penetration	Plunger Gap			Freq Range	Ave. VSWR	Ave. Q
1		.125"	.075"	.008"	.360"	-	8.0-8.9	1.61	16.6
2	10	.125	.075	.008	.180	-			
3	10	.125	.075	.008	.360	-	8.0-8.9	1.79	19.7
4	10	.125	.075	.008	.450	-	7.9-8.9	1.46	13.0
5		.125	.075	.004	.360	-	7.9-8.9	2.27	26.4
6	16	.072	.075	.008	.360	-	8.35-8.75	1.08	4.1
7	11,13	.072	.085	.008	.180	-	8.2-9.0	1.89	22.9
8	11	.072	.085	.008	.270	-			
9	11,16	.072	.085	.008	.360	-	8.2-8.9	1.29	11.1
10	11	.072	.085	.008	.450	-			
11	12,13	.072	.085	.008	-	.180	8.1-9.0	2.17	26.8
12	12	.072	.085	.008	-	.270			
13	12	.072	.085	.008	-	.360			
14	12	.072	.085	.008	-	.450			
15	14	.072	.115	.013	-	.180	8.4-8.85	1.17	9.2
16	15	.072	.115	.009	.150	-	8.3-8.85	1.23	9.6
17	12,15	.072	.115	.009	.180	-	8.3-8.8	1.18	8.1
18	15	.072	.115	.009	.210	-	8.2-8.8	1.31	10.6
19	15,16	.072	.115	.009	.360	-	8.2-8.8	1.34	8.9

Tests Nos. 6, 9 and 19: Probe disc diameters were varied from 0.036 (no disc) to 0.250 inches during the tests. It was found that the 0.072 inch diameter disc gives the best match over a 500 MHz bandwidth at 8 GHz. Tests 6, 9 and 19 show the effect of varying the cavity penetration depth of a probe with the 0.072 inch disc (see Figure 16). The termination position was 0.360 inches and the probe disc to plunger surface spacing was 0.008 to 0.009 inches for all three cases.

Tests Nos. 7, 8, 9 and 10: These tests show the effect of varying termination position using the 0.072 inch probe disc at 0.085 inch cavity penetration (see Figure 11). The results are similar to those of Figure 10.

Test Nos. 11, 12, 13 and 14: The test conditions are identical to those of Test Nos. 7, 8, 9 and 10 except that the terminations have been replaced with movable aluminum shorts. The short positions were varied in the same manner as the termination positions and results plotted in Figure 12. It can be seen that results bear little resemblance to those of the termination loaded combiner (Figure 11) except for the 0.180 position cases, Test Nos. 7 and 11. These two cases (plotted together in Figure 13 for comparison) are very similar indicating little absorption of power when the shorts are exchanged for the terminations. The Q's of these cases are too high, 22.9 to 26.8, and a better matched, but non-absorptive condition is necessary.

Test Nos. 15 and 17: The test conditions are identical to those of Test Nos. 11 and 7, respectively, except that the probe's cavity penetration has been increased to 0.115 inches. The results (plotted together in Figure 14 for comparison) show that match has been improved and the Q lowered to the 8.1 to 9.2 region. The results for both shorts and terminations are similar. The frequency is slightly high and could be adjusted downward by increasing the cavity size.

Test Nos. 16, 17, 18 and 19: In these tests the circuit is the same as in Test 17 except that the termination positions are varied. The results, plotted in Figure 15, show that combiner VSWR changes relatively little with termination position when compared to previous tests (Figures 10 and 11). This, again, indicates a very small power absorption by the terminations. The Q is acceptable (8 to 11) and represents a substantial improvement in bandwidth potential over the original amplifier configuration.

2.10 ACTIVE COMBINER BANDWIDTH TESTS

Using the results of the passive tests, a series of power combiner measurements was made using active devices (IMPATT diodes) in the circuit. Four diodes were used in most of these tests with particular emphasis being placed on amplifier Q under both large and small signal conditions. In addition, the effect of matching the large signal power contributions of the individual diodes on overall amplifier performance was studied. Some of the most significant results are shown in Table 9.

The first circuit tried was the one corresponding to Test No. 17 of the passive test results above. Several types of coax module matching circuits were tried but none gave good amplifier results. It was necessary to reduce the probe's cavity penetration to 75 percent of the cavity height and to change the plunger's position in order to obtain reasonable values of gain and power output. When these changes were allowed, the results of lines 1 and 2 of Table 9 were obtained. The output power of 4.33 watts and the Q of 61 were the best results obtained for two diode operation.

Another modification tried was a reduction in cavity height. It was found that reducing the cavity height from 0.125 to 0.100 inches yielded a slight improvement in bandwidth but that further reductions in height

TABLE 9

COMBINER BANDWIDTH IMPROVEMENT TESTS

	No. of Diodes	RF Input Power (W)	RF Output Power (W)	Gain (dB)	Freq (GHz)	Q
1	2	1.58	4.33	4.4	7.86	107
2	2	.016	.058	16.1	7.84	61
3	[illegible]	3.16	8.44	4.3	7.91	82
4	4	.032	.561	12.5	7.94	49
5	4	.032	.183	7.6	7.98	58
6	4	3.16	7.44	3.7	8.42	102
7	4	.032	.377	10.8	8.45	62
8	4	.032	.167	7.2	8.46	61

tended to degrade performance. It was also necessary to match the power contributions of the individual diodes in large signal quite closely (within 10 percent) in order to maximize power output and minimize the Q. Lines 3 and 4 of Table 9 indicate the performance of a four diode combiner in which all of the above modification were made. It was the best four diode results obtained for both power output and lowest Q. The termination positions were similar to those of passive tests 17 and 18. Line 5 of Table 9 indicates the performance of the same circuit except that the small signal gain was reduced by changing the plunger position. This increased the small signal Q from 49 to 58.

Lines 6 and 7 are data for a circuit similar to that of lines 3 and 4 except that the cavity diameter was reduced from 1.108 to 0.988 inches in order to increase the center frequency to 8.4 GHz. The cavity height was reduced proportionally to 0.089 and the coaxial module matching appropriately adjusted. The results were similar to but not quite as good as those at 7.9 GHz because of the characteristics of the diodes. The small signal performance (line 8) was approximately the same as that of the lower frequency circuit.

In summary, a new probe-cavity transition configuration was developed which has improved the combiner's gain-bandwidth product. Additionally, insight into the proper positioning of the terminations was obtained and a more flexible coax module impedance matching circuit was developed which allows closer power contribution equalization among the individual diodes. The amount of the improvement obtained is illustrated by Figure 17. The dashed line represents the gain versus amplifier Q for four-diode combiner results obtained previous to the latest series of tests (Sections 2.4 and 2.5). The second (solid) line shows the performance of the improved configuration as reported above in Table 9, lines 3 through 8. The third line, labeled "Goal", shows the minimum

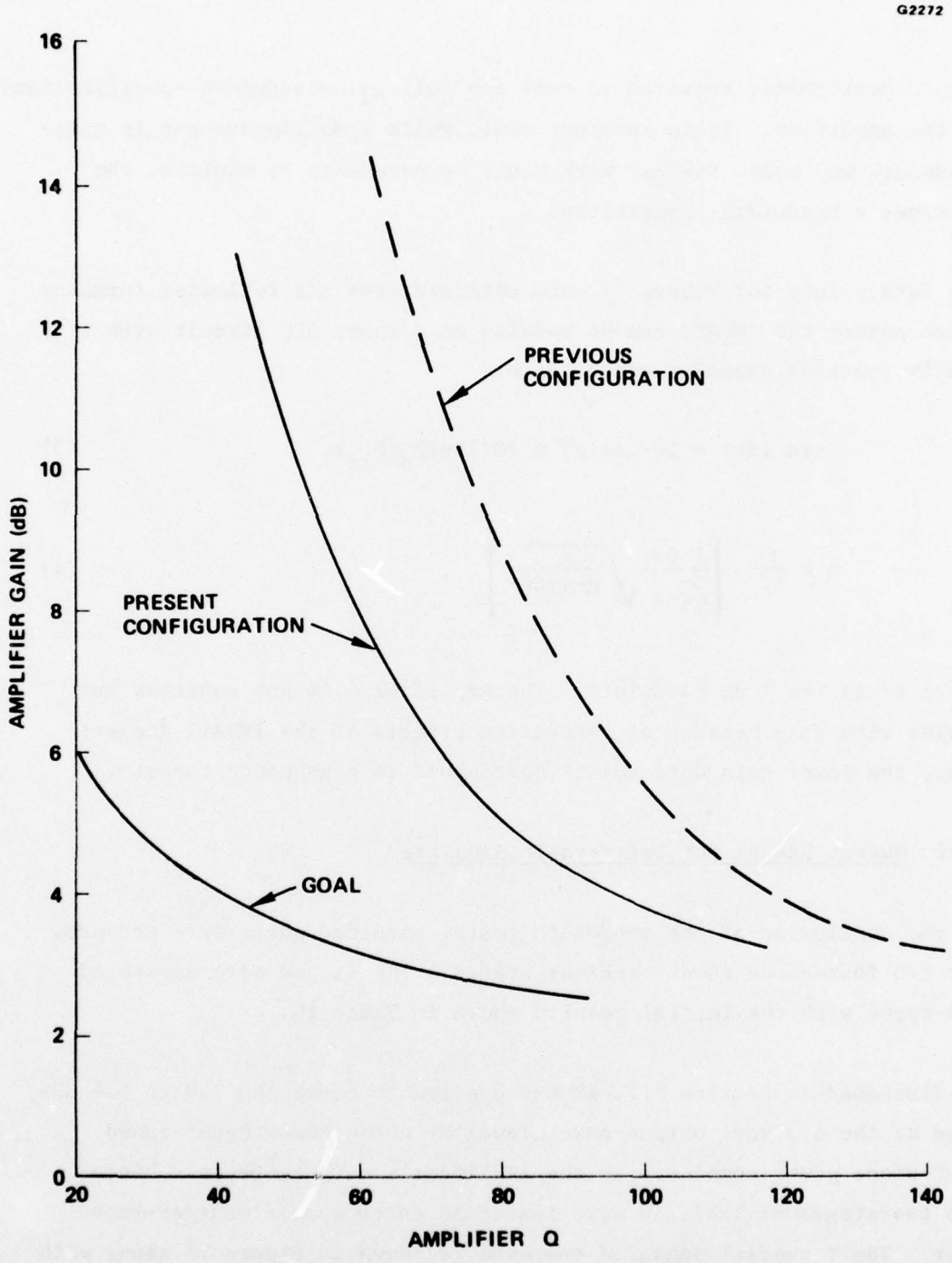

Figure 17 Four-diode power combiner gain versus amplifier Q.

gain-Q performance required to meet the full gain-bandwidth specifications of the amplifier. It is apparent that, while some improvement in gain-bandwidth was made, further work would be necessary to minimize the combiner's bandwidth limitations.

The data points for Figure 17 were obtained from the following formulae which assume the IMPATT can be modeled as a shunt GLC circuit with a nearly constant negative conductance:

$$\text{Gain (dB)} = 10 \cdot \log(g) = 10 \cdot \log(P_o/P_{IN}), \tag{3}$$

$$Q = \frac{f}{\Delta f} \left[\frac{1.02}{\sqrt{g-1}} \sqrt{\frac{g}{g-1.26}} \right] , \tag{4}$$

where Δf is the 1 dB bandwidth. The amplifier Q is not constant but varies with gain because of saturation effects of the IMPATT diodes; i.e., the lower gain data points correspond to high power outputs.

2.11 Output Stages for Deliverable Amplifier

At the conclusion of the bandwidth tests, machined parts were procured for two four-diode power combiner stages. The stages were assembled and tuned with the initial results shown in Table 10.

As discussed in Section 5.1, it was desired to cover the 7.9 to 8.4 GHz band at the 1.5 watt output power level by using two stagger-tuned four-diode power combiners as the amplifier's output stages. Hence, the two stages of Table 10 were tested in cascade as a stagger-tuned pair. Their overall measured response is shown in Figure 18 along with a theoretical response calculated from the data of Table 10. It can be seen that the measured response has less bandwidth and somewhat higher

TABLE 10

DELIVERABLE OUTPUT STAGES

Stage No.	RF Input Power (W)	RF Output Power (W)	Gain (dB)	Freq. (GHz)	Q
7	3.12	6.77	3.36	8.213	160
7	.21	1.84	9.34	8.241	68
8	3.16	7.27	3.62	7.981	135
8	.22	1.91	9.45	8.030	60

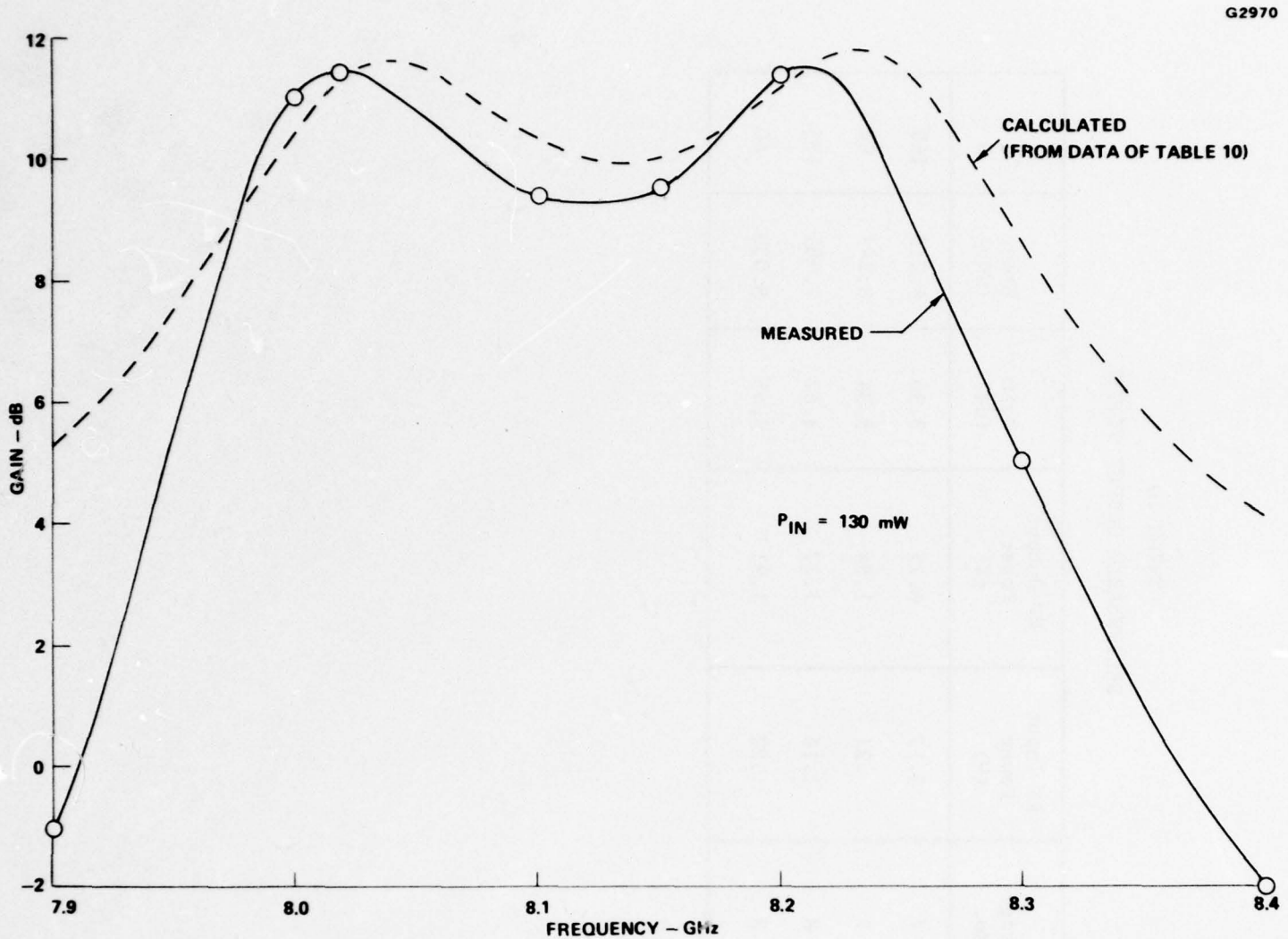

Figure 18 Calculated and measured responses of two cascaded combiner stages.

ripple than the calculated one. It is apparent that the combiners do not stagger tune as well as calculations based on simple 3 dB Q measurements would indicate. It has been found that the power combiner's gain falls off more rapidly with frequency than would a simple single-tuned amplifier stage having the same 3 dB bandwidth. The gain of single-tuned reflection amplifier approaches 0 dB gain assymotically with frequency deviation from center band whereas the combiner's gain approaches a negative value (attenuation). This effect produces the sharp gain fall-off at the band edges of the measured response of Figure 18. It also causes a reduction in bandwidth and higher ripple. The effect was present throughout all of our stagger-tuned measurements and led to reduction in overall amplifier performance below that previously thought possible (see Section 5).

Because of the rather high gain ripple of the response of Figure 18, the stages were retuned for less ripple as shown in Figure 19. This entailed moving the center frequencies of the two stages closer together which caused a further reduction in bandwidth. However, in order to produce an amplifier with useable gain ripple over at least a portion of the band, the output stages were left tuned in this manner.

2.12 FUNDAMENTAL BANDWIDTH LIMITATIONS

Experience with stagger-tuning of the combiner stages late in the program led to the realization that they fall off more rapidly at frequencies beyond the 3 dB points than a simple Q measurement would indicate. It is now known that this effect can be explained by examining a simple model of the combiner circuits. It is, in fact, a fundamental limitation to the bandwidth of any amplifier circuit which employs Kenyon-type coaxial modules for stabilizing.

One coaxial module of the power combiner may be represented by the model shown in Figure 20 where Y_d is the admittance of the IMPATT diode (matching

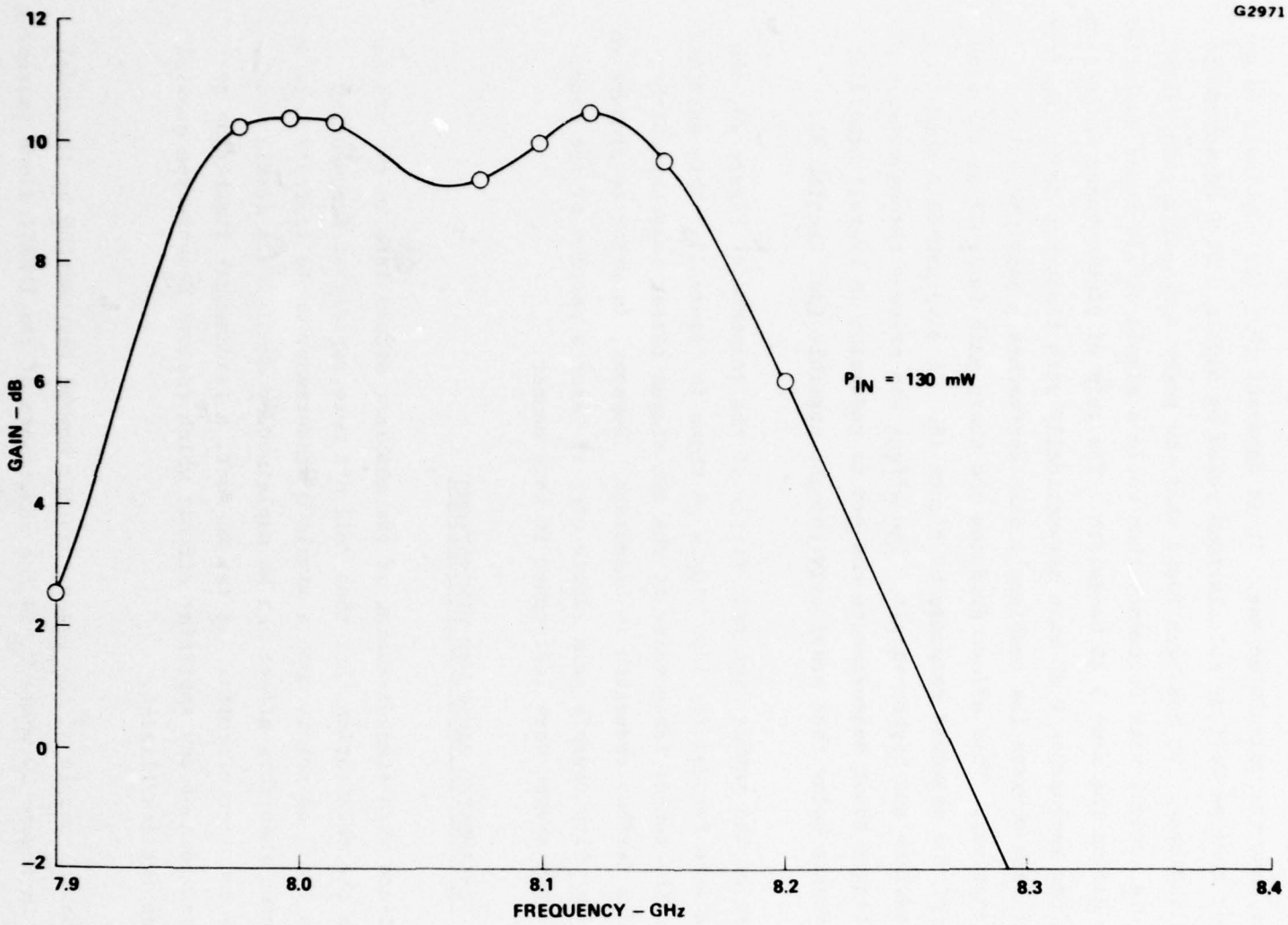

Figure 19 Measured response of cascaded combiner stages (returned for reduced ripple).

circuitry neglected), G_s is the conductance of the coaxial stablilzing load and Y_L is the load presented to the coaxial module by the cavity and probe.

G2972

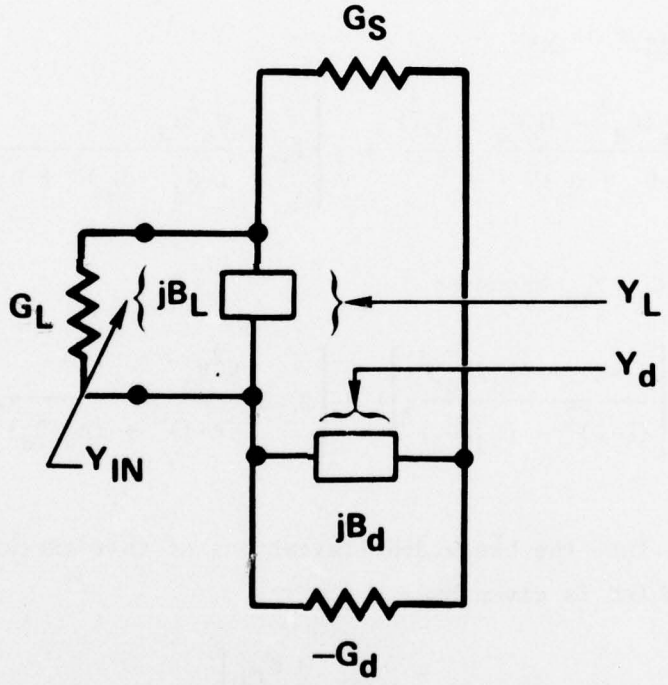

Figure 20 Simplified Model of Power Combiner Coaxial Module.

The gain of this circuit is given by

$$g = \left| \frac{G_L - Y_{IN}}{G_L + Y_{IN}} \right|^2 , \tag{5}$$

$$= \frac{(G_L - G_{IN})^2 + B_{IN}^2}{(G_L + G_{IN})^2 + B_{IN}^2} , \tag{6}$$

where

$$Y_{IN} = G_{IN} + jB_{IN}, \tag{7}$$

$$= \frac{G_s(G_d^2 - G_dG_s + B_d^2)}{(-G_d + G_s)^2 + B_d^2} + j\left[B_L + \frac{G_s^2 B_d}{(-G_d + G_s)^2 + B_d^2}\right] . \tag{8}$$

Letting $K = G_s/G_d$, Y_{IN} becomes:

$$Y_{IN} = KG_d\left[\frac{(1-K) + (B_d/G_d)^2}{(K-1)^2 + (B_d/G_d)^2}\right] + j\left[B_L + \frac{K^2 B_d}{(K-1)^2 + (B_d/G_d)^2}\right] \tag{9}$$

To gain insight into the bandwidth limitations of this circuit, we examine the Q which is given by

$$Q = \frac{1}{G_{IN}} \frac{\omega o}{2} \left.\frac{d\, B_{IN}}{d\omega}\right|_{\omega_o} \tag{10}$$

Differentiating B_{IN} (from equation (9)), we obtain:

$$\frac{dB_{IN}}{d\omega} = \frac{dB_L}{d\omega} + \left[\frac{K^2}{(K-1)^2 + (B_d/G_d)^2}\right]\left[\frac{(K-1)^2 - B_d^2}{(K-1)^2 + B_d^2}\right]\frac{dB_d}{d\omega} \tag{11}$$

At $\omega = \omega o$, $B_d = 0$ and

$$\left.\frac{dB_{IN}}{d\omega}\right|_{\omega o} = \left.\frac{dB_L}{d\omega}\right|_{\omega o} + \left[\frac{K^2}{(K-1)^2}\right] \left.\frac{dB_d}{d\omega}\right|_{\omega o} , \tag{12}$$

$$\left. G_{IN} \right|_{\omega o} = -G_d \left[\frac{K}{K-1}\right] . \tag{13}$$

The negative amplifier Q is then

$$Q = -\frac{1}{G_d} \frac{\omega o}{2} \left[\left(\frac{K-1}{K}\right) \left.\frac{dB_L}{d\omega}\right|_{\omega o} + \left(\frac{K}{K-1}\right) \left.\frac{dB_d}{d\omega}\right|_{\omega o} \right] \tag{14}$$

In practical amplifiers K is made as large as possible in order to minimize absorption by the stabilizing termination, G_s. (K is about 4 to 5 in the delivered combiners.) Additionally, $dB_L/d\omega$ is kept as small as possible whereas $dB_d/d\omega$ is fixed by the IMPATT device; hence, generally

$$\left.\frac{dB_d}{d\omega}\right|_{\omega o} \geq \left.\frac{dB_L}{d\omega}\right|_{\omega o} . \tag{15}$$

When this condition holds, and $K > 1$, it can be shown that

$$\left[\left(\frac{K-1}{K}\right) \left.\frac{dB_L}{d\omega}\right|_{\omega o} + \left(\frac{K}{K-1}\right) \left.\frac{dB_d}{d\omega}\right|_{\omega o} \right] > \left.\frac{dB_L}{d\omega}\right|_{\omega o} + \left.\frac{dB_d}{d\omega}\right|_{\omega o} . \tag{16}$$

The right hand side of (16) is the susceptance slope of the circuit in Figure 20 with G_s removed from the circuit (i.e., $R_s = 0$). Thus, the

presence of the stabilizing termination, G_s, increases the magnitude of the amplifier's Q. The closer G_s is in value to G_d (i.e., the smaller the value of K) the larger is the increase in Q .

In order to observe the effects of K on the amplifier's gain response, equation (6) has been plotted for several values of K and two values of peak gain in Figures 21 and 22. For these plots it was assumed that the Q of the diode $\left(Q_d = \frac{1}{G_d} \frac{\omega o}{2} \left.\frac{dB_d}{d\omega}\right|_{\omega o}\right)$ is 20 which is consistent with experimental measurements. For the probe-cavity-coax transition $\left(Q_L = \frac{1}{G_L} \frac{\omega o}{2} \left.\frac{dB_L}{d\omega}\right|_{\omega o}\right)$ a Q of 10 was used which is consistent with test numbers 15 through 19 of Table 8.

In Figure 21 all of the gain responses have a peak gain of 10 dB. The $K \to \infty$ case has an amplifier $|Q|$ of 39.25 which is somewhat larger than the sum of the circuit and diode $|Q|$ s ($|Q_d| + |Q_L| = 30$). This discrepancy is due to the "mismatch" required between the circuit and diode to achieve 10 dB gain. (The lowest values of $|Q|$ would be obtained for extremely high values of peak gain, approaching oscillation). From the other curves it can be seen that the presence of G_s in the circuit can cause significant bandwidth reduction depending upon its value. It is, of course, obvious that the degree of stabilization provided by G_s and its reduction of bandwidth will trade off. The values of Q shown in parentheses in the figures are calculated using (1) for frequencies close (within ±25 MHz) to the center frequency. If Q is calculated for more distant frequencies it remains constant for the $K \to \infty$ case but increases for lower values of K. For example, if the 6 dB down gain points are used to calculate gain in Figure 21, the results are as follows:

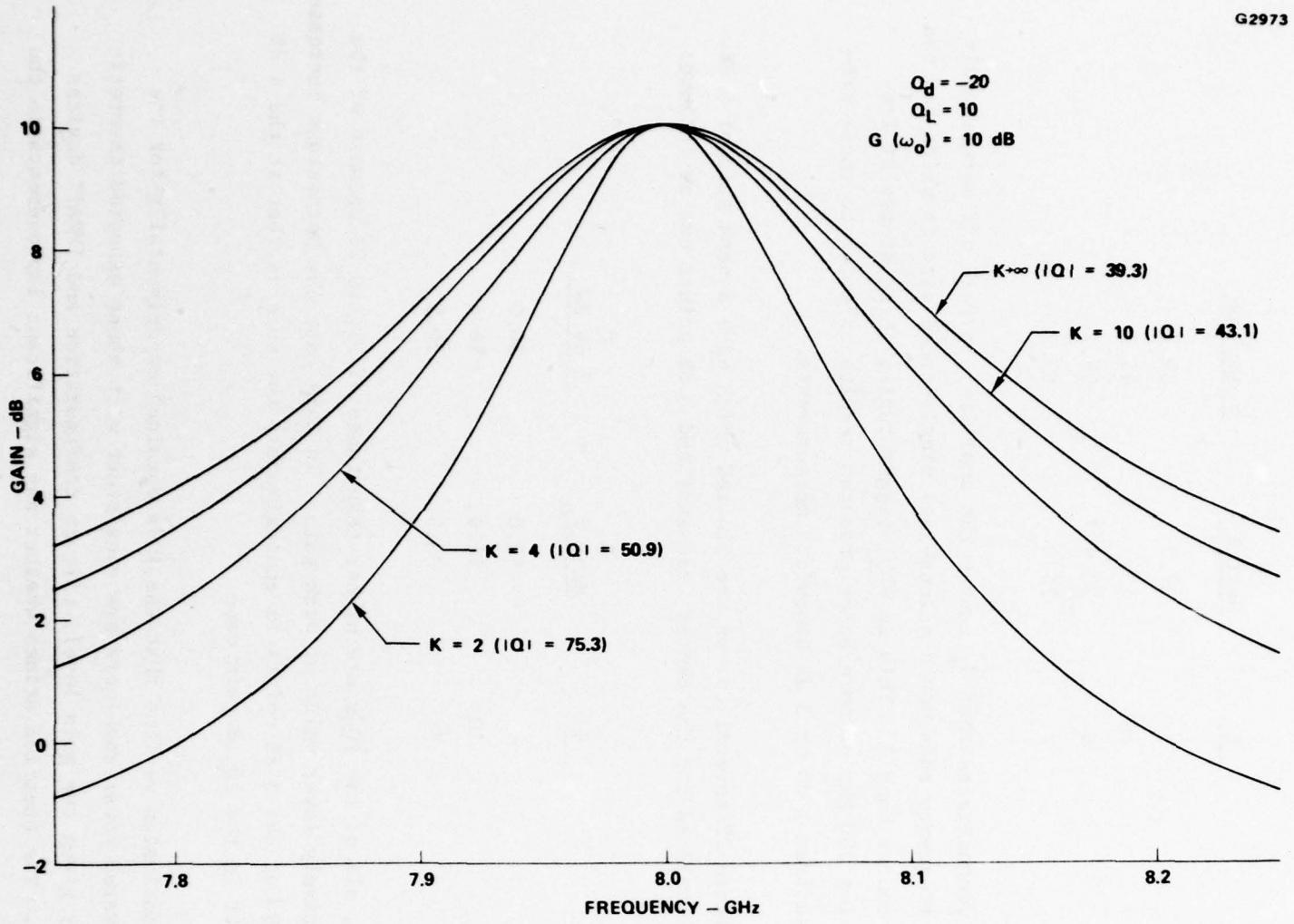

Figure 21 Gain response of coax module model

K	Q Near f_o	6 dB Q BW
∞	39.3	39.3
10	43.1	45.1
4	50.9	56.7
2	75.3	87.7

This demonstrates that G_s causes the amplifier to fall off more rapidly with frequency than would a loss-less single-tuned circuit which had the same center band Q. This is why stagger tuning these stages at frequencies 200 MHz or more apart produces results inferior to those predicted from 1 dB or 3 dB bandwidth measurements.

In Figure 22 several curves are plotted which have a peak gain of 6 dB. Qs calculated for the center frequency and 3 dB points are as follows:

K	Q Near f_o	Q 3 dB BW
∞	50.0	50.0
10	55.9	59.4
5	63.5	70.9

Here, all of the $|Q|$s are higher than those of Figure 21 because of the relatively lower value of peak gain. In this case the percentage increase of $|Q|$ at the 3 dB points in approximately the same as that at the 6 dB points in the 10 dB gain case.

In conclusion we find that the $|Q|$s obtained experimentally for the delivered power combiners are consistent with those expected theoretically given the gain level, circuit configuration and IMPATT devices used. The question arises whether any significant improvements in the

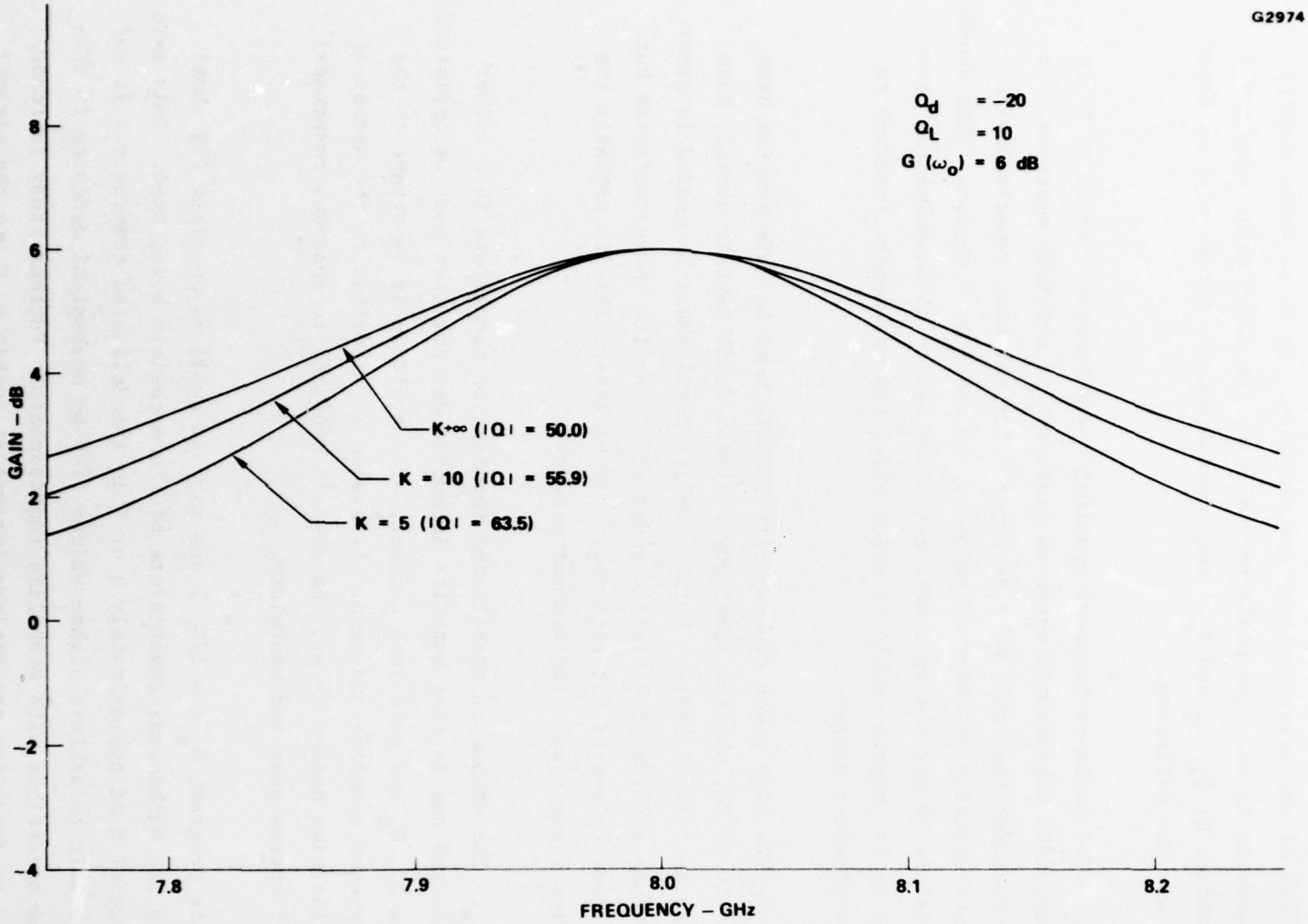

Figure 22 Gain response of coax module model

bandwidth of the power combiner are possible. To do so would require improvements in one (and preferably all) of the three major components of combiner Q; Q_d, Q_L and G_s. Recommendations for future work in these areas are the following.

1. Q_L - The probe-cavity-coax coupling Q was lowered from 28 to 10 in the bandwidth improvement tests as discussed in previous sections. It is recommended that this work be pursued further both experimentally and theoretically in order to reduce Q_L to the 2 to 5 region. This should be possible by performing a more extensive series of experimental tests backed up by computer analysis which allow the parameters involved to vary over wider ranges.

2. Q_d - The high power double drift IMPATTs used in this program have Q's of 16 to 20, whereas lower power single drift devices usually have Q's in the 8 to 12 range. Further device development is needed in order to produce IMPATTs with similar power and linearity characteristics but with lower values of Q_d; preferably, 10 or less. This is probably the most important single improvement needed.

3. G_s. The choice of stabilizing termination parameters is a rather complicated one in that both its impedance and position must be optimized taking Q_L, Q_d and gain into account. Its position is important to the cavity-coax coupling and gain. Its value is important to the amount of stabilization needed (i.e., the diode's tendency to spurious responses) and of course gain and bandwidth.

In this program, R_s (= $1/G_s$) was made as small as possible (20 ohms) within the mechanical constraints of the materials being used. This gave a value of K of approximately 4 or 5 in the delivered combiners. It may be possible to achieve higher values of K by mechanical redesign if this proves compatible with stability requirements. Further study is recommended to establish the optimum interrelationship of G_s to the circuit

parameters. Other more complicated structures might also be considered. For example, a bandstop filter between G_s and the rest of the circuit may allow nearly full bandwidth potential at the fundamental frequency while providing good stabilization at far out of band frequencies.

Figure 23 is a plot of the estimated gain of the combiner if all of the above potential improvements were to be made. It was assumed for these plots that $|Q|$s of 5 and 10 could be achieved for the circuit and diode, respectively. It was also assumed that either a value of K = 10 could be obtained or G_s could be effectively removed at the fundamental frequency band by the use of some filtering arrangement. Note that there is not a great deal of difference between these two cases. Two amplifier stages having a gain response corresponding to the K = 10 case could be stagger-tuned to produce a 500 MHz bandwidth with 1 dB ripple and 11.9 dB minimum gain.

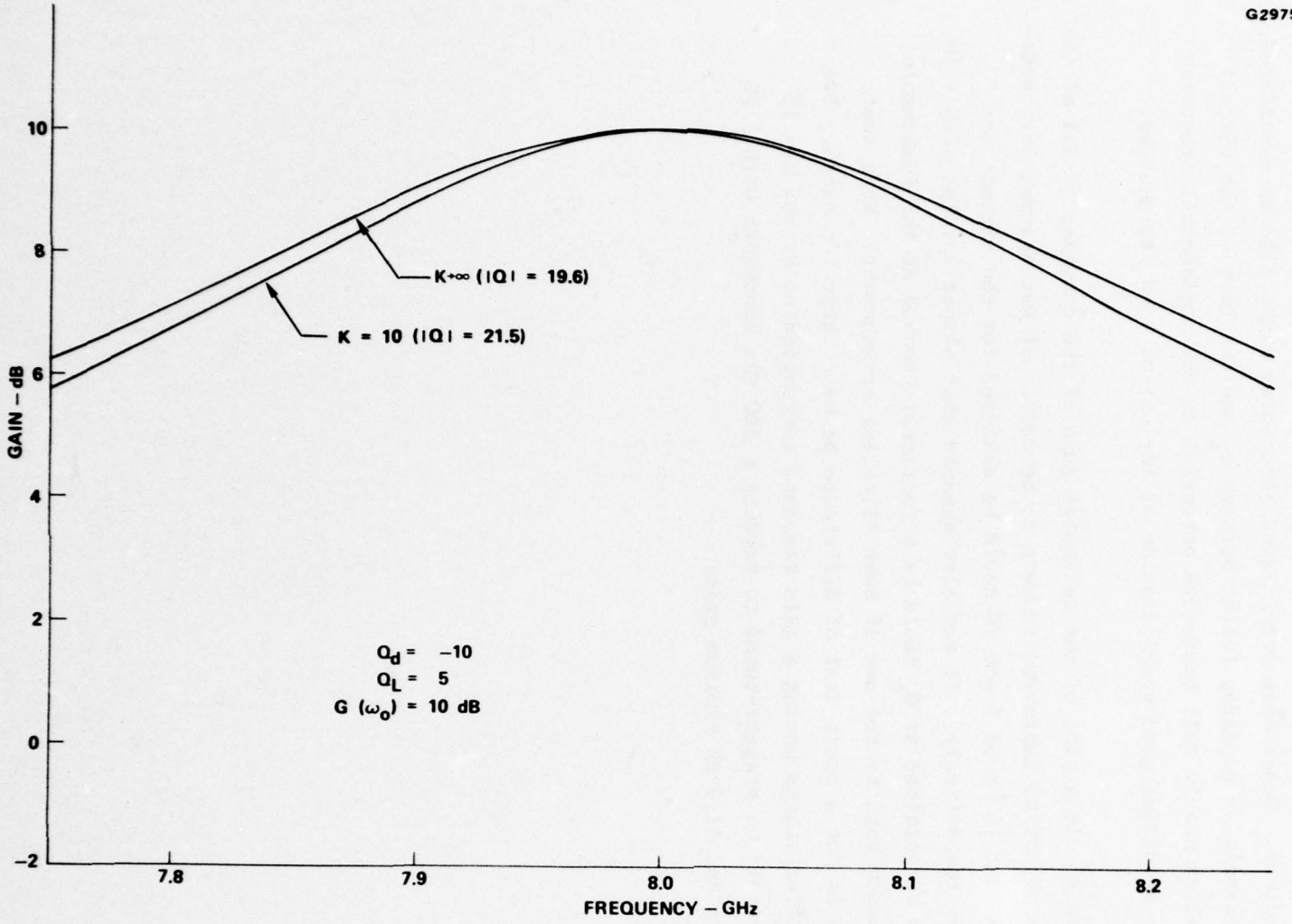

Figure 23 Combiner bandwidth potential

3.0 TASK II - HYBRID STAGE DEVELOPMENT

3.1 Hybrid Coupler Scaling, Fabrication and Evaluation

A two-section maximally flat airstrip hybrid coupler was designed for operation at 8.15 ±0.5 GHz during the first monthly period. A sketch of the airstrip center conductor is shown in Figure 24. It consists of 0.001 inch metallization plated on a 0.010 inch microstrip board for support. The ground plane spacing is 0.100 inch.

The hybrid coupler was assembled and tested using a network analyzer. The results of the hybrid coupler evaluation are summarized in Figure 25. Curves A and B show the isolation between the input and output, ports 1 and 2, and the isolation between the two amplifier ports, 3 and 4. Although the maximum isolation occurs somewhat low in frequency, 7.6 to 7.7 GHz, the isolation remains below 19 dB across the 7.9 to 8.4 band and is considered adequate.

The coupling balance between the input port and the two amplifier ports is shown by curves C and D. The coupling balance between the amplifier ports and the output port is shown by curves E and F. The coupling factors are quite flat over the 7.9 to 8.4 GHz band, exhibit a minimal amount of coupling error and show that the coupler has very little loss. The coupling errors (deviations from 3.0 dB) are ±0.4 dB for all curves except for one point at +0.7 dB in curve E. Other data taken shows that the coupling errors are generally within +0.5 dB from 7.6 to 8.6 GHz indicating that the 1 GHz design bandwidth was achieved.

The phase balance of the coupler was measured by putting a signal into port 1 and recording the phase at ports 3 and 4. The phase difference was found to be 90° $\pm 5^{\circ}$.

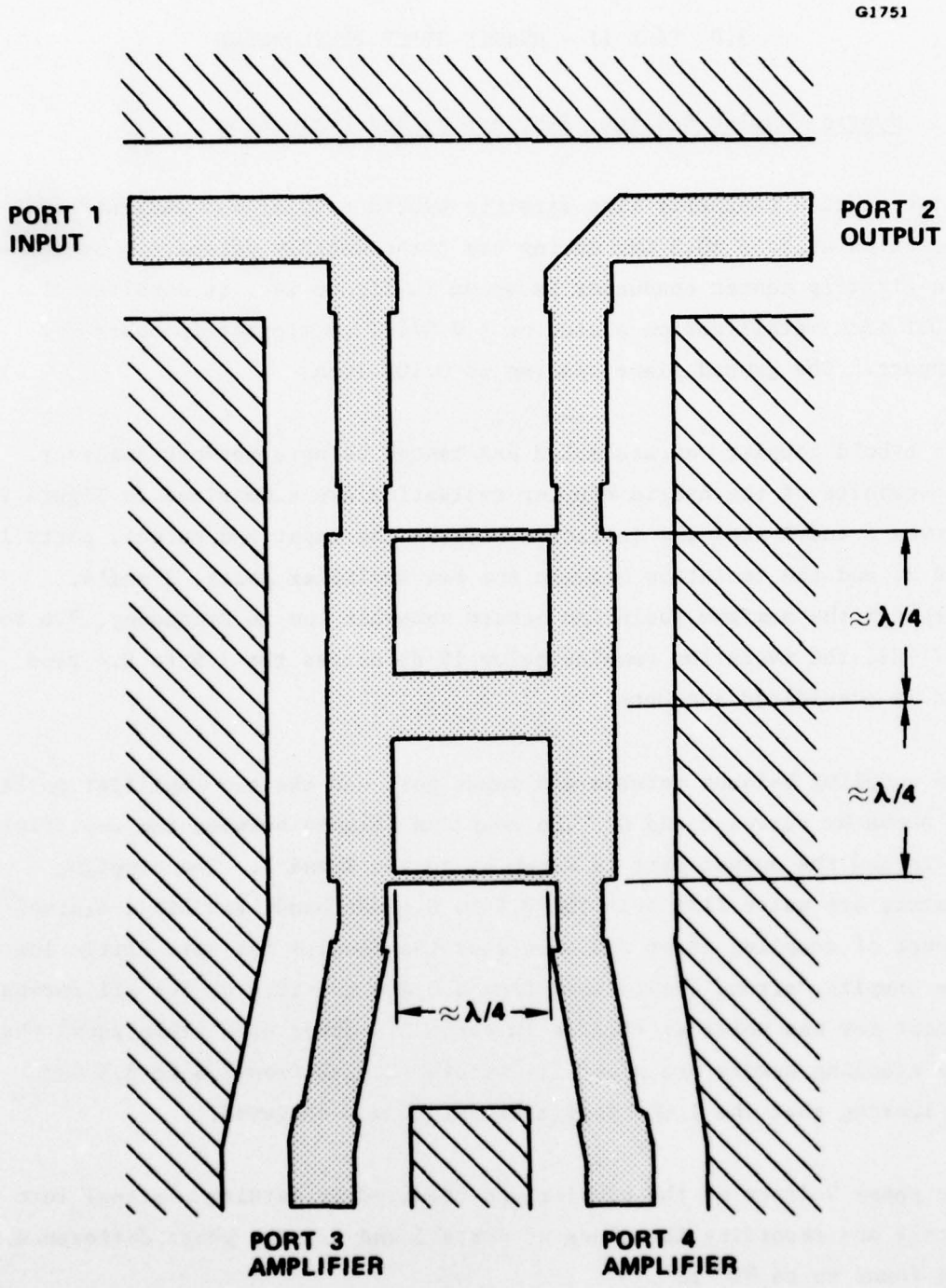

Figure 24 Center conductor of 8.15 GHz airstrip hybrid coupler.

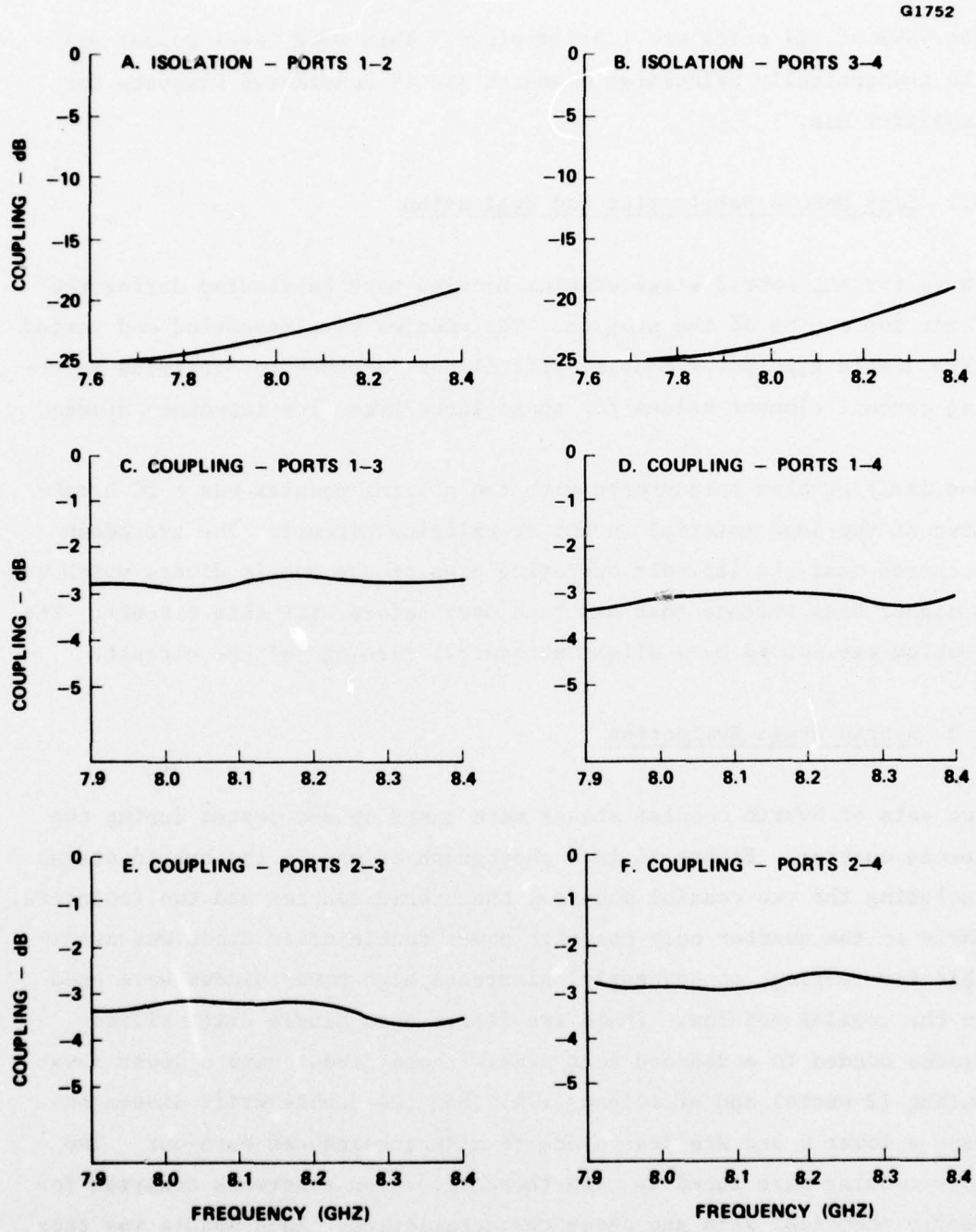

Figure 25 Hybrid coupler performance.

The VSWR at all ports was 1.3:1 maximum. This VSWR level approaches the theoretically calculated mismatch and is considered adequate for amplifier use.

3.2 Coax Module Fabrication and Evaluation

Parts for the hybrid stage coaxial modules were fabricated during the first two months of the program. The modules were assembled and tested with sample high power double drift diodes in order to determine matching circuit element values for these large area, low impedance diodes.

One early problem encountered with the coaxial modules was a DC breakdown of the load material in the stabilizing circuit. The breakdown occurred near the 185 volt operating bias of the double diodes which was a higher bias voltage than had been used before with this circuit. The problem was solved by a slight mechanical redesign of the circuit.

3.3 Hybrid Stage Evaluation

Two sets of hybrid coupled stages were tuned up and tested during the second quarter. Figure 26 is a photograph of one of the hybrid stages including the two coaxial modules, the hybrid coupler and two isolators. Early in the quarter only one high power double drift diode was available for testing, consequently, alternate high power diodes were used in the coaxial modules. These are larger area single drift silicon diodes bonded to a diamond heat sink. These diodes have a lower power rating (2 watts) and efficiency (7%) than the double drift diodes but have a lower Q and are less prone to mismatch-induced burn-out. Two coax modules were tuned up with these diodes on a network analyzer for nearly identical gain and phase characteristics. Each module was then individually placed on the hybrid coupler with a load on the adjacent amplifier port. Each was slightly readjusted so that the gain and phase

E842

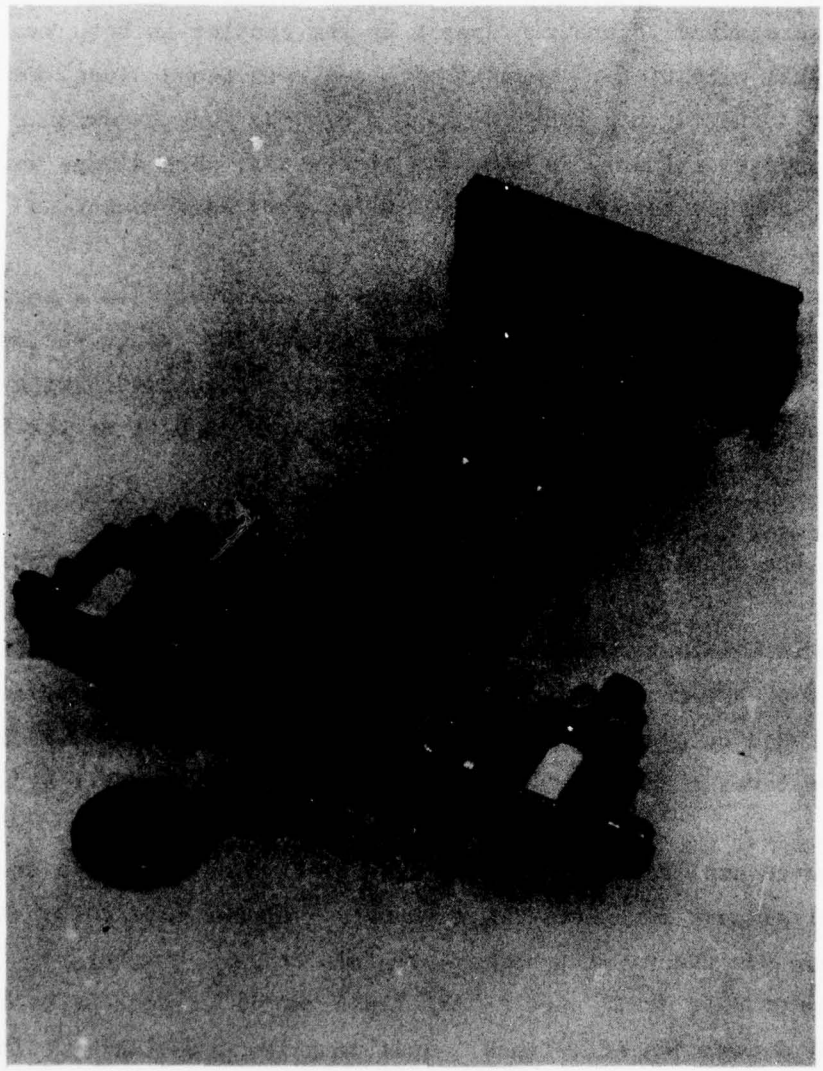

Figure 26 Hybrid coupler amplifier stage.

characteristics were nearly identical when used with the hybrid. Both modules were then connected to the coupler and the overall response measured. It was verified that the gain responses of the two coaxial modules were added together properly by the coupler in both small and large signal conditions. Results obtained with these diodes were 3.8 watts output with 2.8 dB gain and a 620 MHz 1 dB bandwidth. A plot of the bandpass obtained is shown in Figure 27a. The diodes were operating at a junction temperature of 195°C for this measurement.

After the high power double drift diodes became available a second hybrid coupled stage was assembled and tuned. This stage yields 3.9 watts output power with 2.8 dB gain and a 355 MHz 1 dB bandwidth with the diodes operating at 175°C junction temperature. A plot of the frequency response for this stage is shown in Figure 27b.

The Q of the double drift diodes is considerably higher than originally anticipated. However, the amplifier Q measured at Hughes is 16 to 21 which is in agreement with a detailed analysis of these diodes the manufacturer has conducted. This is in contradiction to previous expectations based on simpler analyses that the Q of a double drift diode should be lower than that of the corresponding single drift structure.

The measured amplifier Q for the single drift diodes used in the first hybrid stage test is substantially lower -- approximately 12. This is the reason for the wider bandwidth of this stage. However, the double drift diodes were still used in the final amplifier because of their higher RF generation efficiency. Additionally, the single drift diodes operate at 125 volts which would cause a further loss in efficiency if used with a 200 volt power supply. The performance of Figure 27b was improved somewhat by raising the junction temperatures to 200°C.

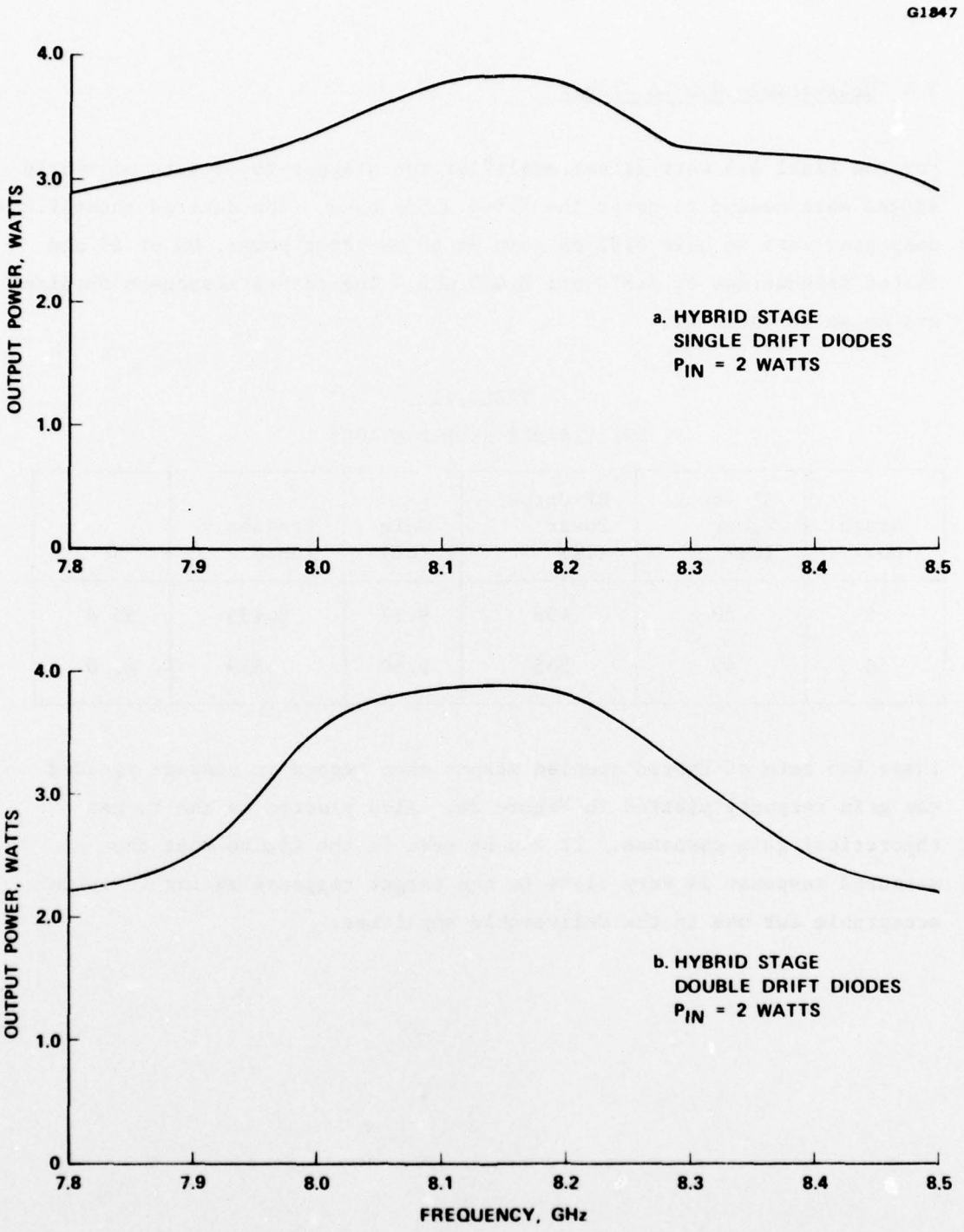

Figure 27 Hybrid coupled stage test results.

3.4 Deliverable Hybrid Stages

For the final 1.5 watt linear amplifier two stagger-tuned sets of hybrid stages were needed to cover the 7.9-8.4 GHz band. The desired theoretical responses were to have 8.85 dB gain at 60 mW input power, Qs of 43 and center frequencies of 7.870 and 8.430 GHz. The actual responses obtained are shown in Table 11.

TABLE 11

DELIVERABLE HYBRID STAGES

Stage No.	RF Input Power (mW)	RF Output Power (mW)	Gain (dB)	Frequency (GHz)	Q
5	60	496	9.17	8.435	56.8
6	60	535	9.50	7.859	41.0

These two sets of hybrid coupled stages when tested in cascade yielded the gain response plotted in Figure 28. Also plotted is the target theoretical gain response. It can be seen in the figure that the measured response is very close to the target response making it quite acceptable for use in the deliverable amplifier.

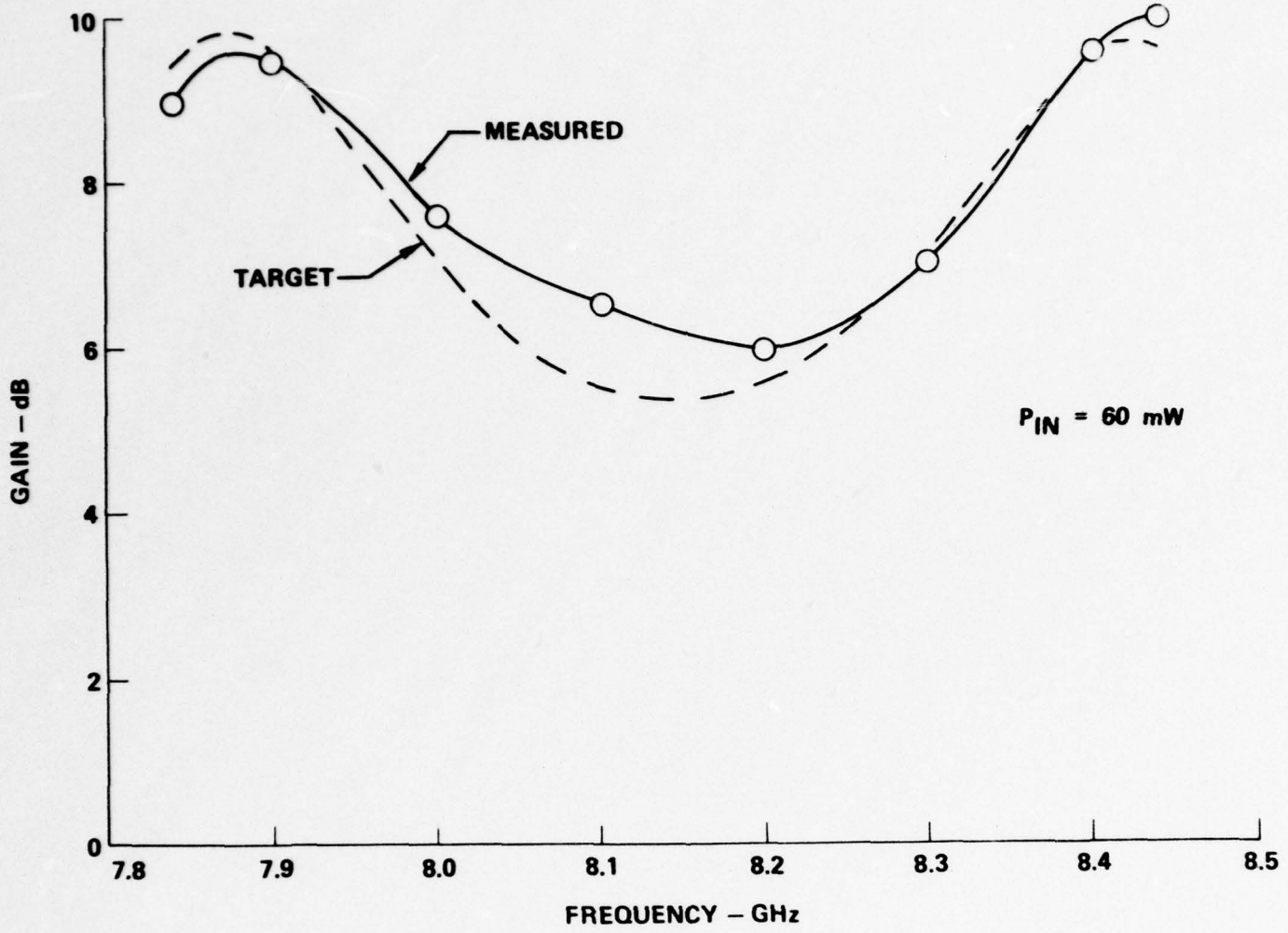

Figure 28 Measured and theoretical target gain responses of two cascaded hybrid states.

4.0 KEY PURCHASED COMPONENTS

4.1 Circulators

Four four-port circulators with 15-watt loads and four isolators with 5-watt loads were delivered to Hughes, Electron Dynamics Division during the second quarter of the program and subsequently evaluated. Figure 29 shows some typical network analyzer measurements of the amplifier port impedances of two of the circulators. The plots are on expanded Smith Charts whose outermost circle corresponds to a VSWR of 1.5:1. It can be seen that the circulators meet our specifications which allow a 1.15:1 maximum VSWR in the 7.9 to 8.4 GHz frequency band from $-30^{o}C$ to $+80^{o}C$ and a VSWR change of no more than 1.14 at any given frequency over the temperature range.

4.2 Sample Diode Procurement and Testing

In September 1974 one IMPATT diode manufacturer informed us that they were nearing the completion of development of a high power, high efficiency double drift silicon diode at 8 GHz. A letter of quotation was received specifying 2.75 watts oscillator power with at least 9% efficiency at 8 GHz. Estimated delivery times were six devices in four weeks and 30 devices in six weeks.

At that time four engineering model diodes were ordered for evaluation purposes. The diodes were delivered in December 1974, and some preliminary evaluation completed. In a coax amplifier stage, these diodes typically give 2.5 watts of output power at 8 GHz with 5 dB gain and 6 to 7 percent generation efficiency at conservative bias levels. This approximates closely the proposed operating level of each diode in the output combiner stage. At maximum recommended bias, the diodes are

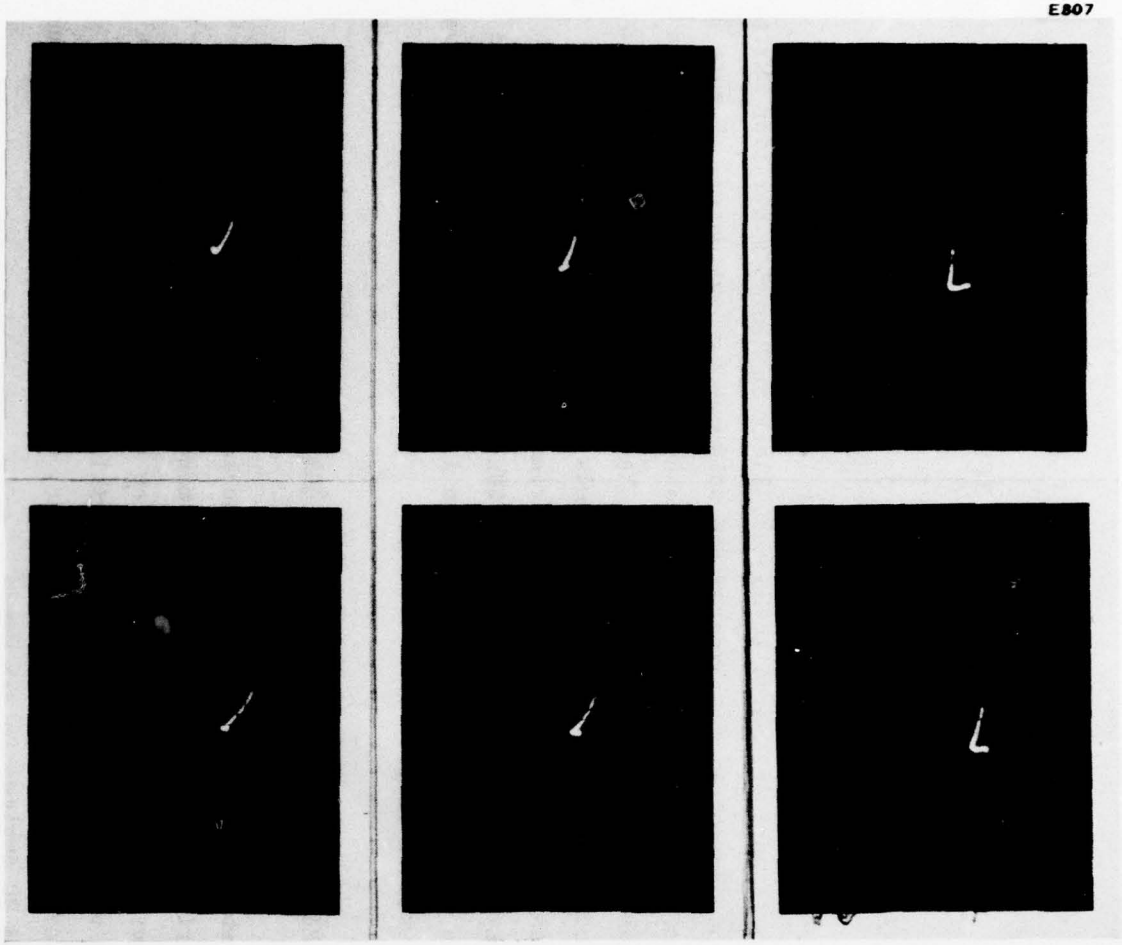

Figure 29 Measured impedances of amplifier ports for two of the four-part circulators plotted on expanded Smith charts.

capable of 2.8 watts output with 5.5 dB gain. Diode impedance measurements were made with a network analyzer to aid in the design of the amplifier matching circuitry. These measurements showed that the real part of the diodes' impedances are very low, 2 to 2.5 ohms. This value is about one quarter that of a single-chip single drift diode which means that much more impedance inversion is needed to match to them. The Q measured for these diodes (as determined from the reactance slope of the impedance measurements) is as high as 21 at 8 GHz. When operated in a coaxial amplifier the large distributed impedance inverter required and the loss of the circulator increase the apparent stage Q to between 28 and 35. A value of Q this high was not anticipated because it is substantially higher than the same circuit used with single drift diodes. With this level of Q, and a required 1 dB bandwidth of 500 MHz, the maximum gain obtainable per stage is 4 to 5 dB according to equation (4). Alternatively, one may obtain higher levels of gain across the required band by stagger tuning pairs of stages.

The vendor was contacted regarding the Q of double drift diodes. He said that our measured amplifier Q of 16 to 21 is in agreement with a detailed analysis of these diodes that he has conducted. The analysis predicts an oscillator Q of 40 for the diodes and that the amplifier Q should be lower than the oscillator Q. This is in contradiction to previous expectations based on simpler analyses that the Q of a double drift diode should be lower than that of the corresponding single drift structure. The diode Q had unfortunate effects on the amplifier program as it seriously affected the gain-bandwidth performance of all of the stages from the drivers to the hybrids and power combiners.

4.3 Production Diode Procurement

At the beginning of the program a production quantity of 32 of the high power double drift diodes was ordered. The original promised delivery schedule was 8 diodes on 2/12/75, 8 on 3/12/75 and 16 on 5/17/75. Early in the program the vendor experienced several problems affecting the manufacture and reliability of the devices. These included silver contamination and/or migration and barrier metal damage due to the silicon etch. The problems were solved but they delayed delivery of the first lot of 13 devices from February 12 to the last week of April. The first lot delivered was sufficient for initial evaluation of the hybrid and combiner stages. The remaining 19 diodes were delivered during the first part of July.

Of the 32 production diodes 16 were shipped with the final amplifier, 3 unused diodes were left over and 13 failed during the course of the program. Of the failures approximately two thirds were "explainable"; i.e., those caused by tuning induced mismatches, sudden bias disconnections, etc. The remaining failures were of the "unexplainable" type, ocurring during stabilized amplifier operation at conservative bias levels while no tuning was being performed. Several diodes seemed to degrade with time and finally fail.

5.0 TASK III - AMPLIFIER CONFIGURATION, ASSEMBLY AND TEST

5.1 Change of Technical Approach

The original program objective was to develop a solid state amplifier which would deliver 20 watts of output power across the 7.9 to 8.4 GHz band with 14 dB gain. The amplifier was to consist of three reflection amplifier stages connected by circulators as shown in Figure 30. The second and third stages were to be cavity power combiners containing four and eight 2.0 watt IMPATT diodes respectively. The first stage was to be a conventional hybrid-coupled amplifier combining the output of two coax amplifier modules. This stage would use two IMPATT diodes also rated at 2.0 watts each. As shown in Figure 30, the first stage was to operate at 6.5 dB gain with an added power of 3.28 watts, the second was to have a gain of 4.0 dB with an added power of 7.53 watts and the third was to have a gain of 3.5 dB with an added power of 13.73 watts. Small signal gains of the three stages would be 12.0 dB, 6.8 dB and 5.2 dB respectively. At the three quarter point in program it became evident that insufficient funds remained to complete the program as originally conceived due primarily to the bandwidth problems discussed in previous sections. Three alternative directions the program could take from this point were considered:

1) Build two 20 watt, 14 dB gain, amplifiers per contract except under the existing bandwidth restrictions.

2) Build one amplifier optimized for use as a linear intermediate power amplifier specifically designed to drive high power TWTs. Under existing bandwidth restrictions it would be necessary to stagger-tune the stages in order to cover the 500 MHz bandwidth at the TWT drive power level (approximately 1.5 W). Eight stages would be incorporated to

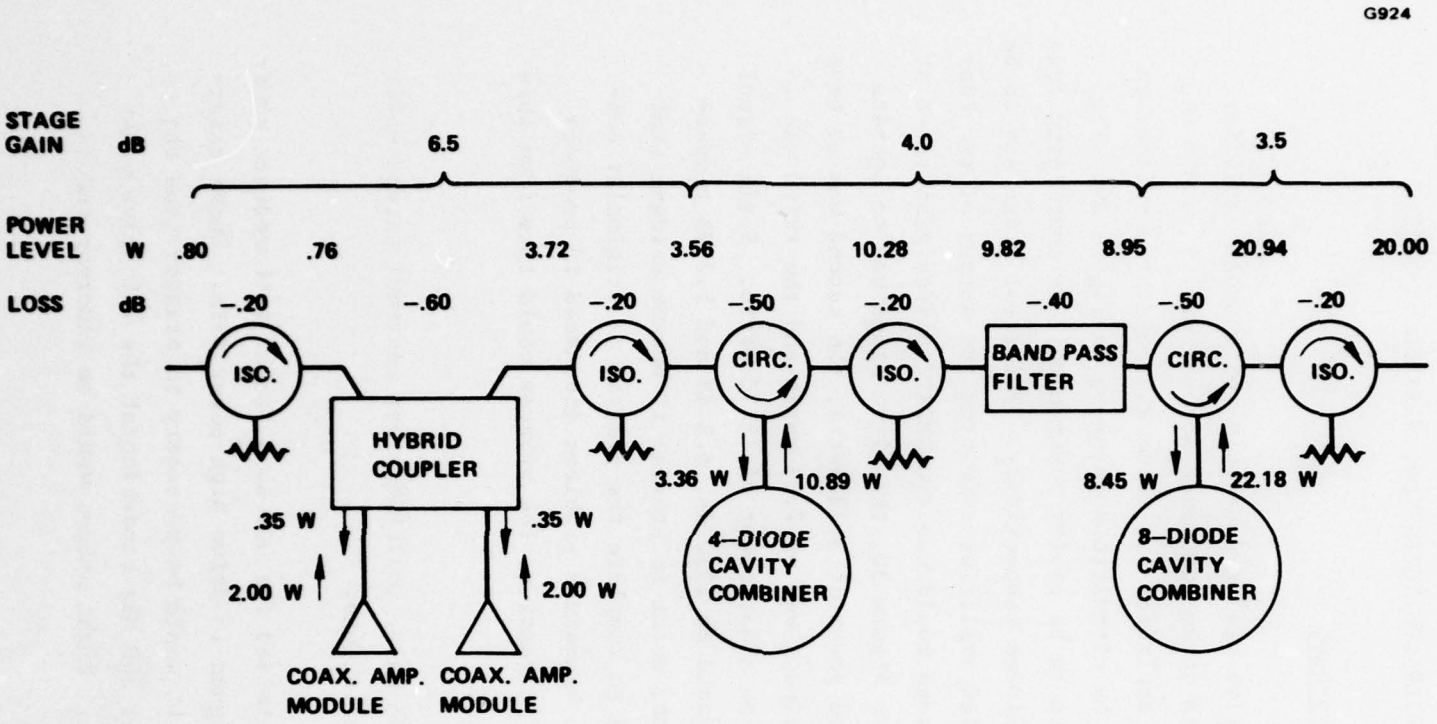

MODULE GAIN	dB	7.5	5.1	4.2
POWER ADDED	W	3.28	7.53	13.73
SMALL SIGNAL GAIN	dB	12.0	6.8	5.2
DC INPUT	W	44	88	176

Figure 30 20 watt, 7.9 - 8.4 GHz IMPATT Amplifier.

provide approximately 40 dB gain at this power level. In order to have good (30 dBc) intermodulation products the amplifier would have to have a 6 to 10 watt saturated output power capability, and for this reason, combiners would still be used in the two output stages. The amplifier would be optimized, however, at the 1.5 W output power level for broadest bandwidth and flatest gain characteristics.

3) Divert full efforts into solving the bandwidth problem before continuing with other aspects of the program. Additional funding would then be needed in order to complete two 20 watt, full bandwidth amplifiers.

A decision was made to proceed with option number 2 of the above alternatives. Under option 2 the solid state amplifier work was to be redirected toward development of a linear TWT driver and the specifications were changed accordingly. The primary specification changes were as follows:

a) The operating power level was changed from 20 watts saturated to 1.5 watts linear.

b) The saturated power was reduced to 10 watts nominal at center band.

c) The gain was increased from 14 dB to 38 dB minimum (40 dB goal).

d) The 20 dB dynamic operating range was retained.

e) An intermodulation product requirement of 30 dBc at 200 mW output was added.

Typical data for a high power TWT, representative of the type which would be driven by the solid state amplifier, is shown in Figures 31, 32 and 33. It is assumed that it is desired to operate the TWT in a system at

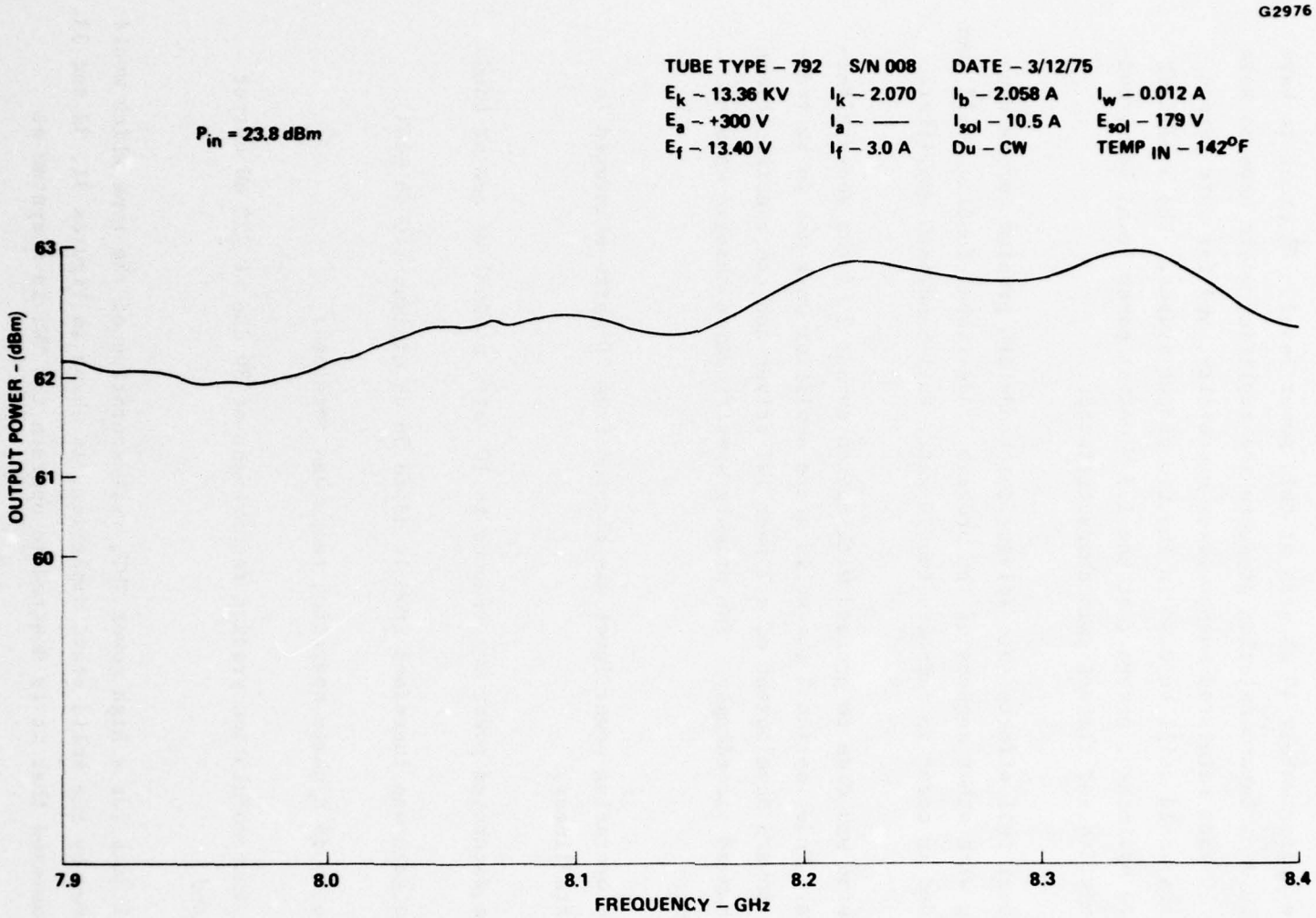

Figure 31 Power output versus frequency at 5 dB below rated power.

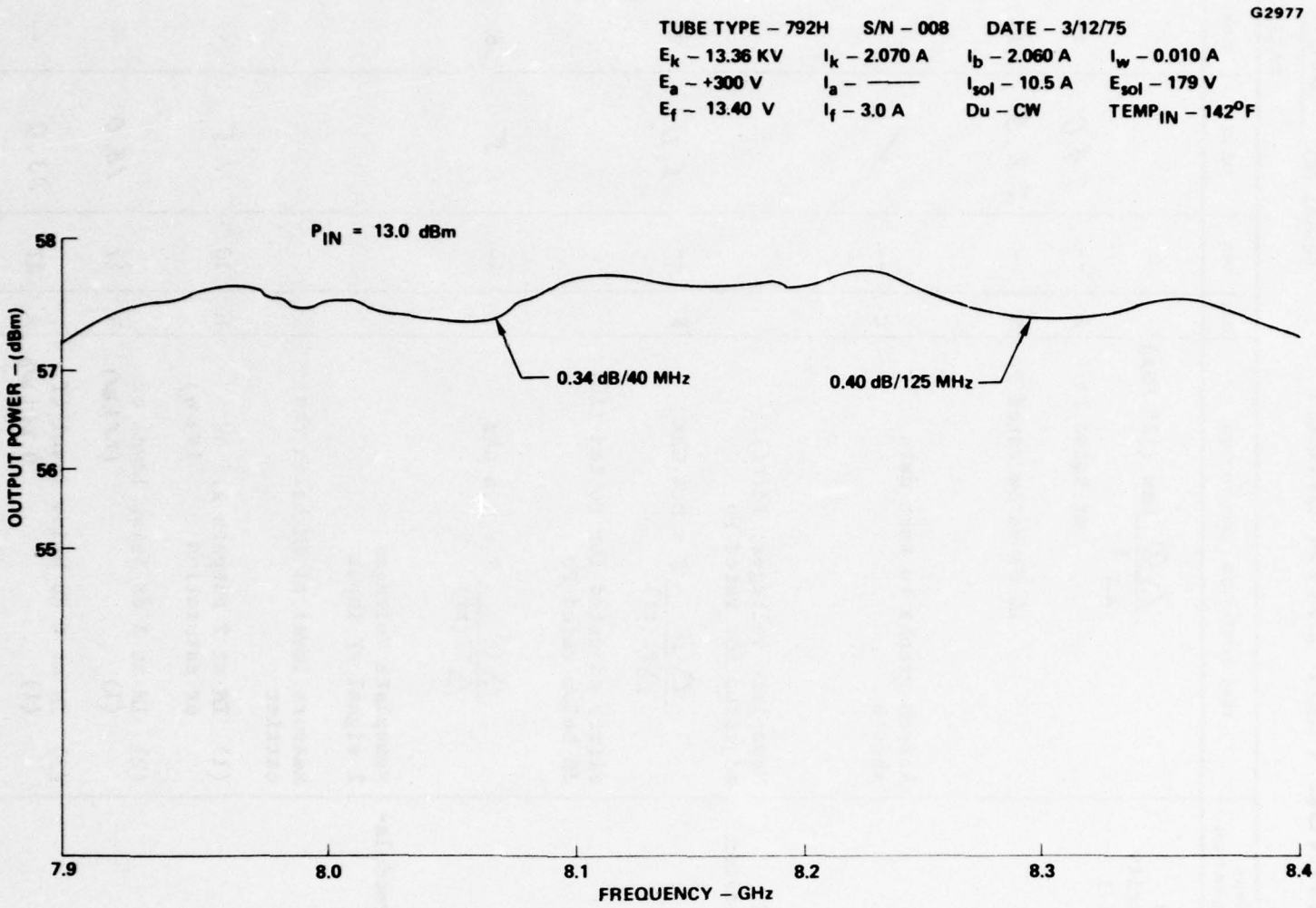

Figure 32 Power output versus frequency at 10 dB below rated power

HUGHES ELECTRON DYNAMICS DIVISION
HUGHES AIRCRAFT COMPANY
3100 West Lomita Boulevard, Torrance, California 90509. Tel (213) 534-2121

DATA SHEET NO. DSB151738
REV. A
SERIAL NO. 008

ACCEPTANCE TEST DATA SHEET

CODE IDENT. 73293

ITEM	SPEC. PAR. No.	TEST DESIGNATION	TEST CONDITION / DESCRIPTION	R/C	MIN.	DATA	MAX.	UNITS
20	4.3.18	Phase Linearity (Cont.)	$\frac{\Delta\phi}{\Delta F}$ Max (125 MHz)					
			at Rated Po	R	--	±4.0	±4	deg
			10 dB below rated Po	R	--	±2.5	±4	deg
			Attach graphs to test data sheets	C	--	✓	--	--
21.	4.3.19	AM-PM Conversion	Nameplate voltages; Pi(rf) adjusted for rated Po					
			$\frac{\Delta\phi}{\Delta Pi(rf)}$ F = 8.4 GHz	R	--	5.0	6	°/dB
			Pi(rf) adjusted for Po ten (10) dB below rated Po					
			$\frac{\Delta\phi}{\Delta Pi(rf)}$ F = 8.4 GHz	R	--	1.5	6	°/dB
22.	4.3.20	Intermodulation	Nameplate Voltages 2 signal RF input					
			Measure level of IM below the carrier					
			(1) IM at 2 outputs 2.5 kW or saturation (5 kW)	R	10.5	11.5	--	dB
			(2) IM at 3 dB below level of (1) (2.5 kW)	R	17	18.0	--	dB
			(3) IM at 6 dB below level of (1) (1.25 kW)	R	23	23.0	--	dB

Figure 33

60 dBm output power with intermodulation products at least 24 dB below the carriers. From the data of Figures 31 and 32 we deduce that the drive power needed for 60 dBm output is between 18 and 19 dBm. Assuming 3 to 4 dB system losses before the TWT's input, the output required of the solid state driver amplifier is approximately 23 dBm, or 200 mW. (The power required to fully saturate the TWT is 1.5 watts accounting for the maximum power requirement of the solid state driver.)

Figure 33 shows that the TWT intermodulation products are 23 dB below the carriers at the 1.25 kW level and are decreasing with output power level at the rate of 2 dB/dB. Thus, at 1 kW output the TWT intermod products would be 25 dB below the carriers. It is our experience at Hughes that the intermodulation powers of two cascaded amplifiers simply add according to the relation:

$$IM_t = -10 \log \left[10^{-IM_1/10} + 10^{-IM_2/10} \right] \qquad (17)$$

where IM_t is the total third order intermodulation product level (dB below the carriers) and IM_1 and IM_2 are the intermodulation product levels of the first and second amplifiers, respectively. If the TWT intermod level, IM_2, is 25 dBc and the desired IM_t is 24 dBc, solving for IM_1 gives 30.9 dBc as the required intermod level for the solid state driver. In IMPATT amplifiers the third order intercept is typically at or near the saturated output power. Thus, and IMPATT amplifier with an intermod level of 30.9 dBc at 23 dBm output is required, having a saturated output power of 38.45 dBm, or 7.0 watts.

The amplifier configuration designed to meet the requirements of the revised specification is shown in Figure 34. It consists of four pairs of stagger-tuned stages for a total eight stages. Two four-diode power combiners are used as the output pair of stages in order to

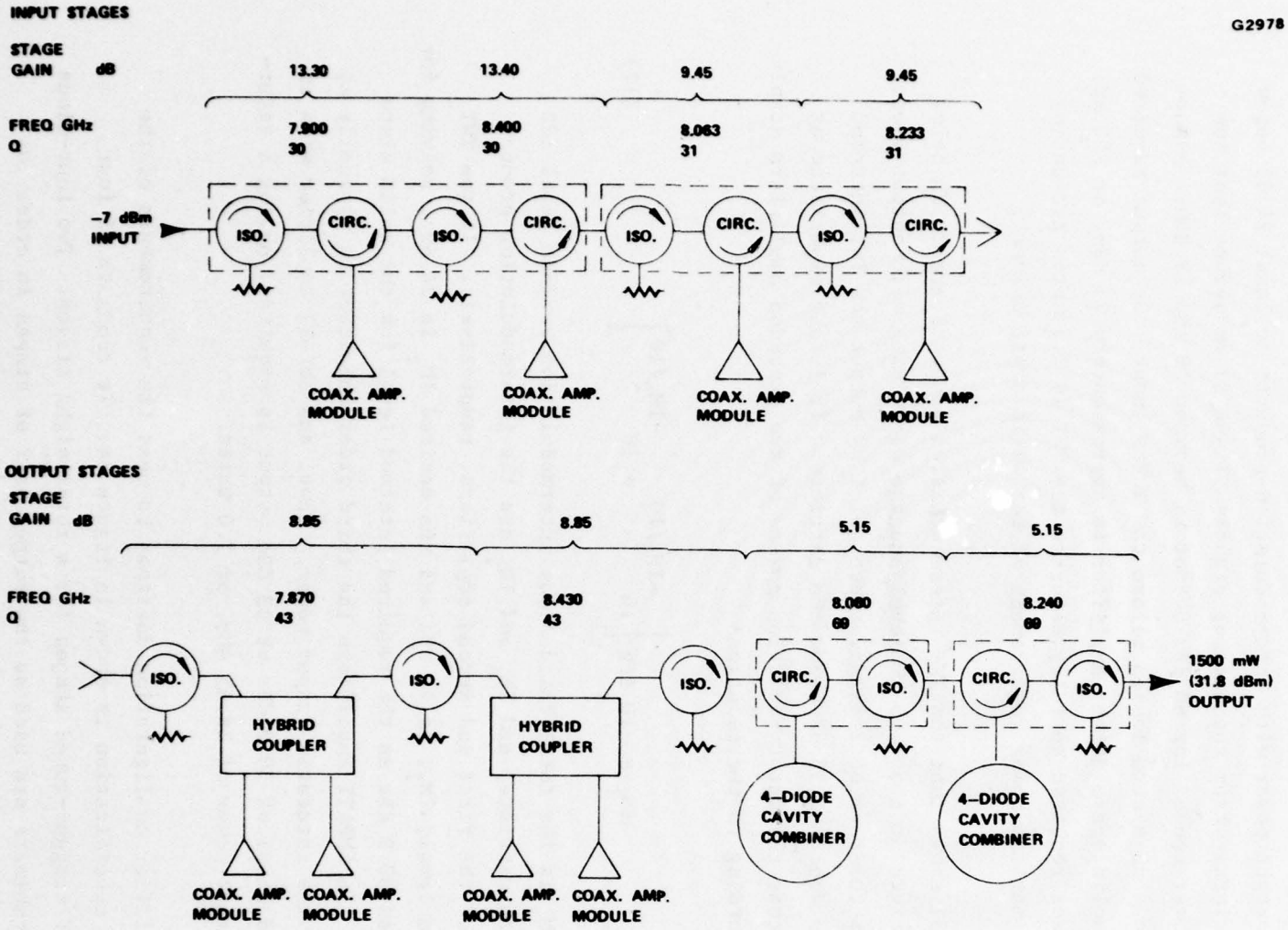

Figure 34 Eight-stage amplifier configuration.

obtain the high saturated output power capability required. The individual stage gains and frequencies were chosen to optimize gain-bandwidth performance at 1.5 watts output.

A computer program has been written at Hughes to predict the overall performance of a multistage amplifier given the individual stage characteristics (gain, center frequency and Q) and to study the trade-offs between gain, bandwidth, ripple and output power. The eight stage amplifier's overall gain response at several power levels has been predicted theoretically via computer based on the performances obtained for individual stages. The computed responses for 1.5 watts output and for small signal conditions are shown in Figure 35. It can be seen that the minimum predicted gain for 1.5 watts output is 38.1 dB and is approximately 2 dB into compression. The computed saturated gain of the amplifier is shown in Figure 36. The peak power output is 10 watts with 21.5 dB gain.

5.2 Assembly and Test of Driver Stages

Upon making the above program direction decision parts fabrication for the output stages of the final amplifier was begun. The parts for the four single diode driver stages and two two-diode hybrid stages were procured earlier in the program. These stages were assembled and initially tuned individually. The six stages and their regulators were then mounted into the final amplifier's chassis and tested as a chain without the combiners. The gain data from these tests is shown in Figure 37 for a wide range of input power levels. The nominal operating input power (for 1.5 watts output from the final amplifier) is 0.2 mW and the small signal input power level is 0.02 mW. It can be seen from the data that the gain at these two levels is nearly identical indicating linear operation over this region. Also, the full 7.9 to 8.4 GHz band is

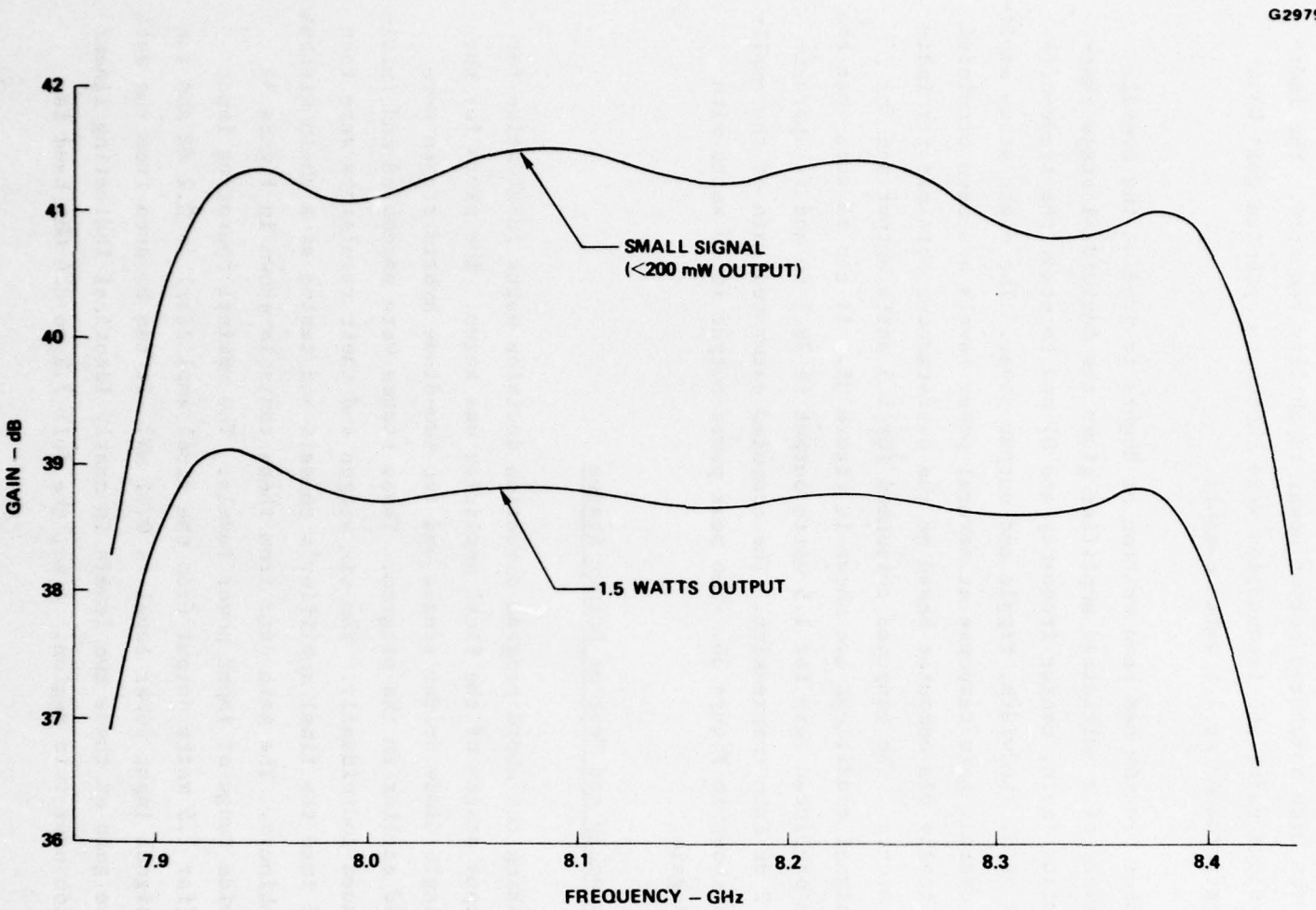

Figure 35 Computed response of amplifier - linear gain region.

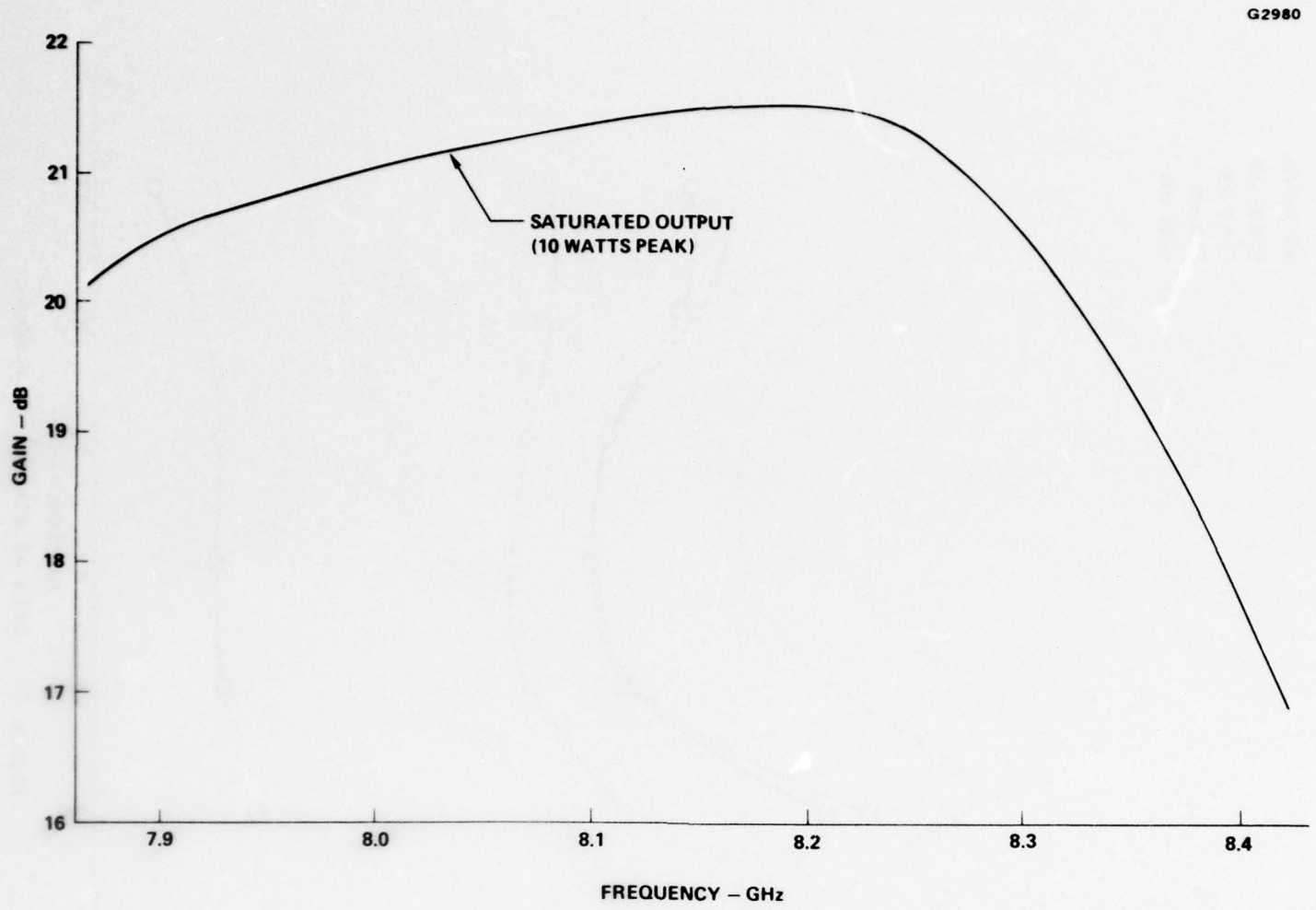

Figure 36 Computed response of amplifier at saturation

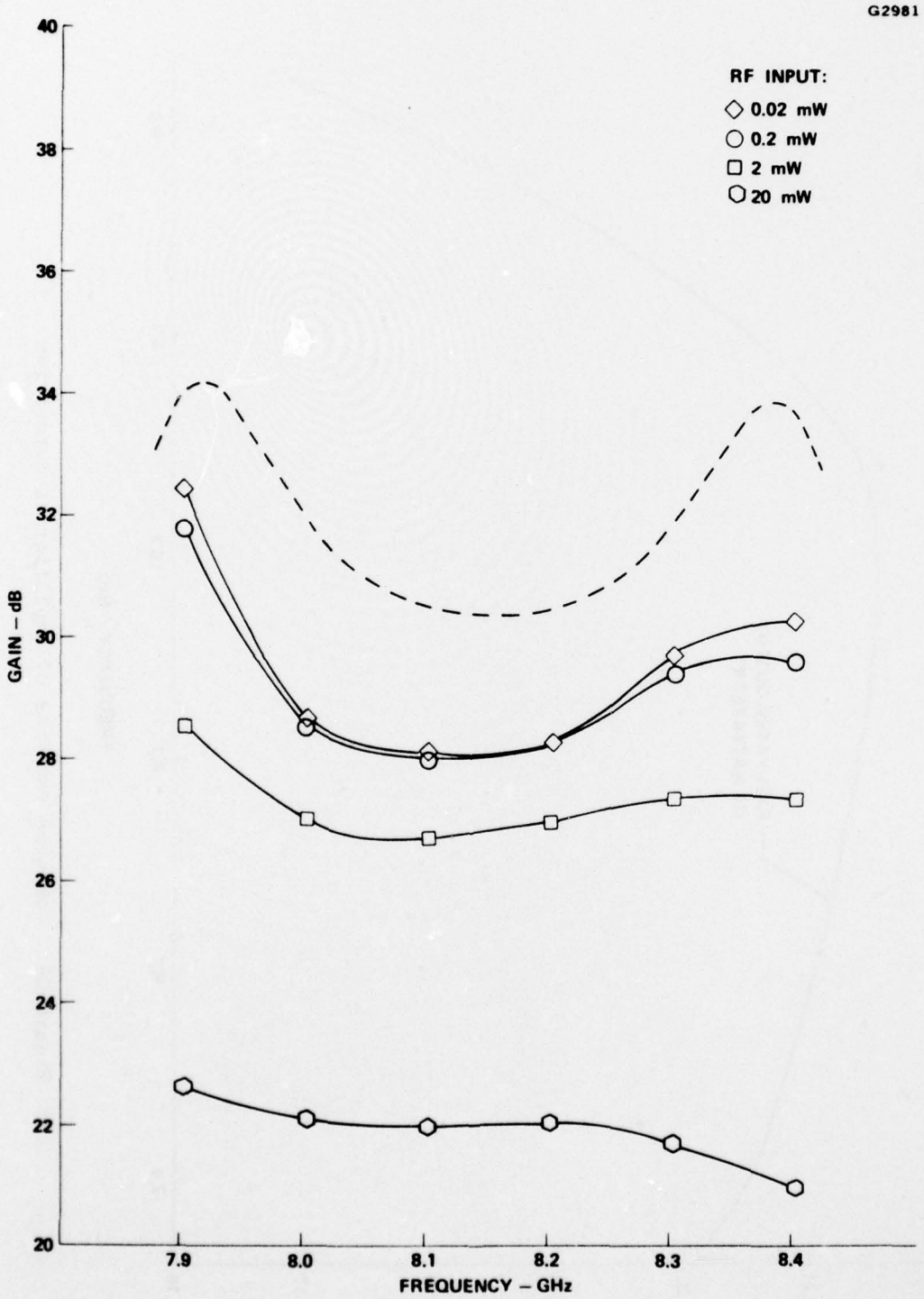

Figure 37 Gain of six driver stages.

covered throughout the operating region. The 20 mW drive level is approximately that necessary to drive the final amplifier to its saturated output. A substantial amount of gain compression occurred at these higher drive levels but with only a very small amount of frequency shift. For this reason the final amplifier was expected to maintain a flat gain characteristic over a very wide dynamic range which is unusual for IMPATT amplifiers. Amplifiers employing single drift diodes usually exhibit a substantial frequency shift between the small signal and saturated power levels.

The dashed line shown in Figure 37 is the calculated target gain response for the six driver stages at the 0.2 mW input power level. The measured gain is somewhat lower than the theoretical because the Q's of the coaxial and hybrid stages are slightly higher than those used in the computer model. The calculated and measured responses for the pair of hybrid stages alone was shown in Figure 28.

5.3 Assembly and Test of Complete Amplifier

Upon receipt of the output stage machined parts two combiners were assembled and tested as discussed in Section 2.11. Their composite response was shown in Figure 19. The combiners were then assembled into the final amplifier chassis along with the six driver stages. Photographs of the completed amplifier assembly (less cover) are shown in Figures 38 and 39. Figure 39 is a plan view of the amplifier assembly showing the relative locations of the various major components. (The "T" numbers are temperature measurement points referred to Section 6.4).

Figure 40 is a plot of the complete amplifier's gain response at the 1.5 watt output level. The figure shows that the 500 MHz bandwidth goal was not achieved. Upon comparison of Figures 19, 37 and 40 it is readily

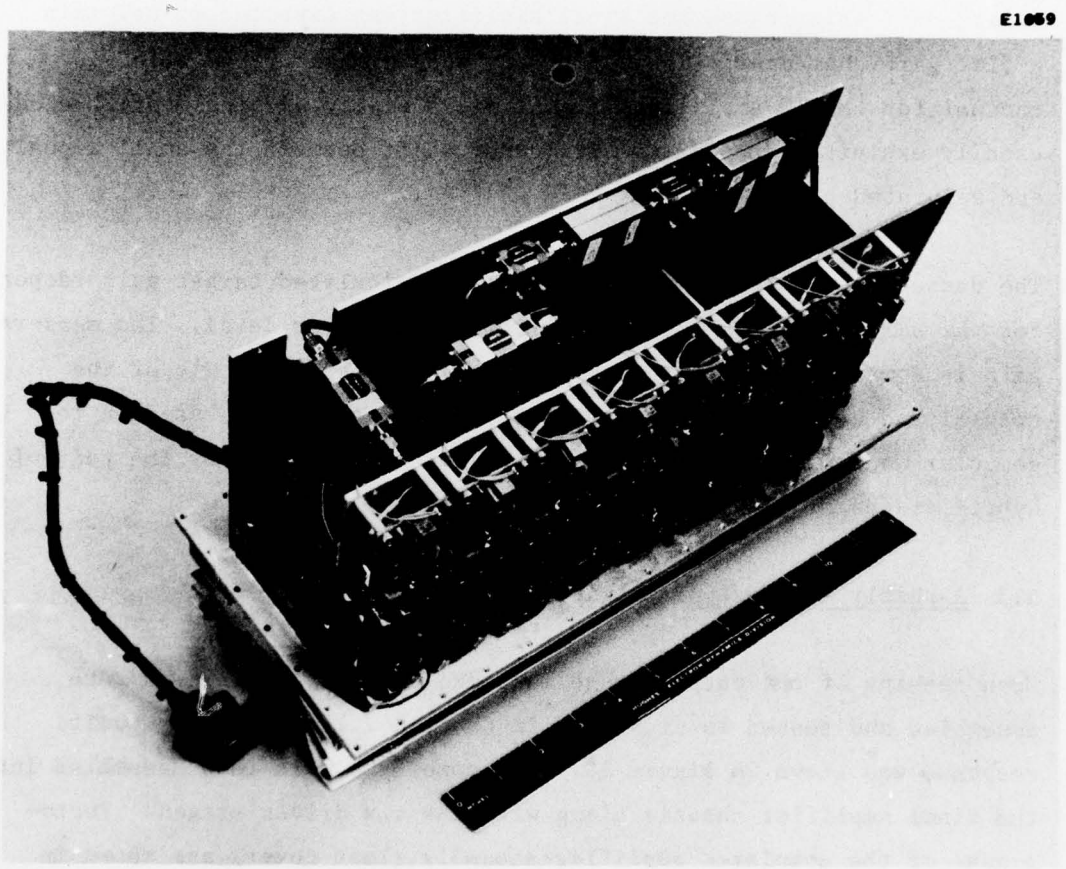

Figure 38. Eight stage amplifier assembly.

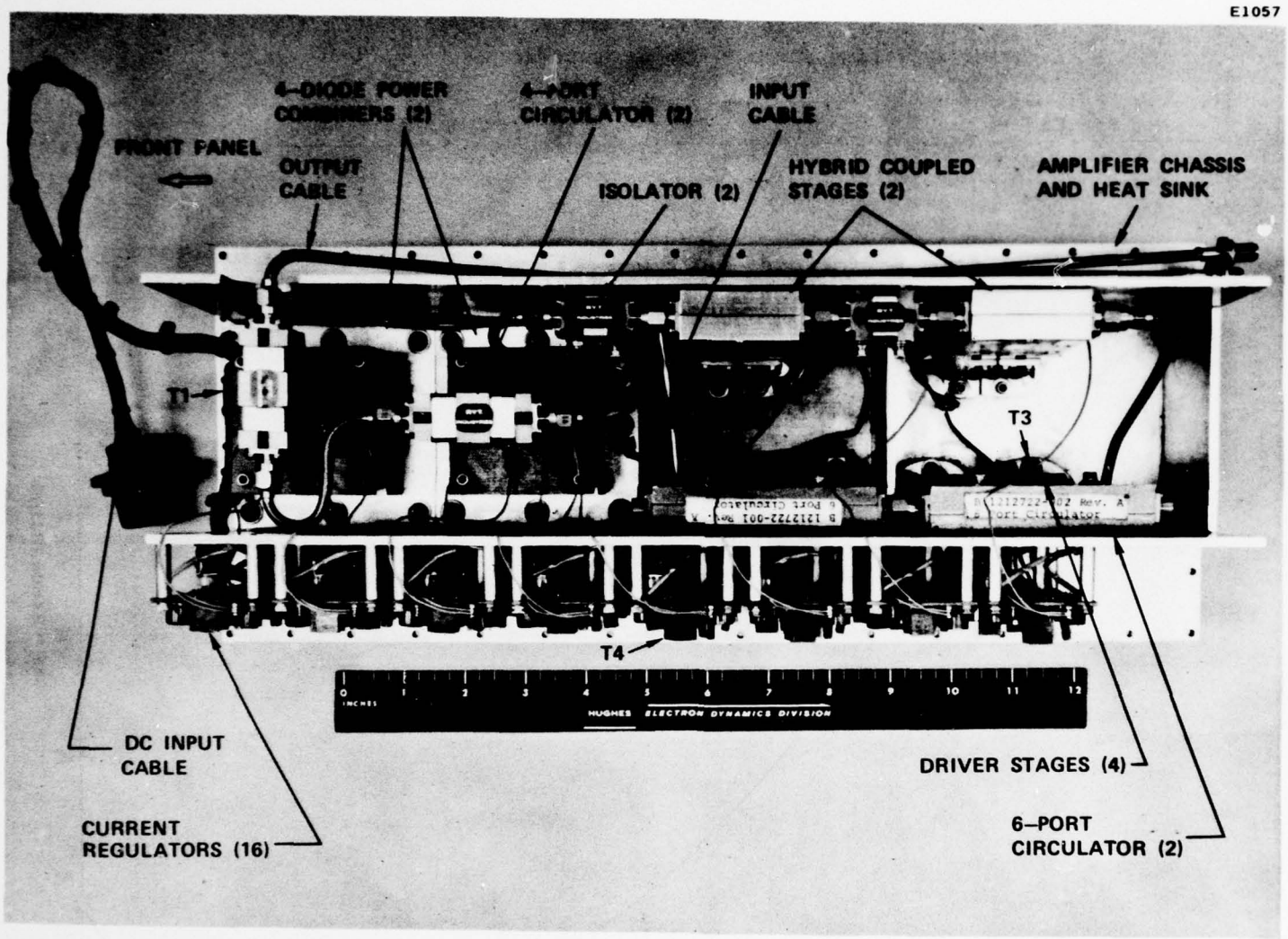

Figure 39 Plan view of eight stage amplifier assembly.

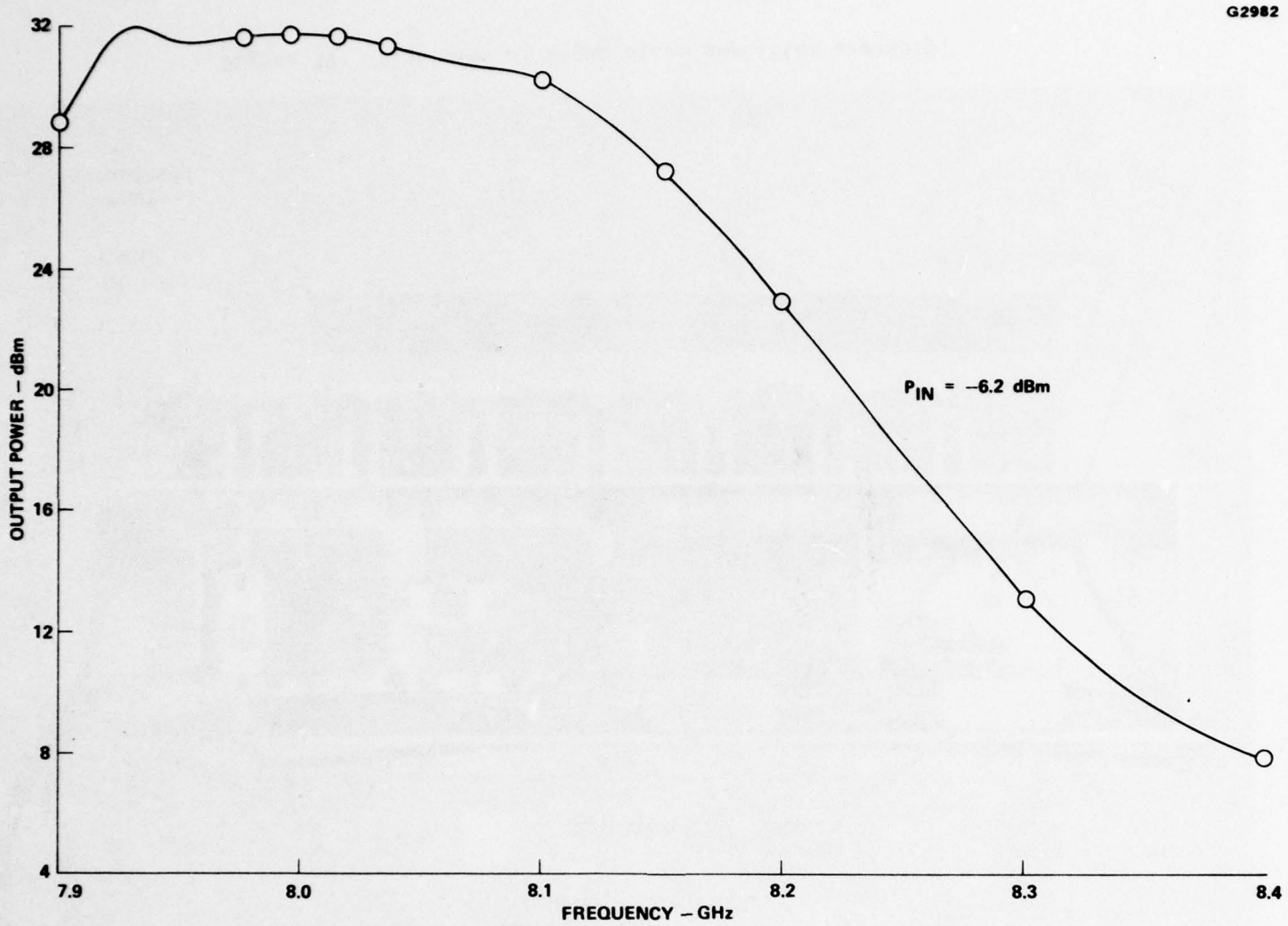

Figure 40 Amplitude response of eight-stage amplifier assembly.

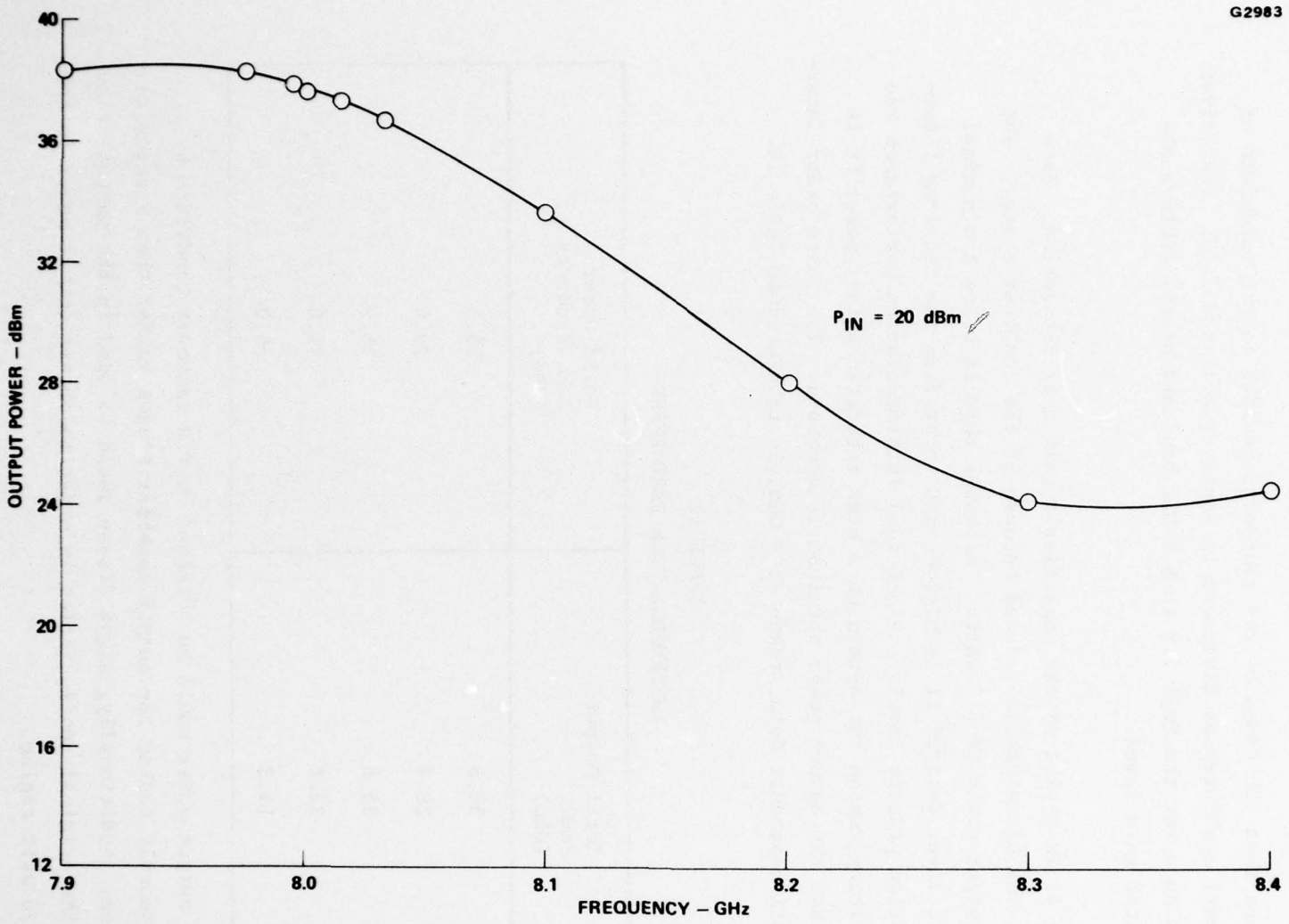

Figure 41 Amplitude response of eight-stage amplifier assembly near saturation.

apparent that the cause of the reduced bandwidth is the bandwidth of the power combiners as discussed in Sections 2.11 and 2.12. The driver stages do cover the full 7.9 to 8.4 GHz band and nearly achieve the predicted gain level.

Figure 41 is a plot of the amplifier's gain near saturation. Here again, the bandwidth is reduced because of the combiner stages. The peak output power is 6.7 watts. Although this is below the nominal 10 watt level desired it is high enough to produce the required intermodulation product levels. Since good intermodulation performance was the primary reason for obtaining a high saturated output power it is felt that the output power obtained is adequate. The third order intermodulation product data, taken at 8 GHz, is tabulated in Table 12.

TABLE 12

INTERMODULATION PERFORMANCE

Total Output Power (dBm)	Third Order I.M. Products (dBc)
31.8	16.5
28.8	20.5
25.8	25.0
22.8	30.0
19.8	35.0

Higher output power could be obtained over a narrower bandwidth by synchronously tuning the output combiner stages rather than stagger tuning them. Additionally, eight diodes could be used in the output stage as in the original configuration in order to obtain output power in the 15 to 20 watt region.

5.4 Engineering Design Test

An Engineering Design Test Plan was written during the first half of the program per the original specification. This test plan was generally followed during the final testing except that minor changes were made during the testing (with customer concurrence) as were made necessary by the specification revisions. The results of the final tests are included in Appendices A, B and C. Appendix A contains operating instructions and saturated output power data. Appendix B is a set of Engineering Design Test data sheets marked per revised specifications. Appendix C contains clarifications pertaining to the reduction of the test data in Appendix B and certain additional data not called for by the test plan.

It is felt that several observations should be made about the data in Appendices B and C.

1) The gain data of Paragraphs 4.3.1 and 4.3.2 is shown graphically in Figures 40 and 41.

2) The gain variation data (4.3.3) and phase linearity data (4.3.4) are shown on the data sheets as being considerably out of spec. However, it can be seen from the X-Y gain and phase plots (Appendix C, Sections 3.0, 4.0 and 14.0) that these worst case data points are bad because of the reduced bandwidth of the amplifier. Within the actual 1 dB bandwidth of the amplifier these variations are in fact quite small and generally within specification. The X-Y plots also show that the amplifier exhibits very little frequency shift with power level and operates over at least a 20 dB dynamic range.

3) The AM-PM conversion (4.3.5) and VSWR data (4.3.6 and 4.3.7) are within specification throughout the frequency band.

4) No spurious outputs (4.3.8) were observed. The second harmonic output is within specification without the use of a low pass filter.

5) The noise figure is within specification at 39 dB.

6) The hum modulation (4.3.11) is out of specification throughout the band and the residual AM modulation (4.3.10) is slightly out of specification at one frequency. These are both caused by high ripple on the 200 volt power supply and can be brought within specification by using an external laboratory supply with better regulation. It is recommended that any future units incorporate a voltage regulator after the 200 volt power supply even though efficiency would be slightly reduced.

7) Gain stability (4.3.12) is within specification. The slight variations measured were due to slight variations in ambient temperature.

8) The intermodulation product goal (4.3.13) was achieved within the amplifier's usable bandwidth.

9) Time remaining on the program did not allow for conductance of the prime power test (4.3.14) and the environmental test (5.0) with the exception of the high temperature test (5.5.1). This test simulates the high ambient temperature extremes expected in system operation. The X-Y plot in Appendix C, Sections 13.0 and 14.0, shows that only minor gain variations occur.

5.5 Low Pass Filter

A coaxial seven element low pass filter was designed and constructed for use with the final amplifier. It was designed to be removable from the amplifier should it not be required to optimize system performance. The filter (less connectors) is 0.5 inches in diameter and 0.52 inches in length. Its theoretically predicted attenuation and measured data points are shown in Figure 42. As can be seen, the insertion loss in the 7.9 to 8.4 band is 0.8 dB and the attenuation in the second harmonic frequency range is well over 40 dB.

As mentioned above, the harmonic content of the final amplifier is such that it was not necessary to incorporate this filter.

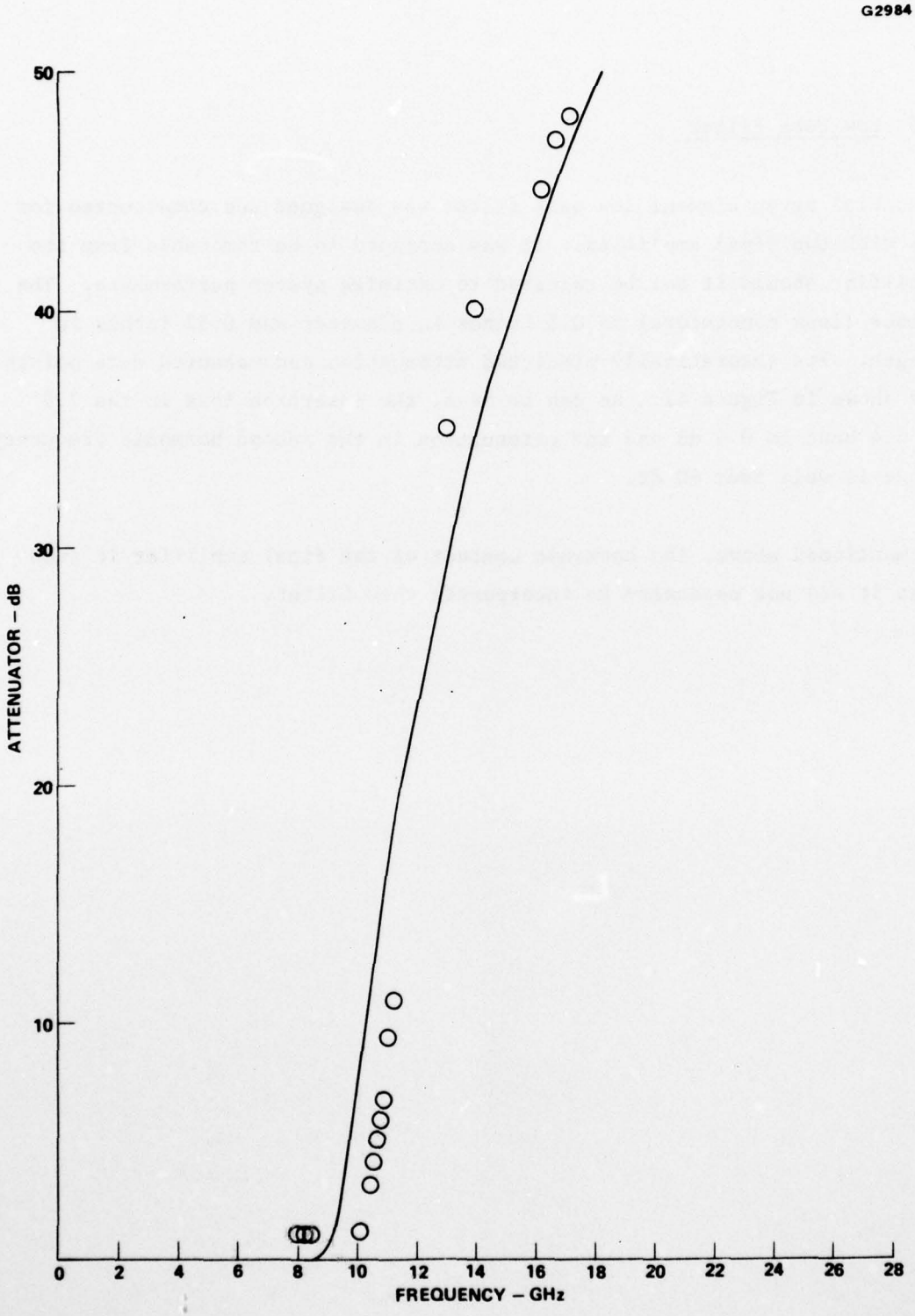

Figure 42 Attenuation of low pass filter.

6.0 TASK IV - POWER SUPPLY AND PACKAGING

6.1 Current Regulator Revision

Since double drift diodes operate at substantially higher voltages than single drift, the components in the existing current regulator design used at Hughes had to be correspondingly upgraded. This work was completed early in the program.

The revised regulator schematic is shown in the block designated R1 in Figure 43. These regulators attenuate the input voltage ripple by 40 dB and have a variable current versus temperature slope which can be set to track the temperature characteristics of the individual diodes. They also employ an over-temperature voltage limit and an over-voltage protection feature which shuts the regulators off if they experience an over-voltage or short circuit condition. Each regulator is individually fused to provide for a "gracefull failure" of the amplifier if an IMPATT should fail in the short circuit mode.

The regulators require a minimum voltage drop of 5 volts and will operate with up to 30 volts drop. In the delivered unit each regulator operates with 200 volts input and 180 to 184 volts output at 130 millamps. Thus, the power dissipated by each regulator is 2.0 to 2.6 watts.

6.2 Power Supply Design and Fabrication

Because the power dissipated by the IMPATT diodes and regulators is quite high (435 watts) it was decided that a high efficiency power supply would be needed to hold down the total power dissipation of the amplifier. Several approaches were considered and several discussions with outside vendors took place during the first month of the program regarding a high voltage, high efficiency power supply. A saturating

transformer design capable of 80% efficiency was decided upon and a power supply manufacturer contracted to do the power supply design and fabrication.

The major specifications of the supply are as follows:

Voltage	200 ±5% VDC
Current	2.8 amps DC max.
Power	560 watts
Input	120 VAC, 50/60 Hz
Efficiency	80% min.
Regulation	±1% from 1/2 to full load
Ripple	2 volts peak to peak
Size	6" x 6" x 12"
Protection	Fused to protect against short circuits

A schematic diagram of the power supply is shown in block PS1 of Figure 43, the overall amplifier schematic.

Some of the power supply test results supplied by the vendor are tabulated in Table 13.

TABLE 13

POWER SUPPLY DATA

V_{in} (AC)	V_o @ 2.8 A (DC)	Ripple @ 2.8 A (pk-pk)	Power Input @ 2.8 A (watts)	Full Load Efficiency (%)
107	201.2	2 V	680	82.8
127	202.0	2 V	820	68.9
115	201.8	2 V	750	75.3

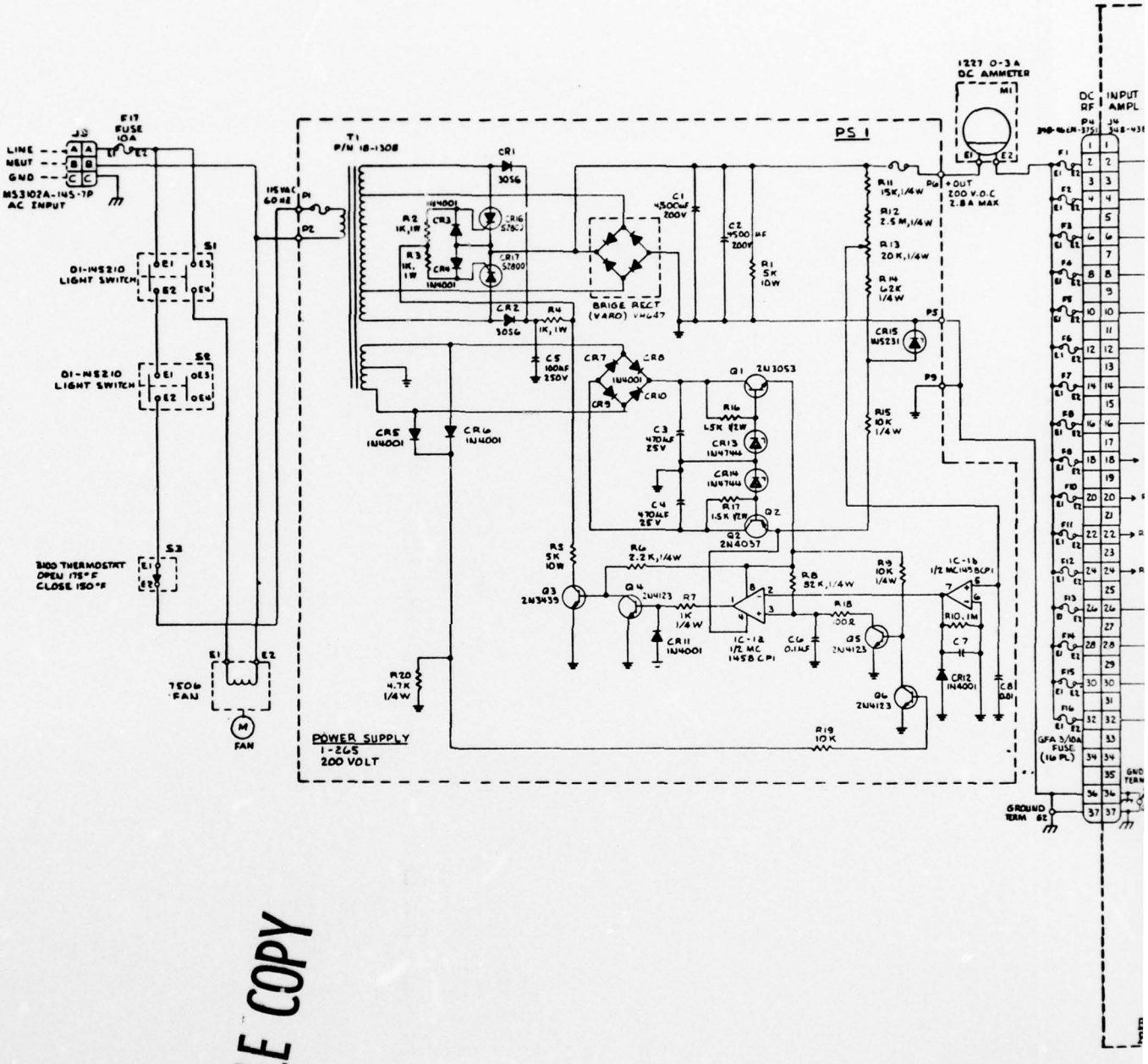

BEST AVAILABLE COPY

- (D) COMPONENT MOUNTED ON AMPLIFIER CHASSIS
- E. ALL CAPACTANCE VALUES ARE IN $\mu F \pm 10\%$, 200V
- I. ALL RESISTANCE VALUES ARE IN OHMS $\pm 5\%$, 1/8W
- NOTES: UNLESS OTHERWISE SPECIFIED

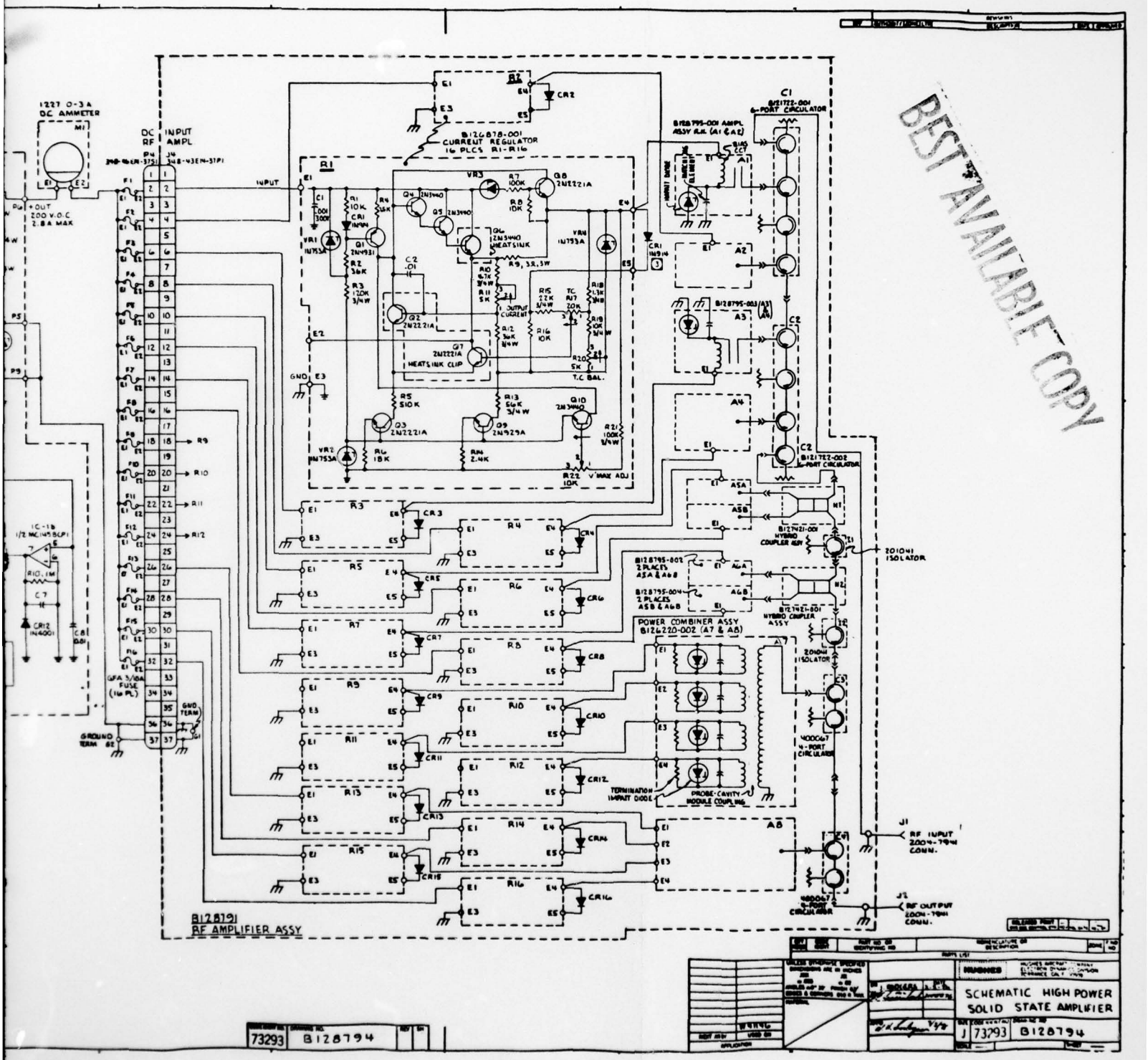

Figure 43 Schematic high power solid state amplifier.

AD-A047 503 HUGHES AIRCRAFT CO TORRANCE CALIF ELECTRON DYNAMICS DIV F/G 9/5
20 WATT SOLID STATE X-BAND POWER AMPLIFIER.(U)
JUN 76 W LOCKYEAR
UNCLASSIFIED EDD-W-41146-F ECOM-75-0023-F DAAB07-75-C-0023
NL

2 OF 2
AD
A047503

END
DATE FILMED
1 -78
DDC

The power supply was tested at Hughes with both resistor and current regulated IMPATT loads. Certain of the test results are shown in Figure 44. Curve 44a shows the ripple on the power supply's output voltage at less than full load (1.2 Amps). Curve 44b and 44c are plots of the voltage ripple at the output of one of the amplifier's current regulators with a double drift diode as a load and the ripple of curve 44a at the input. It can be seen that the regulator attenuates the ripple by approximately 40 dB which is consistent with other data taken on these regulators. In order to determine the effect of the ripple on RF performance an amplifier stage was biased with the above mentioned power supply and current regulator combination. The output power of the amplifier stage was measured with a power meter and its "recorder" output plotted on an expanded scale (curve 44d). This plot shows a 0.2 mV, peak to peak, ripple whose peaks are not strongly correlated to those of the regulator's ripple. The same regulator when powered by a laboratory supply had no measurable ripple (curve 44e). The ripple on the RF power meter signal, curve 44f, has approximately the same amplitude as that of curve 44d. Based on these measurements, it was not expected that the power supply ripple would have any adverse effects on RF performance.

It was found, however, in the final amplifier that current regulators do not attenuate the full load power supply ripple enough to meet the hum modulation specification. This is probably aggravated by the high gain multi-stage nature of the unit. It will therefore be necessary on any future amplifiers using this type of power supply to incorporate a voltage regulator between the power supply and the current regulators in order to attenuate the ripple an additional 30 dB. The voltage regulator would reduce the apparent power supply efficiency from 80% to approximately 75%.

E811

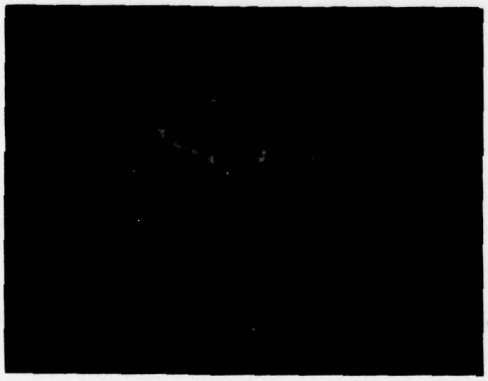

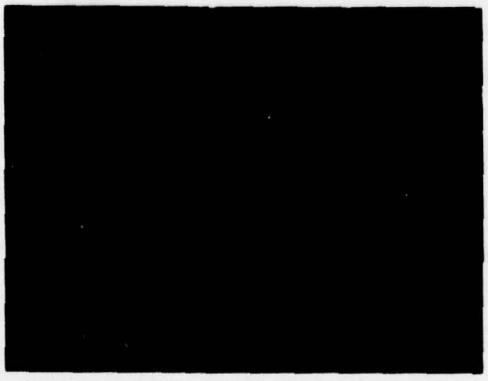

Figure 44 High voltage power supply ripple test results.

a. Power supply output voltage ripple with 1.2 A. load; .96 volts, pk-pk, 120 Hz.

b. Current regulator output voltage ripple with IMPATT load; 9 mV, pk-pk, 120 Hz.

c. Same as b.

d. Ripple on RF power meter output signal .2 mV, pk-pk.

e. Same as b. except with standard laboratory supply as source.

f. Ripple on RF power meter output signal; laboratory supply .2 mV, pk-pk.

6.3 Package Configuration

Photographs of the overall package configuration of the delivered amplifier are shown in Figures 45 and 46. Figure 45 shows the unit with the top covers in place while Figure 46 shows the relative locations of the major components. It can be seen that the RF amplifier assembly and 200 volt power supply are enclosed in a rack mounted case on opposite sides of a high capacity heat sink assembly in order to obtain maximum cooling. The RF and DC connectors are located on the back panel of the unit. Figure 47 is an outline and mounting drawing which details the unit's size and mounting nut and connector locations. The 16 regulator fuses are located between the front panel and the RF amplifier.

6.4 Thermal Calculations and Data

The general package configuration was determined early in the program primarily to determine thermal design parameters. The total power dissipation was originally calculated as follows:

P_{DC} into 14 diodes @ 28 W (worst case)	392 watts
Current regulator efficiency 90%, divided by 0.9	435 watts
Power supply efficiency 80%, divided by 0.8	544 watts
Fan (Pamotor 7506)	40 watts
Total AC Power Input, P_{AC}	584 watts

A standard heat sink extrusion was selected for use in the cooling duct which offers a very good combination of thermal properties and physical characteristics. According to data published by the manufacturer, the thermal resistance for a pair of these extrusions 6 inches long is

E1060

Figure 45 Packaged high power solid state amplifier.

E1061

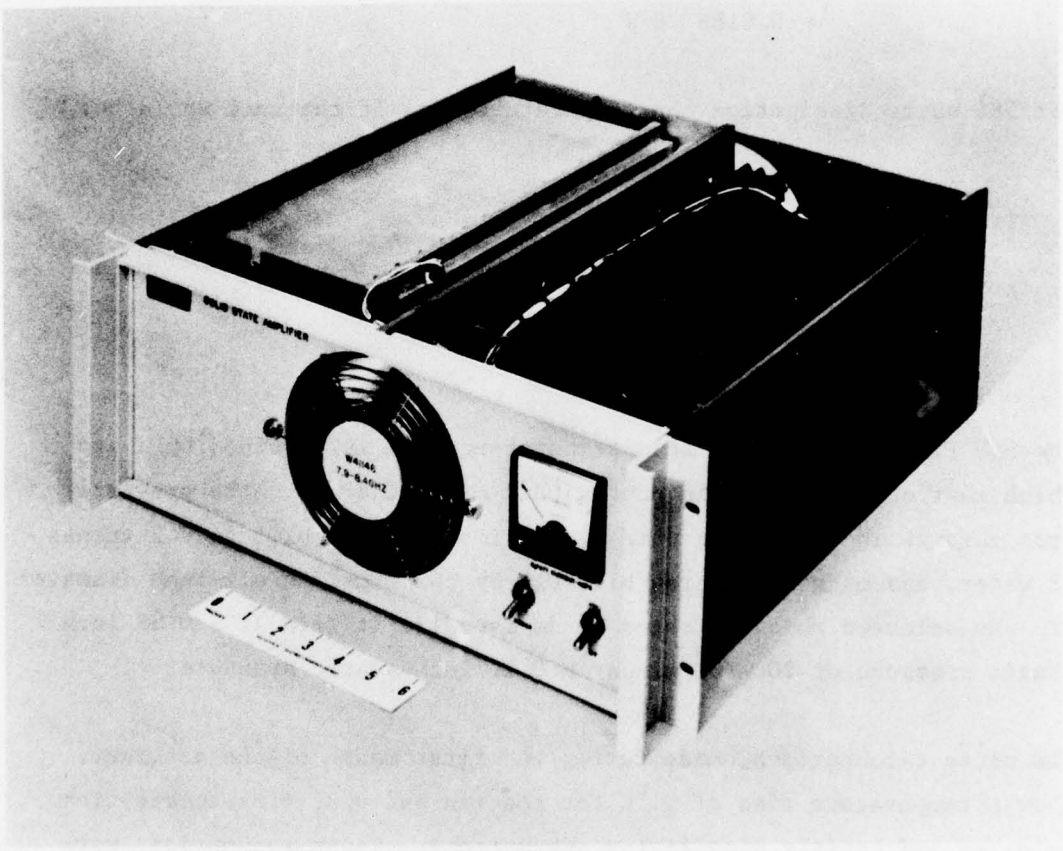

Figure 46 Major component locations; high power solid state amplifier.

0.05° C/W for 90 ft^3/min. ducted air flow. For a 12-inch length and 120 ft^3/min. air flow the thermal resistance would be approximately:

$$\theta = (0.05^{\circ}\ C/W)\left(\frac{90\ ft^3/min}{120\ ft^3/min}\right)\left(\frac{6''}{12''}\right)$$

$$= 0.0188^{\circ}\ C/W$$

For 584 watts dissipation the temperature rise of the unit would be:

$$\Delta T = \theta \times P_{AC}$$

$$\Delta T = (0.0188^{\circ}C/W)\ (584\ W)$$

$$= 10.95^{\circ}C$$

The air flow required for this temperature rise is provided by a fan which must operate into the ducted pair of heat sinks. The pressure drop through the heat sink pair was estimated to be 0.15 to 0.2 inches of water, assuming a 60% area blockage by the fins. A six-inch diameter fan was selected which is rated to deliver 120 ft^3/min at a 0.29 inch static pressure or 200 ft^3/min at a 0.20 inch static pressure.

The above calculations, made during the first month of the contract, show a temperature rise of $11^{\circ}C$ for the fan and heat sink combination selected and certain simplifying assumptions. These assumptions were (a) an even distribution of heat into the heat sink, and (b) a negligible rise in air temperature as it flows through the heat sink. These assumptions turned out to be somewhat different from actual operating conditions and the thermal calculations were subsequently revised. The amplifier layout as originally conceived had two power combiners located

PART NO.
B128793-001

SOLID STATE AMPLIFER
MFR: 73293 MOD: W41146
S/N 001
VOLTAGE: 120 VAC, 60Hz
CURRENT: 6A
RF FREQUENCY 7.9-8.4GHz

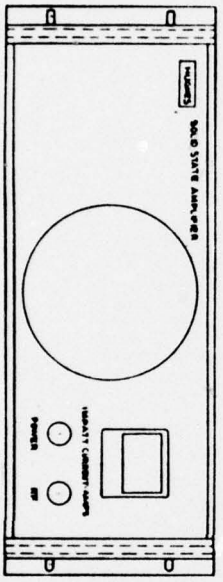

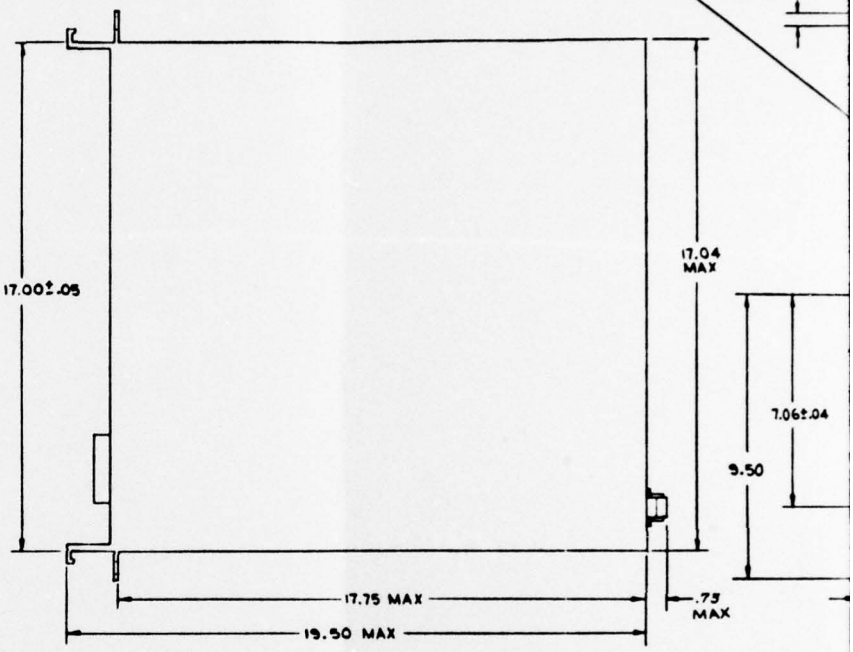

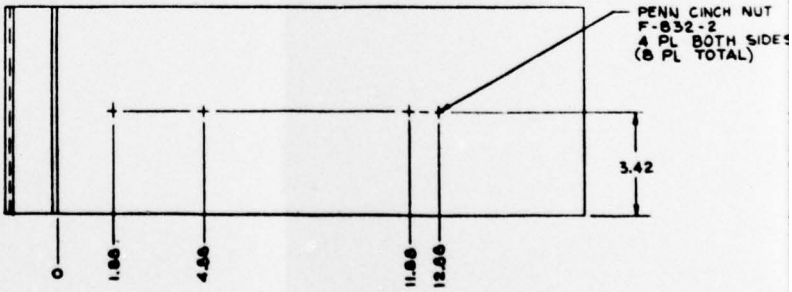

NOTES:

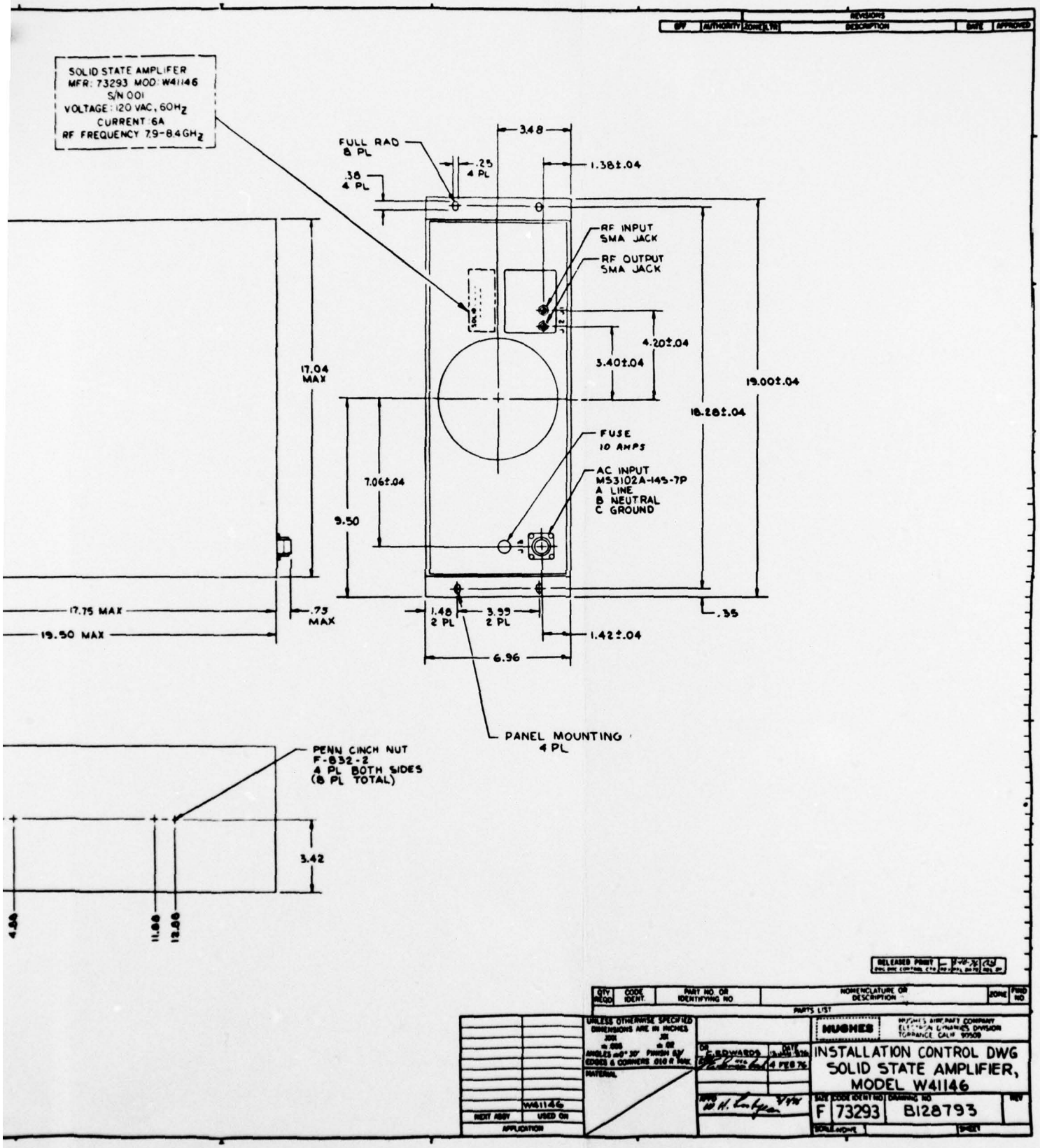

Figure 47 Outline and mounting of high power solid state amplifier.

near one end of one side of the heat sink and the power supply on the other side as shown in Figure 48a. The combiners, each occupying a 3 x 3 inch square, dissipate 372 watts (including regulator dissipation) into a six-inch length of one side of the heat sink. It was assumed that relatively little of this heat is conducted either to the other side of the heat sink or farther down the same side. Thus, all of this heat must be removed by this six-inch length on one side of the sink and the thermal impedance in this region is:

$$\theta_A = 2\ (0.05^\circ\ C/W)\left(\frac{90\ ft^3/min}{120\ ft^3/min}\right) = 0.075^\circ\ C/W$$

The temperature rise at point A is:

$$\Delta T_A = \theta_A \times 372\ W = 27.9^\circ C$$

The hybrid stage dissipates 62 watts in a three-inch length on one side of the heat sink. The thermal impedance in this region is:

$$\theta_B = 2(0.05^\circ\ C/W)\left(\frac{90\ ft^3/min}{120\ ft^3/min}\right)\left(\frac{6\ in}{3\ in}\right) = 0.150^\circ\ C/W$$

The temperature rise of this stage will be determined by θ_B plus the "induced thermal impedance" due to warming of the air flow by heat from the combiners. This additional thermal impedance, θ_I, was estimated to be 0.05° C/W. The temperature rise at point B is then calculated to be:

$$\Delta T_B = (\theta_B + \theta_I) \times 62\ W$$

$$= (0.15^\circ\ C/W + 0.05^\circ\ C/W) \times 62\ W = 12.4^\circ C$$

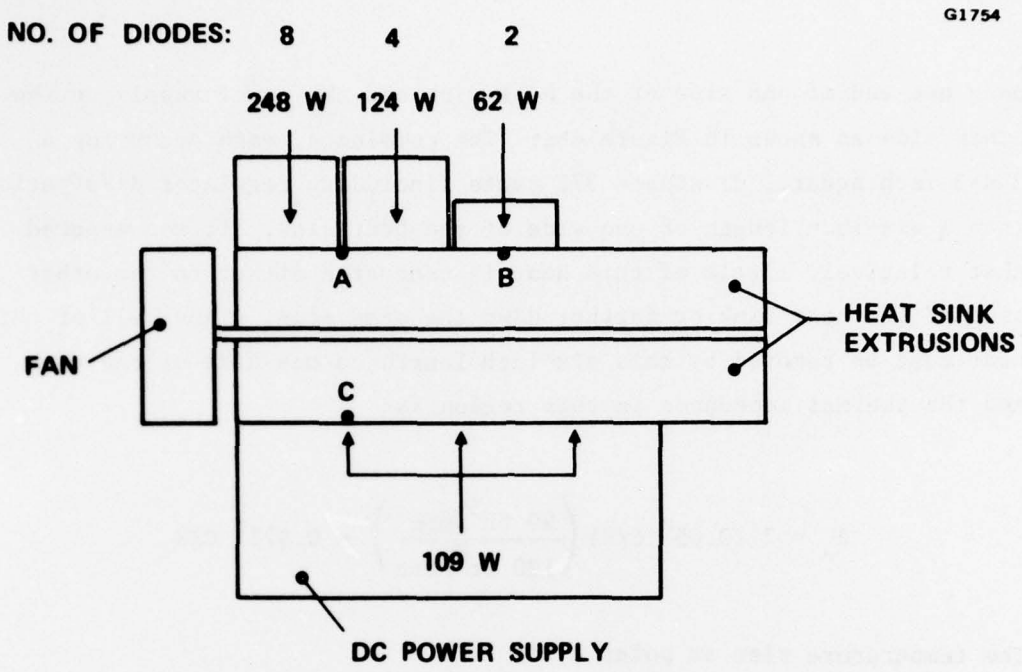

(a) ORIGINAL AMPLIFIER LAYOUT

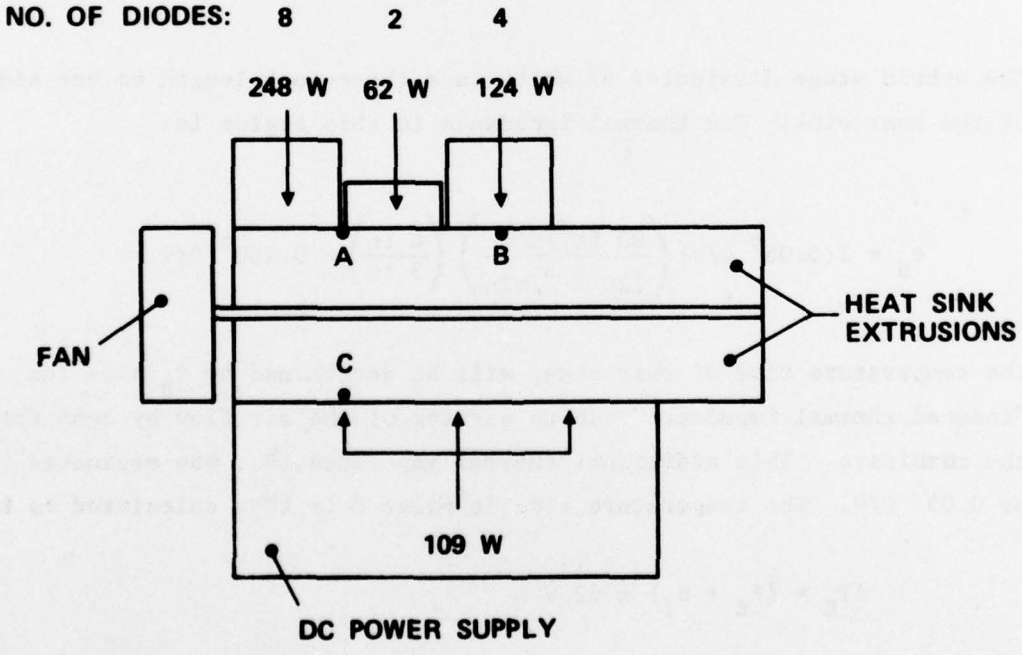

(b) REVISED AMPLIFIER LAYOUT

Figure 48

The power supply dissipates 109 watts over a twelve-inch length on the other side of the heat sink. Assuming no other significant heat paths, the thermal impedance in this region is:

$$\theta_C = 2(0.05^\circ \text{ C/W}) \left(\frac{90 \text{ ft}^3/\text{min}}{120 \text{ ft}^3/\text{min}}\right)\left(\frac{6 \text{ in}}{12 \text{ in}}\right)$$

$$= 0.0375^\circ \text{ C/W}$$

The temperature rise at point C is:

$$\Delta T_C = \theta_C \times 109 \text{ W} = 4.1^\circ\text{C}$$

Clearly the RF circuit side of the heat sink will operate hotter than the power supply side. It was thought that a heat pipe might be employed to conduct heat from one side to the other and more nearly equalize the temperatures. The calculations for a Hughes, EDD, Model 1370H, 0.5 inch diameter by 6 inch long heat pipe proceed as follows. The thermal impedance of the heat pipe including connections to the heat sink is $\theta_P = 0.40^\circ$ C/W. The temperature drop across the pipe is (initially):

$$\Delta T_P = \Delta T_A - \Delta T_C = 23.8^\circ\text{D}$$

The heat carried by the pipe is:

$$\frac{\Delta T_P}{\theta_P} = \frac{23.8^\circ\text{C}}{0.40^\circ \text{ C/W}} = 59.5 \text{ watts}$$

The temperature at points A and C are recalculated to be:

$$\Delta T_A' = (372\ W - 59.5\ W) \times 0.075^{\circ}\ C/W = 23.44^{\circ}C$$

$$\Delta T_C' = (109\ W + 59.5\ W) \times 0.0375^{\circ}\ C/W = 6.3^{\circ}C$$

These values for $\Delta T_A'$ and $\Delta T_C'$ are refined as follows:

$$\Delta T_P = \Delta T_A' - \Delta T_C' = 17.1^{\circ}D$$

$$\frac{\Delta T_P}{\theta_P} = \frac{17.12}{0.4} = 42.8 \text{ watts}$$

$$\Delta T_A' = (372 - 42.8) \times 0.075 = 24.7^{\circ}C$$

$$\Delta T_C' = (109 + 42.8) \times 0.0375 = 5.7^{\circ}C$$

Thus, the heat lowers the temperature at point B about $3^{\circ}C$. Additional heat pipes could be used but each one would have slightly less effect than the previous one because of the lessening difference between $\Delta T_A'$ and $\Delta T_C'$.

A six-inch diameter, 250 CFM fan and two fifteen-inch lengths of the heat sink extrusion used for the calculations were used for testing the thermal design early in the program. The fan was attached to one end at a variable distance from the heat sink. Cardboard shrouding was used for experimental purposes. Twelve 50 watt chassis-mount power resistors were attached to one side of the heat sink in an arrangement designed to simulate the power distribution of the RF circuitry. Three power resistors were mounted to the other side to simulate the power supply. The experimental and calculated temperatures are summarized in Table 14. The measured temperatures agree reasonably well with the

TABLE 14

HEAT SINK PERFORMANCE

CONDITIONS	TEMPERATURES, ^{o}C, $T_{AMB.} = 24^{o}C$					
	T_A	ΔT_A	T_B	ΔT_B	T_C	ΔT_C
Calculated Temperature Even heat distribution (240 Watts input, θ = .0188)	28.5	4.5	-	-	-	-
Measured Temperature Nearly even heat distribution (240 Watts input)	30.0	6.0	(θ = .0250)		-	-
Calculated Temperatures No heat pipe	51.9	27.9	36.4	12.4	28.1	4.1
Measured Temperatures No heat pipe						
(a) Fan at ¼" from heat sink No shroud	53	29	42	18	31.5	7.5
(b) Fan at ½" from heat sink No shroud	56	32	44	20	-	-
(c) Fan at ½" from heat sink With shroud	61	37	45	21	-	-
Calculated Temperatures With one heat pipe	48.7	24.7	-	-	29.7	5.7
Measured temperatures With heat pipe near 8-diode combiner						
(a) Fan at ¼" from heat sink No shroud	53	29	43	19	35	11
(b) Fan at ½" from heat sink No shroud	54	30	44	20	34.5	10.5
(c) Fan at ½" from heat sink With shroud	51.5	27.5	43.5	19.5	34	10
Revised Amplifier Layout (Figure 12b)						
Calculated Temperatures With one heat pipe	44.4	20.4	48.8	24.8	29.5	5.5
Measured temperatures With heat pipe near 8-diode combiner						
(a) Fan at ½" from heat sink No shroud	51.5	27.5	45	21	34	10
(b) Fan at ½" from heat sink With shroud	50	26	42	18	32	8

calculated ones although they are generally a few degrees higher. About half of the discrepancy can be explained by the fact that 480 watts and 120 watts were used in the experiments as the powers dissipated in the RF and power supply sides of the heat sink, respectively, whereas 434 watts and 109 watts were used in the calculations.

It was expected that the performance of the heat sink could be improved by changing the layout of the amplifier to that shown in Figure 48b. In this figure, the positions of the four-diode combiner and hybrid stage have been interchanged. (Additional cabling would be needed to reroute the RF energy flow.) The total power dissipated by the first six-inch length of heat sink is now 310 watts, hence.

$$\Delta T_A = 310\ W \times \theta_A = 23.3^{\circ}C$$

Similarly,

$$\Delta T_B = 124\ W \times (\theta_B + \theta_I) = 24.8^{\circ}C$$

ΔT_C remains unchanged at $4.1^{\circ}C$.

If a heat pipe is employed in this case, we take as an initial guess for ΔT_P,

$$\Delta T_P \approx 20^{\circ}C - 5^{\circ}C = 15^{\circ}C$$

Then,

$$\frac{\Delta T_P}{\theta_P} = \frac{15^{\circ}C}{0.4^{\circ}\ C/W} = 37.5\ \text{watts},$$

$$\Delta T_A' = (310 - 37.5) \times \theta_A = 20.4^{\circ}C$$

$$\Delta T_C' = (109 + 39.5) \times \theta_C = 5.5^{\circ}C$$

As a check,

$$T_P = 20.4 - 5.5 = 14.9^{\circ}C$$

Thus, rearranging the layout should lower the temperature of the 8-diode combiner by over $4^{\circ}C$. This change was checked by rearranging the simulation power resistors and measuring the heat sink temperatures. It was found that the temperature at the output stage was lowered by 1.5° to $2.5^{\circ}C$ (rather than 4° as predicted) with this arrangement. These measurements are shown in the bottom two lines of Table 14.

A series of tests was performed in a manner similar to those above except that the fan was reversed so as to pull air through the heat sink fins rather than pushing it. This was done to determine whether the more nearly laminar "pulled" airflow cools as effectively as the turbulent "pushed" flow. It was found that the "pulled" case gave consistently higher heat sink temperatures and that the difference was 2 to $14^{\circ}C$ depending on configuration and measurement location. Therefore the "pushed" configuration was used in the final amplifier.

The final eight amplifier layout is rather different than that shown in Figure 48b in that two four-diode combiners and two hybrid stages are used but no eight-diode stage is present. The final layout also has four driver stages. However, the total dissipation (435 watts) is the same and is more evenly distributed than in Figure 48b. Because of previous calculations and measurements it was deemed unnecessary to repeat them for this layout. No heat pipe was used in the final unit

because it was felt that the small improvement achieved did not warrant the extra mechanical complication. The temperatures actually obtained in the final amplifier are as follows (referring to Figure 39):

T1) Temperature near output combiner, stage 8: 51°C

T2) Temperature between first combiner, stage 7 and second hybrid, stage 6: 45°C

T3) Temperature near last driver, stage 4: 42°C

T4) Case temperature measured at edge of base plate: 43°C

6.5 Reliability Mathematical Model

A realibility mathematical model of the amplifier was constructed based on the schematics and parts lists for the power supply, the current regulators and the revised eight-stage RF amplifier configuration.

The reliability estimate for the W-41146 Amplifier indicates a MTBF of 30,392 hours. The amplifier consists of 16 current regulators, one power supply, and some miscellaneous components (16 IMPATT diodes, 6 four-port circulators, 3 isolators, and a fan).

The mathematical model for this estimate is a series dependent model: that is, the failure of any one component is considered a system failure. This type of model provides the most conservative estimate of unit MTBF. Such a model can be expressed mathematically as:

$$R_T = e^{-\lambda_T T_T} = \prod_{i=1}^{i=T} \left(e^{-\lambda_i T_i} \right)$$

where

R_T = total unit reliability

T_T = total unit operating time which equals T_i (all on all the time)

λ_T = total unit failure rate, equals summation of λ_i

T_i = individual part on time

λ_i = individual piece part failure rate

since

$$\lambda_T = \Sigma \lambda_i$$

and by definition

$$\text{MTBF Total} = \frac{1}{\lambda_T} = \frac{1}{\Sigma \lambda_i}$$

The unit MTBF is equal to the reciprocal of the sum of the piece part failure rates. The failure rate of each assembly is summarized below.

ASSEMBLY	$\lambda(10^{-6})$	QTY	TOTAL λ (10^{-6})
Current Regulator	0.951	16	15.216
Power Supply	4.987	1	4.987
Miscellaneous Components	12.700	1	12.700
			32.903

The MTBF for the Amplifier is as follows:

$$MTBF = \frac{1}{\lambda} = \frac{1}{32.903 \times 10^{-6}} = 30,392$$

7.0 CONCLUSIONS

Technical problems encountered with the gain-bandwidth performance of the power combiner and earlier delays due to late delivery of vendor supplied IMPATT diodes made it impossible to achieve the original program goals within the time frame allowed. The bandwidth of the power combiner was improved but not enough to meet the full specifications of the contract. It was therefore necessary to re-evaluate the program goals and alter the program objectives according to one of the alternatives discussed in Section 5.1. These were, briefly:

1) Build two 20 watt, 14 dB gain, narrow band amplifiers.

2) Build one full bandwidth amplifier, optimized at 1.5 watts output as a linear TWT driver, having a saturated output of approximately 10 watts.

3) Solve the bandwidth problem first and complete the original program on additional funding.

Most of the program objectives, revised per alternative number 2 above, were basically achieved with the major exception of bandwidth. The bandwidth restrictions are due to the Q's of the IMPATT diodes, the gain-bandwidth of the power combiners and the failure of the combiners to stagger-tune as predicted. The saturated power output, although lower than the specified nominal of 10 watts, is high enough to achieve the required intermodulation performance. The flatness of the gain and phase responses are reasonably good within the amplifier's usable bandwidth. The 20 dB dynamic range requirement was achieved. The hum modulation is somewhat high but could be brought into specification with better power supply regulation. Although complete environmental

qualification was not completed the amplifier's performance over the limited temperature range expected in system operation was verified.

All of the major circuit development tasks were completed. An existing power combiner design was scaled to 8 GHz and power combination of several devices successfully demonstrated with deliverable hardware. The full gain-bandwidth requirements of the combiners were not realized due to both device and circuit limitations. A hybrid-coupled stage was designed which successfully combines the outputs of two diodes. A high efficiency 200 volt power supply was developed. The thermal and packaging problems associated with the amplifier were solved.

8.0 RECOMMENDATIONS

This report has shown that the primary technical problem encountered in the program was the bandwidth of the power combiners. It has been shown that although the bandwidth of the combiners was improved during the course of the program, the full gain-bandwidth potential has not yet been achieved. It is therefore recommended that further work be undertaken to improve the combiner's bandwidth and that the work be concentrated in three main areas:

1) IMPATT diode Q. A device program should be undertaken to improve the Q of the high power double drift diodes while maintaining power, power linearity and frequency linearity comparable to those of the present diodes. This is the most important single improvement needed and would improve the performance of every stage in the amplifier, not just the combiners.

2) Probe-cavity-coax coupling Q. A much more extensive theoretical and experimental program should be undertaken to reduce this Q by at least a factor of 2.

3) Stabilizing termination. A program should be undertaken to optimize the value, position and configuration of the stabilizing termination taking into account bandwidth, the amount of stabilization needed and the numerous other trade-offs involved.

Other recommendations for improvement of the existing design include:

Install a voltage regulator between the power supply and the current regulators in order to reduce hum modulation.

Reduce the specified temperature range to $0^{o}C$ to $50^{o}C$. This would eliminate the need for the temperature-sloping feature of the current regulators and significantly reduce their parts count.

Certain manufacturing improvement techniques should be implemented to reduce size and weight and lower costs.

With these recommendations implemented it is believed that the solid state amplifier in basically its present form could become a viable alternative to the TWT intermediate power amplifier.

9.0 REFERENCES

1. "Microwave Power Combinatorial Development." Interim Rept., 15 January 73 through 14 July 73. R. Harp and K. Russell, Hughes Research Labs, Malibu, CA. F33615-73-C-1056

2. R. S. Harp and H. L. Stover, "Power Combining of X-band IMPATT Circuit Modules." International Solid State Circuit Conference, Philadelphia, February 14-16, 1973.

3. W. J. Getsinger, "Prototype for use in Broadbanding Reflection Amplifiers," IEEE Trans. on MTT, MTT-11, pp. 486-497, Nov. 1963.

4. G. L. Mattaei, L. Young, and E. M. T. Jones, "Microwave Filters, Independence Matching Networks, and Coupling Structures," McGraw Hill Book Company, Inc., New York, 1964.

TEST AND DEMONSTRATION REPORTS

APPENDIX

A	DATA AND OPERATING INSTRUCTIONS
B	ACCEPTANCE TEST DATA SHEETS
C	SUPPLEMENTARY DATA

APPENDIX A

DATA AND OPERATING INSTRUCTIONS

APPENDIX A

HUGHES MODEL W41146

X-BAND SOLID STATE AMPLIFIER

DATA AND OPERATING INSTRUCTIONS

SALES ORDER NUMBER: W-41146

SERIAL NUMBER: 001

DATE: 22 March 1976

1.0 OPERATING INSTRUCTIONS:

1.1 Rack Mounting:

The amplifier is designed for bench or a standard rack mount configuration. The unit is 7.0 inches in height and requires side mounted rails for installation. Adapters and cables are provided for connection to the system waveguide ports.

1.2 Environmental Limitations:

The amplifier is designed to operate in a temperature environment from $-18^{o}C$ to $52^{o}C$. Precautions must be taken not to block the air outlet at the rear of the unit.

1.3 Power Requirements:

For the protection of operating personnel, the National Electrical Manufacturer's Association (NEMA) recommends that the instrument panel and cabinet be grounded. The instrument is grounded when its three conductor power cable is plugged into a U blade receptacle (Power connector Pin C). Power requirements are 120 Vac ± 10%, 50 to 60 Hz at 6 amps maximum. Actual power consumption is approximately 600 watts.

Turn the power and RF switches on and allow approximately one minute for the power supplies to achieve full voltage and the microwave diodes to achieve thermal equilibrium. Check the Impatt Current meter to verify that it is registering a current consistent with that recorded in the data of Section 2.0. A substantial deviation from this current (6%) would indicate that one of the diodes is not operating. Small deviations (2-3%) may occur due to changes in ambient temperature.

Once the amplifier is operating, a large system bias transient can cause one or more of the internal regulators to turn off. If this

occurs, turn the amplifier off, wait one to two minutes for the power supply voltages to return to zero, then turn the unit back on.

1.4 RF Port Loading:

Although the amplifier will operate into any VSWR without damage, it is recommended that the RF input and output ports be terminated with a VSWR less than 1.5:1 when the amplifier is operating.

1.5 RF Power Input:

The amplifier is designed to operate with an RF input power of 20 dBm or less at frequencies between 7.9 and 8.4 GHz. The unit can be driven with higher power levels (up to 30 dBm) without damage but at input power levels above 20 dBm degradation of its performance may result.

2.0 DATA:

2.1 Currents:

Total Impatt Diode Current: 2.18 Amps

2.2 Frequency Response (RF Power Input = 20 dBm):

Frequency (GHz)	7.9	8.0	8.1	8.2	8.3	8.4
RF Output Power (W)	6.69	5.71	2.33	.64	.26	.28
Gain (dB)	18.3	17.6	13.7	8.0	4.1	4.5

APPENDIX B

ACCEPTANCE TEST DATA SHEETS

HUGHES AIRCRAFT COMPANY

ELECTRON DYNAMICS DIVISION

3100 West Lomita Boulevard, Torrance, California 90509. Tel (213) 534-2121

DATA SHEET NO. DSB126546 M/P

PRODUCT Solid State Amp

MODEL W-41146

PART NO.

APPENDIX B

ACCEPTANCE TEST DATA SHEET

CODE IDENT. 73293

TEST NAME	SPEC. No.	TEST POS. No.	SERIAL No.
Engineer Design Test	EDTB126546	193013	001

REV.	AUTHORITY	DATE	APPROVAL	REV.	AUTHORITY	DATE	APPROVAL

QUALITY: J. J. Haupt

DATE OF ISSUE: 4 September 1975

EFFECTIVITY:

ITEM	SPEC. PAR. No.	TEST DESIGNATION	TEST CONDITION / DESCRIPTION	R/C	MIN.	DATA	MAX.	UNITS
	4.0		INITIAL FUNCTIONAL TEST					
	4.2	Visual and Mechanical Inspection	Inspect for compliance with Applicable drawing	C	--		--	--
			Weight	R	--		--	lbs
	4.3.1	Rated Output Power vs. Frequency	Steps 1-2 Ein (ac) = 120V ± 10%					
			F = 7.9 GHz; Po = ~~20~~ 1.5 W Pi(rf)	R	--	0.33	~~196~~ 100	mW
			F = 8.0 GHz; Po = ~~20~~ 1.5 W Pi(rf)	R	--	0.33	~~196~~ 100	mW
			F = 8.1 GHz; Po = ~~20~~ 1.5 W Pi(rf)	R	--	1.36	~~196~~ 100	mW
			F = 8.2 GHz; Po = ~~20~~ 0.64 W Pi(rf)	R	--	77.6	~~196~~ 100	mW
			F = 8.3 GHz; Po = ~~20~~ 0.24 W Pi(rf)	R	--	77.6	~~196~~ 100	mW
			F = 8.4 GHz; Po = ~~20~~ 0.17 W Pi(rf)	R	--	77.6	~~196~~ 100	mW
			Steps 3-4 Ein (ac) = 120V ± 10%					
			F = 7.9 GHz; Pi(rf) = ~~196~~ 100 mW Po	R	~~20~~	6.69	--	W
			F = 8.0 GHz; Pi(rf) = ~~196~~ 100 mW Po	R	~~20~~	5.71	--	W

EDD 1045 REV JUN74

PRECEDING PAGE BLANK-NOT FILMED

HUGHES ELECTRON DYNAMICS DIVISION
3100 West Lomita Boulevard, Torrance, California 90509, Tel (213) 534-2121

DATA SHEET NO. DSB126546
REV.
SERIAL NO. 001

ACCEPTANCE TEST DATA SHEET

CODE IDENT. 73293

ITEM	SPEC PAR. No	TEST DESIGNATION	TEST CONDITION / DESCRIPTION	R/C	MIN.	DATA	MAX.	UNITS
	4.3.1	Rated Output Power vs. Frequency (Cont.)	Steps 3-4 Ein (ac) = 120V ± 10%					
			F = 8.1 GHz; Pi(rf) = ~~296~~ 100 mW Po	R	~~20~~ -	2.33	--	W
			F = 8.2 GHz; Pi(rf) = ~~296~~ 100 mW Po	R	~~20~~ -	0.64	--	W
			F = 8.3 GHz; Pi(rf) = ~~296~~ 100 mW Po	R	~~20~~ -	0.26	--	W
			F = 8.4 GHz; Pi(rf) = ~~296~~ 100 mW Po	R	~~20~~ -	0.28	--	W
			Step 5 T amb	R	65	75	85	°F
	4.3.2	Gain versus Frequency at Saturation	Calculate gain at rated Po(~~20W~~ 1.5)					
			G at F = 7.9 GHz	R	~~14~~ 38	36.6	--	dB
			F = 8.0 GHz	R	~~14~~ 38	36.6	--	dB
			F = 8.1 GHz	R	~~14~~ 38	30.4	--	dB
			F = 8.2 GHz	R	~~14~~ 38	-	--	dB
			F = 8.3 GHz	R	~~14~~ 38	-	--	dB
			F = 8.4 GHz	R	~~14~~ 38	-	--	dB
			Calculate gain at max Pi(rf)					
			G at F = 7.9 GHz	R	~~14~~ -	18.3	--	dB
			F = 8.0 GHz	R	~~14~~ -	17.6	--	dB
			F = 8.1 GHz	R	~~14~~ -	13.7	--	dB
			F = 8.2 GHz	R	~~14~~ -	8.0	--	dB
			F = 8.3 GHz	R	~~14~~ -	4.1	--	dB
			F = 8.4 GHz	R	~~14~~ -	4.5	--	dB

HUGHES **ELECTRON DYNAMICS DIVISION**

3100 West Lomita Boulevard, Torrance, California 90509 Tel (213) 534-2121

DATA SHEET NO. DSB126546

REV.

SERIAL NO. 001

ACCEPTANCE TEST DATA SHEET

CODE IDENT 73293

ITEM	SPEC PAR. No	TEST DESIGNATION	TEST CONDITION / DESCRIPTION	R/C	MIN	DATA	MAX	UNITS
	4.3.3	Gain Variation	Ein (ac) = 120V ± 10% Pi(rf) adj for rated Po at F = 7962 MHz F = 7900 to 8025 MHz					
			G(var) w.c. (40 MHz)	R	--	± 1.5	±0.15	dB
			G(var) w.c. (125 MHz)	R	--	± 1.5	±0.25	dB
			Pi(rf) adj for rated Po at F = 8337 MHz F = 8275 to 8400 MHz					
			G(var) w.c. (40 MHz)	R	--	± 1.7	±0.15	dB
			G(var) w.c. (125 MHz)	R	--	± 3.3	±0.25	dB
			Freq varied ± 63 MHz in region exhibiting greatest gain variation					
			G(var) w.c. (40 MHz)	R	--	± 1.7	±0.15	dB
			G(var) w.c. (125 MHz)	R	--	± 3.3	±0.25	dB
			Center freq w.c.	R	7962	8337	8337	MHz
			Pi(rf) adj for Po = ~~200~~ 15 mW at F = 7962 MHz F = 7900 to 8025 MHz					
			G(var) w.c. (40 MHz)	R	--	± 1.6	±0.15	dB
			G(var) w.c. (125 MHz)	R	--	± 1.7	±0.25	dB
			Pi(rf) adj for Po = ~~200~~ 15 mW at F = 8337 MHz F = 8275 to 8400 MHz					
			G(var) w.c. (40 MHz)	R	--	—	±0.15	dB
			G(var) w.c. (125 MHz)	R	--	—	±0.25	dB

HUGHES ELECTRON DYNAMICS DIVISION
3100 West Lomita Boulevard, Torrance, California 90509, Tel (213) 534-2121

DATA SHEET NO. DSB126546
REV.
SERIAL NO. 001

ACCEPTANCE TEST DATA SHEET

CODE IDENT 73293

ITEM	SPEC. PAR. No.	TEST DESIGNATION	TEST CONDITION / DESCRIPTION	R/C	MIN.	DATA	MAX.	UNITS
	4.3.3	Gain Variation (Cont.)	Freq varied ± 63 MHz in region exhibiting greatest gain variation					
			G(var) w.c. (40 MHz)	R	--	± 2.5	±0.15	dB
			G(var) w.c. (125 MHz)	R	--	± 5.0	±0.25	dB
			Center freq w.c.	R	7962	8163	8337	MHz
			Pi(rf) adj for Po between 200 mW and 20 W which exhibits greatest gain variation at F = 7962 MHz F = 7900 to 8025 MHz					
			G(var) w.c. (40 MHz)	R	--	± 1.6	±0.15	dB
			G(var) w.c. (125 MHz)	R	--	± 1.7	±0.25	dB
			Po	R	~~0.2~~ 15	15	~~20~~ 1500	mW
			Pi(rf) adj for Po between 200 mW and 20 W which exhibits greatest gain variation at F = 8337 MHz F = 8275 to 8400 MHz					
			G(var) w.c. (40 MHz)	R	--	± 2.1	±0.15	dB
			G(var) w.c. (125 MHz)	R	--	± 3.7	±0.25	dB
			Po	R	~~0.2~~ 15	150	~~20~~ 1500	mW
			Freq varied ± 63 MHz in region exhibiting greatest gain variation					
			G(var) w.c. (40 MHz)	R	--	± 2.5	±0.15	dB
			G(var) w.c. (125 MHz)	R	--	± 5.0	±0.25	dB
			Po	R	~~0.2~~ 15	15	~~20~~ 1500	mW
			Center freq (w.c.)	R	7962	8163	8337	MHz
			T amb	R	65	75	85	°F

DATA SHEET NO. DSB126546
REV.
SERIAL NO. 061

ACCEPTANCE TEST DATA SHEET

CODE IDENT 73293

ITEM	SPEC PAR. No.	TEST DESIGNATION	TEST CONDITION / DESCRIPTION	R/C	MIN.	DATA	MAX.	UNITS
	4.3.4	Phase Linearity	Ein (ac) = 120V ± 10% Pi(rf) adj for rated Po at F = 7962 MHz F = 7900 to 8025 MHz					
			$\frac{\Delta\angle}{\Delta F}$ w.c. (40 MHz)	R	--	± 5	±1	deg
			$\frac{\Delta\angle}{\Delta F}$ w.c. (125 MHz)	R	--	± 8	±3	deg
			Pi(rf) adj for rated Po at F = 8337 MHz F = 8275 to 8400 MHz					
			$\frac{\Delta\angle}{\Delta F}$ w.c. (40 MHz)	R	--	± 6	±1	deg
			$\frac{\Delta\angle}{\Delta F}$ w.c. (125 MHz)	R	--	± 15	±3	deg
			Freq varied ± 63 MHz in region exhibiting greatest phase deviation from linear					
			$\frac{\Delta\angle}{\Delta F}$ w.c. (40 MHz)	R	--	± 6	±1	deg
			$\frac{\Delta\angle}{\Delta F}$ w.c. (125 MHz)	R	--	± 15	±3	deg
			Center freq (w.c.)	R	7962	8337	8337	MHz
			Pi(rf) adj for Po = ~~200~~ 15 mW at F = 7962 MHz F = 7900 to 8025 MHz					
			$\frac{\Delta\angle}{\Delta F}$ w.c. (40 MHz)	R	--	± 5.5	±1	deg
			$\frac{\Delta\angle}{\Delta F}$ w.c. (125 MHz)	R	--	± 9.5	±3	deg

HUGHES ELECTRON DYNAMICS DIVISION
3100 West Lomita Boulevard, Torrance, California 90509, Tel (213) 534-2121

DATA SHEET NO. DSB126546
REV.
SERIAL NO. 001

ACCEPTANCE TEST DATA SHEET

CODE IDENT. 73293

ITEM	SPEC. PAR. No.	TEST DESIGNATION	TEST CONDITION / DESCRIPTION	R/C	MIN.	DATA	MAX.	UNITS
	4.3.4	Phase Linearity (Cont.)	Pi(rf) adj for Po = ~~200~~ 15 mW at F = 8337 MHz F = 8275 to 8400 MHz					
			$\frac{\Delta\phi}{\Delta F}$ w.c. (40 MHz)	R	--	± 18	±1	deg
			$\frac{\Delta\phi}{\Delta F}$ w.c. (125 MHz)	R	--	± 35	±3	deg
			Freq varied ± 63 MHz in region exhibiting greatest phase deviation from linear					
			$\frac{\Delta\phi}{\Delta F}$ w.c. (40 MHz)	R	--	± 18	±1	deg
			$\frac{\Delta\phi}{\Delta F}$ w.c. (125 MHz)	R	--	± 35	±3	deg
			Center freq (w.c.)	R	7962	8337	8337	MHz
			Pi(rf) adj for Po between 200 mW and 20 watts which exhibits greatest phase deviation from linear at F = 7962 MHz F = 7900 to 8025 MHz					
			$\frac{\Delta\phi}{\Delta F}$ w.c. (40 MHz)	R	--	± 5.5	±1	deg
			$\frac{\Delta\phi}{\Delta F}$ w.c. (125 MHz)	R	--	± 9.5	±3	deg
			Po	R	~~2~~ 15	15	~~20~~ 1500	mW
			Pi(rf) adj for Po between 200 mW and 20 watts which exhibits greatest phase deviation from linear at F = 8337 MHz F = 8275 to 8400 MHz					
			$\frac{\Delta\phi}{\Delta F}$ w.c. (40 MHz)	R	--	± 18	±1	deg
			$\frac{\Delta\phi}{\Delta F}$ w.c. (125 MHz)	R	--	± 35	±3	deg
			Po	R	~~2~~ 15	15	~~20~~ 1500	mW

DATA SHEET NO. DSB126546
REV.
SERIAL NO. 001

ACCEPTANCE TEST DATA SHEET

CODE IDENT 73293

ITEM	SPEC. PAR. No.	TEST DESIGNATION	TEST CONDITION / DESCRIPTION	R/C	MIN.	DATA	MAX.	UNITS
	4.3.4	Phase Linearity (Cont.)	Freq varied ± 63 MHz in region exhibiting greatest phase deviation from linear					
			$\frac{\Delta\phi}{F}$ w.c. (40 MHz)	R	--	±18	±1	deg
			$\frac{\Delta\phi}{F}$ w.c. (125 MHz)	R	--	±35	±3	deg
			Po	R	~~2~~ 15	15	~~20~~ 1500	m W
			Center freq (w.c.)	R	7962	8337	8337	MHz
			T amb	R	65	75	85	°F
	4.3.5	AM-PM Conversion	Ein (ac) = 120V ± 10% Pi(rf) varied ± 0.5 dB of rated Po					
			$\frac{\Delta\phi}{\Delta Pi(rf)}$ at F = 7.9 GHz	R	--	2	5	°/dB
			F = 8.15GHz	R	--	2	5	°/dB
			F = 8.4 GHz	R	--	2	5	°/dB
			T amb	R	65	75	85	°F
	4.3.6	Output Load VSWR	Ein(ac) = 120V ± 10% Pi(rf) adj for rated Po Load VSWR = 1.3:1 Unit meets requirements of Par. 4.3.1 and 4.3.2	C	--	✓	--	--
			Adj load VSWR to 2.0:1 Pi(rf) adj for rated Po Return unit operation to Par 4.3.1 and 4.3.2 Unit operates satisfactorily	C	--	✓	--	--

DATA SHEET NO. DSB126546
REV.
SERIAL NO. 001

ACCEPTANCE TEST DATA SHEET

CODE IDENT 73293

ITEM	SPEC. PAR. No.	TEST DESIGNATION	TEST CONDITION / DESCRIPTION	R/C	MIN.	DATA	MAX.	UNITS
	4.3.6	Output Load VSWR (Cont.)	Load VSWR varied through all possible values of magnitude and phase Unit remains stable at all frequencies above 8.4 GHz and below 7.9 GHz	C	--	✓	--	--
			Load VSWR varied through all possible values of magnitude and phase. No Pi(rf). Unit remains stable at all frequencies above 8.4 GHz and below 7.9 GHz.	C	--	✓	--	--
			T amb	R	65	75	85	°F
	4.3.7	Input/ Output VSWR and Impedance	Ein (ac) = 120V ± 10% Pi(rf) adj for rated Po Input VSWR no greater than 1.20:1	C	--	✓	--	--
			Output VSWR no greater than 1.40:1	C	--	✓	--	--
			T amb	R	65	75	85	°F
	4.3.8	Spurious Output and Harmonic Content	Ein (ac) = 120V ± 10% Pi(rf) adj for rated Po					
			Po(rf) 1.5 W spo(max) at F = 7.9 GHz	R	--	< -48.2	-48.2 ~~-37~~	dBm
			1.1 W F = 8.15GHz	R	--	< -48.2	-48.2 ~~-37~~	dBm
			0.29 W F = 8.4 GHz	R	--	< -48.2	-48.2 ~~-37~~	dBm
			No Pi(rf) spo(max)	R	--	< -48.2	-48.2 ~~-37~~	dBm
			Measure second harmonic power output Ph2 at F = 7.9 GHz	R	--	< -50	--	dBm
			F = 8.15 GHz	R	--	-38	--	dBm
			F = 8.4 GHz	R	--	< -50	--	dBm

HUGHES ELECTRON DYNAMICS DIVISION
3100 West Lomita Boulevard, Torrance, California 90509, Tel (213) 534-2121

DATA SHEET NO. DSB126546
REV.
SERIAL NO. 001

ACCEPTANCE TEST DATA SHEET

CODE IDENT 73293

ITEM	SPEC. PAR. No.	TEST DESIGNATION	TEST CONDITION / DESCRIPTION	R/C	MIN.	DATA	MAX.	UNITS
	4.3.8	Spurious Output and Harmonic Content (Cont.)	Calculate ratio of total harmonic output power to fundamental power					
			Pht at F = 7.9 GHz	R	~~60~~	> 80	~~60~~	dBc
			F = 8.15 GHz	R	~~60~~	68	~~60~~	dBc
			F = 8.4 GHz	R	~~60~~	> 80	~~60~~	dBc
			T amb	R	65	75	85	°F
	4.3.9	Noise Figure	Calculate noise figure					
			N.F.	R	--	39.0	40	dB
			T amb	R	65	75	85	°F
	4.3.10	Residual AM Modulation	Ein (ac) = 120V ± 10% Pi(rf) adj for rated Po Measure residual AM modulation below fundamental					
			AM Mod at F = 7.9 GHz	R	70	60	--	dBc
			F = 8.15 GHz	R	70	> 70	--	dBc
			F = 8.4 GHz	R	70	> 70	--	dBc
			T amb	R	65	75	85	°F
	4.3.11	Hum Modulation	Ein (ac) = 120V ± 10% Calculate level of hum modulation below the carrier					
			HM at F = 7.9 GHz	R	78	52.1	--	dBc
			F = 8.15 GHz	R	78	61.5	--	dBc
			F = 8.4 GHz	R	78	46.3	--	dBc
			T amb	R	65	75	85	°F

DATA SHEET NO. DSB126546
REV.
SERIAL NO. 001

ACCEPTANCE TEST DATA SHEET

CODE IDENT. 73293

ITEM	SPEC. PAR. No.	TEST DESIGNATION	TEST CONDITION / DESCRIPTION	R/C	MIN.	DATA	MAX.	UNITS
	4.3.12	Gain Stability	Unit operating per Par. 4.3.1 Step 1					
			f = 8 GHz G (8 hours)	R	~~14~~ 38	36.01	--	dB
			T amb (8 hours)	R	65	76	85	°F
			G (16 hours)	R	~~14~~ 38	36.49	--	dB
			T amb (16 hours)	R	65	72	85	°F
			G (24 hours)	R	~~14~~ 38	36.29	--	dB
			T amb (24 hours)	R	65	75	85	°F
			Gain stability within ± 0.25 dB/ 24 hours	C	--	✓	--	--
	4.3.13	Inter-modulation Products	Ein (ac) = 120V ± 10% Determine third order IM Products below carrier					
			IM at P0(rf) = ~~29~~ dBm 31.8	R	--	16.5	--	dBc
			P0(rf) = ~~19~~ dBm 28.8	R	--	20.5	--	dBc
			P0(rf) = ~~9~~ dBm 25.8	R	--	25.0	--	dBc
			P0(rf) = ~~-1~~ dBm 22.8	R	--	30.0	--	dBc
			P0(rf) = ~~-11~~ dBm 19.8	R	--	35.0	--	dBc
			T amb	R	65	75	85	°F
	4.3.14	Prime Power	Steps 1-2 Ein (ac) = 132V at 60 Hz ± 5% Perform tests of Par. 4.3.1 and 4.3.2 Data recorded on attached pages	C	--		--	--
			Steps 3-4 Ein (ac) = 108V at 60 Hz ± 5% Perform tests of Par. 4.3.1 and 4.3.2 Data recorded on attached pages	C	--		--	--

DATA SHEET NO. DSB126546
REV.
SERIAL NO.

ACCEPTANCE TEST DATA SHEET

CODE IDENT 73293

ITEM	SPEC PAR. No.	TEST DESIGNATION	TEST CONDITION / DESCRIPTION	R/C	MIN	DATA	MAX.	UNITS
	4.3.14	Prime Power (Cont.)	Step 5 Ein (ac) = 132V at 50 Hz ± 5% Perform tests of Par. 4.3.1 and 4.3.2 Ein (ac) = 108V at 50 Hz ± 5% Perform tests of Par. 4.3.1 and 4.3.2					
			Data recorded on attached pages	C	--		--	--
			Step 6 Ein (ac) = 120V at 66 Hz t = 1 minute	C	--		--	--
			Step 7 Ein (ac) = 144V at 66 Hz t = 1 minute	C	--		--	--
			Ein (ac) = 96V at 66 Hz t = 1 minute	C	--		--	--
			Step 8 Ein (ac) = 120V at 45 Hz t = 1 minute	C	--		--	--
			Ein (ac) = 144V at 45 Hz t = 1 minute	C	--		--	--
			Ein (ac) = 96V at 45 Hz t = 1 minute	C	--		--	--
			Step 9 Ein (ac) = 120V ± 10% 60 Hz ± 5% Perform tests of Par. 4.3.1 and 4.3.2					
			Data recorded on attached pages	C	--		--	--

HUGHES
HUGHES AIRCRAFT COMPANY
ELECTRON DYNAMICS DIVISION

PAR 4.3.14 PRIME POWER

DATA SHEET NO. DSB126546
REV. _____
SERIAL NO. _____

ACCEPTANCE TEST DATA SHEET

	PAR	TEST DESCRIPTION	R/C	MIN	MAX	UNIT	Steps 1-2 132 Vac 60Hz ± 5%	Steps 3-4 108 Vac 60Hz ± 5%	Step 5 132 Vac 50Hz ± 5%	Step 5 108 Vac 50Hz ± 5%	Step 9 120Vac±10% 60Hz ± 5%
	4.3.1	Rated Output Power vs. Frequency									
		Steps 1-2 Ein (ac) = 120V ± 10%									
		F = 7.9 GHz; Po = 20W Pi(rf)	R	--	796	mW					
		F = 8.0 GHz; Po = 20W Pi(rf)	R	--	796	mW					
		F = 8.1 GHz; Po = 20W Pi(rf)	R	--	796	mW					
		F = 8.2 GHz; Po = 20W Pi(rf)	R	--	796	mW					
		F = 8.3 GHz; Po = 20W Pi(rf)	R	--	796	mW					
		F = 8.4 GHz; Po = 20W Pi(rf)	R	--	796	mW					
		Steps 3-4 Ein (ac) = 120V ± 10%									
		F = 7.9 GHz; Pi(rf) = 796 mW Po	R	20	--	W					
		F = 8.0 GHz; Pi(rf) = 796 mW Po	R	20	--	W					
		F = 8.1 GHz; Pi(rf) = 796 mW Po	R	20	--	W					
		F = 8.2 GHz; Pi(rf) = 796 mW Po	R	20	--	W					

HUGHES ELECTRON DYNAMICS DIVISION
HUGHES AIRCRAFT COMPANY

PAR 4.3.14 PRIME POWER

DATA SHEET NO. DSB126546
REV. _____
SERIAL NO. _____

ACCEPTANCE TEST DATA SHEET

	PAR	TEST DESCRIPTION	R/C	MIN	MAX	UNIT	Steps 1-2 132 Vac 60Hz ± 5%	Steps 3-4 108 Vac 60Hz ± 5%	Step 5 132 Vac 50Hz ± 5%	Step 5 108 Vac 50Hz ± 5%	Step 9 120Vac±10% 60Hz ± 5%
	4.3.1	Rated Output Power vs. Frequency (Cont.)									
		F = 8.3 GHz; Pi(rf) = 796 mW Po	R	20	--	W					
		F = 8.4 GHz; Pi(rf) = 796 mW Po	R	20	--	W					
		Step 5 T amb	R	65	85	°F					
	4.3.2	Gain vs Frequency at Saturation									
		Calculate gain at rated Po G at F = 7.9 GHz	R	14	--	dB					
		F = 8.0 GHz	R	14	--	dB					
		F = 8.1 GHz	R	14	--	dB					
		F = 8.2 GHz	R	14	--	dB					
		F = 8.3 GHz	R	14	--	dB					
		F = 8.4 GHz	R	14	--	dB					

HUGHES AIRCRAFT COMPANY — ELECTRON DYNAMICS DIVISION

PAR 4.3.14 PRIME POWER

DATA SHEET NO. DSB126546

REV. _____

SERIAL NO. _____

PAGE 14 OF 38

ACCEPTANCE TEST DATA SHEET

	PAR	TEST DESCRIPTION	R/C	MIN	MAX	UNIT	Steps 1-2 132 Vac 60Hz ± 5%	Steps 3-4 108 Vac 60Hz ± 5%	Step 5 132 Vac 50Hz ± 5%	Step 5 108 Vac 50Hz ± 5%	Step 9 120Vac±10% 60Hz ± 5%
	4.3.2	Gain vs. Frequency at Saturation (Cont.)									
		Calculate gain at max Pi(rf) G at F = 7.9 GHz	R	14	--	dB					
		F = 8.0 GHz	R	14	--	dB					
		F = 8.1 GHz	R	14	--	dB					
		F = 8.2 GHz	R	14	--	dB					
		F = 8.3 GHz	R	14	--	dB					
		F = 8.4 GHz	R	14	--	dB					

EDD 1045F—REV JULY74

DATA SHEET NO. DSB126546
REV.
SERIAL NO.

ACCEPTANCE TEST DATA SHEET

CODE IDENT 73293

ITEM	SPEC PAR. No	TEST DESIGNATION	TEST CONDITION / DESCRIPTION	R/C	MIN	DATA	MAX	UNITS
	5.0		ENVIRONMENTAL TEST					
	5.1	Vibration Test	Unit operating during test Date completed_____					
	5.1.4	Mechanical Inspection	Visual inspection for evidence of mechanical damage	C	--		--	--
	5.1.5	Post Vibration Test	Perform the tests of Par. 4.3.1, 4.3.2, 4.3.3, 4.3.4 and 4.3.9 Data recorded on attached pages	C	--		--	--
	5.2	Bench Handling Test	Unit non operating during test Date completed_____					
	5.2.2	Mechanical Inspection	Visual inspection for evidence of mechanical damage	C	--		--	--
	5.2.3	Post Bench Handling Test	Perform the tests of Par. 4.3.1, 4.3.2, 4.3.3, 4.3.4 and 4.3.9 Data recorded on attached pages	C	--		--	--
	5.3	Transit Drop Test	Date completed_____					
	5.3.2	Mechanical Inspection	Visual inspection for evidence of mechanical damage	C	--		--	--
	5.3.3	Post Transit Drop Test	Perform the tests of Par. 4.3.1, 4.3.2, 4.3.3, 4.3.4 and 4.3.9 Data recorded on attached pages	C	--		--	--

HUGHES ELECTRON DYNAMICS DIVISION
3100 West Lomita Boulevard, Torrance, California 90509, Tel (213) 534-2121

DATA SHEET NO. DSB126546
REV.
SERIAL NO. 001

ACCEPTANCE TEST DATA SHEET

CODE IDENT 73293

ITEM	SPEC. PAR. No.	TEST DESIGNATION	TEST CONDITION / DESCRIPTION	R/C	MIN.	DATA	MAX.	UNITS
	5.4	Altitude Test	T = 75° ± 10°F					
			Step 2: P = 87.5 mmHg(50,000 ft) t = 1 hour	C	--		--	--
			Step 3: P = 523 mmHg(10,000 ft)					
			Perform tests of Par 4.3.1 and 4.3.2					
			Data recorded on attached pages	C	--		--	--
			Date completed _____	C	--		--	--
	5.4.2	Post Altitude Test	Perform the tests of Par. 4.3.1, 4.3.2, 4.3.3, 4.3.4 and 4.3.9					
			Data recorded on attached pages	C	--		--	--
	5.4.3	Mechanical Inspection	Visual inspection for evidence of mechanical damage	C	--		--	--
	5.5.1	High Temperature Test Procedure	Step 2: T = +155°F; t = 48 hours	C	--		--	--
			Steps 3-4: T = ~~+125°F~~ 113°F					
			Perform the tests of Par. 4.3.1, 4.3.2, and 4.3.3					
			Steps 5-6: T = amb 77°F					
			Perform the tests of Par. 4.3.1, 4.3.2, and 4.3.3.					
			~~Data~~ X-Y PLOTS recorded on attached pages	C	--	✓	--	--
			Date completed 19 MAR 76	C	--	✓	--	--
	5.5.2	Mechanical Inspection	Visual inspection for evidence of mechanical damage					

DATA SHEET NO. DSB126546
REV.
SERIAL NO.

ACCEPTANCE TEST DATA SHEET

CODE IDENT 73293

ITEM	SPEC PAR. No.	TEST DESIGNATION	TEST CONDITION / DESCRIPTION	R/C	MIN.	DATA	MAX.	UNITS
	5.6.1	Low Temperature Test Procedure	Step 2: T = -65°F; t = 12 hours	C	--		--	--
			Steps 3-4: T = 0°F					
			Perform the tests of Par. 4.3.1, 4.3.2 and 4.3.3					
			Steps 5-6: T = Amb					
			Perform the tests of Par. 4.3.1, 4.3.2, and 4.3.3					
			Data recorded on attached pages	C	--		--	--
			Date completed_____	C	--		--	--
	5.6.2	Mechanical Inspection	Visual inspection for evidence of mechanical damage	C	--		--	--
	5.7	Humidity Test	Steps 2, 3 & 4: T = 129°F; t = 24 hours					
			Perform test of Par. 4.3.1					
			Steps 5 & 6: Five (5) continuous 48 hour cycles per Figure 10					
			Perform test of Par. 4.3.1 at specified intervals					
			Data recorded on attached pages	C	--		--	--
			Date completed_____					
	5.7.2	Mechanical Inspection	Visual inspection for evidence of mechanical damage	C	--		--	--

HUGHES ELECTRON DYNAMICS DIVISION
HUGHES AIRCRAFT COMPANY

PAR 5.0 ENVIRONMENTAL TEST

DATA SHEET NO. DSB126546
REV. _____
SERIAL NO. _____

ACCEPTANCE TEST DATA SHEET

	PAR	TEST DESCRIPTION	R/C	MIN	MAX	UNIT	POST VIBRATION	POST BENCH HANDLING	POST TRANSIT DROP	ALTITUDE TEST	POST ALTITUDE
	4.3.1	Rated Output Power vs. Frequency									
		Steps 1-2 Ein (ac) = 120V ± 10%									
		F = 7.9 GHz; Po = 20W Pi(rf)	R	--	796	mW					
		F = 8.0 GHz; Po = 20W Pi(rf)	R	--	796	mW					
		F = 8.1 GHz; Po = 20W Pi(rf)	R	--	796	mW					
		F = 8.2 GHz; Po = 20W Pi(rf)	R	--	796	mW					
		F = 8.3 GHz; Po = 20W Pi(rf)	R	--	796	mW					
		F = 8.4 GHz; Po = 20W Pi(rf)	R	--	796	mW					
		Steps 3-4 Ein (ac) = 120V ± 10%									
		F = 7.9 GHz; Pi(rf) = 796 mW Po	R	20	--	W					
		F = 8.0 GHz; Pi(rf) = 796 mW Po	R	20	--	W					
		F = 8.1 GHz; Pi(rf) = 796 mW Po	R	20	--	W					
		F = 8.2 GHz; Pi(rf) = 796 mW Po	R	20	--	W					

EDD 1045F-REV JULY74

HUGHES ELECTRON DYNAMICS DIVISION
HUGHES AIRCRAFT COMPANY

PAR 5.0 ENVIRONMENTAL TEST

DATA SHEET NO. DSB126546
REV. _____
SERIAL NO. _____
PAGE 19 OF 38

ACCEPTANCE TEST DATA SHEET

	PAR	TEST DESCRIPTION	R/C	MIN	MAX	UNIT	POST VIBRATION	POST BENCH HANDLING	POST TRANSIT DROP	ALTITUDE TEST	POST ALTITUDE
	4.3.1	Rated Output Power vs. Frequency (Cont.)									
		F = 8.3 GHz; Pi(rf) = 796 mW Po	R	20	--	W					
		F = 8.4 GHz; Pi(rf) = 796 mW Po	R	20	--	W					
		Step 5 T amb	R	65	85	°F					
	4.3.2	Gain vs. Frequency at Saturation									
		Calculate gain at rated Po G at F = 7.9 GHz	R	14	--	dB					
		F = 8.0 GHz	R	14	--	dB					
		F = 8.1 GHz	R	14	--	dB					
		F = 8.2 GHz	R	14	--	dB					
		F = 8.3 GHz	R	14	--	dB					
		F = 8.4 GHz	R	14	--	dB					

EDD 1045F-REV JULY74

HUGHES AIRCRAFT COMPANY — ELECTRON DYNAMICS DIVISION

PAR. 5.0 ENVIRONMENTAL TEST

DATA SHEET NO. DSB126546

REV. _____

SERIAL NO. _____

ACCEPTANCE TEST DATA SHEET

	PAR	TEST DESCRIPTION	R/C	MIN	MAX	UNIT	POST VIBRATION	POST BENCH HANDLING	POST TRANSIT DROP	ALTITUDE TEST	POST ALTITUDE
	4.3.2	Gain vs. Frequency at Saturation (Cont.)									
		Calculate gain at max Pi(rf) G at F = 7.9 GHz	R	14	--	dB					
		F = 8.0 GHz	R	14	--	dB					
		F = 8.1 GHz	R	14	--	dB					
		F = 8.2 GHz	R	14	--	dB					
		F = 8.3 GHz	R	14	--	dB					
		F = 8.4 GHz	R	14	--	dB					
	4.3.3	Gain Variation									
		Ein (ac) = 120V ± 10% Pi(rf) adj for rated Po									
		Calculate max gain variations G(var) w.c. (40 MHz)	R	--	±0.15	dB				--	
		G(var) w.c. (125 MHz)	R	--	±0.25	dB				--	
		Center freq w.c.	R	7962	8337	MHz				--	

HUGHES ELECTRON DYNAMICS DIVISION
HUGHES AIRCRAFT COMPANY

PAR. 5.0 ENVIRONMENTAL TEST

DATA SHEET NO. DSB126546
REV.
SERIAL NO.

ACCEPTANCE TEST DATA SHEET

	PAR	TEST DESCRIPTION	R/C	MIN	MAX	UNIT	POST VIBRATION	POST BENCH HANDLING	POST TRANSIT DROP	ALTITUDE TEST	POST ALTITUDE
	4.3.3	Gain Variation (Cont.)									
		Pi(rf) adj for Po = 200 mW Calculate max gain variations									
		G(var) w.c. (40 MHz)	R	--	±0.15	dB				--	
		G(var) w.c. (125 MHz)	R	--	±0.25	dB				--	
		Center freq w.c.	R	7962	8337	MHz				--	
		Pi(rf) adj for Po between 200 mW and 20W which exhibits									
		greatest gain variation Calculate max gain variations									
		G(var) w.c. (40 MHz)	R	--	±0.15	dB				--	
		G(var) w.c. (125 MHz)	R	--	±0.25	dB				--	
		Po	R	.2	20	W				--	
		Center freq (w.c.)	R	7962	8337	MHz				--	
		T amb	R	65	85	^{o}F				--	

EDD 1045F-REV JULY74

HUGHES ELECTRON DYNAMICS DIVISION
HUGHES AIRCRAFT COMPANY

PAR. 5.0 ENVIRONMENTAL TEST

DATA SHEET NO. DSB126546
REV. _____
SERIAL NO. _____

ACCEPTANCE TEST DATA SHEET

	PAR	TEST DESCRIPTION	R/C	MIN	MAX	UNIT	POST VIBRATION	POST BENCH HANDLING	POST TRANSIT DROP	ALTITUDE TEST	POST ALTITUDE
	4.3.4	Phase Linearity									
		Pi(rf) adj for rated Po at F = 7962 MHz									
		F = 7900 to 8025 MHz $\frac{\Delta\varphi}{\Delta F}$ w.c. (40 MHz)	R	--	±1	deg				--	
		$\frac{\Delta\varphi}{\Delta F}$ w.c. (125 MHz)	R	--	±3	deg				--	
		Pi(rf) adj for rated Po at F = 8337 MHz; F = 8275to 8400									
		MHz $\frac{\Delta\varphi}{\Delta F}$ w.c.(40 MHz)	R	--	±1	deg				--	
		$\frac{\Delta\varphi}{\Delta F}$ w.c.(125 MHz)	R	--	±3	deg				--	
		Freq varied ± 63 MHz in region exhibiting greatest									
		phase deviation from linear									
		$\frac{\Delta\varphi}{\Delta F}$ w.c.(40 MHz)	R	--	±1	deg				--	
		$\frac{\Delta\varphi}{\Delta F}$ w.c. (125 MHz)	R	--	±3	deg				--	
		Center freq (w.c.)	R	7962	8337	MHz				--	

EDD 1045F—REV JULY74

HUGHES ELECTRON DYNAMICS DIVISION
HUGHES AIRCRAFT COMPANY

PAR. 5.0 ENVIRONMENTAL TEST

DATA SHEET NO. DSB126546
REV. _____
SERIAL NO. _____

ACCEPTANCE TEST DATA SHEET

	PAR	TEST DESCRIPTION	R/C	MIN	MAX	UNIT	POST VIBRATION	POST BENCH HANDLING	POST TRANSIT DROP	ALTITUDE TEST	POST ALTITUDE
	4.3.4	Phase Linearity (Cont.)									
		Pi(rf) adj for Po = 200 mW at F = 7962 MHz									
		F = 7900 to 8025 MHz $\frac{\Delta\phi}{\Delta F}$ w.c. (40 MHz)	R	--	±1	deg				--	
		$\frac{\Delta\phi}{\Delta F}$ w.c. (125 MHz)	R	--	±3	deg				--	
		Pi(rf) adj for Po = 200 mW at F = 8337 MHz									
		F = 8275 to 8400 MHz $\frac{\Delta\phi}{\Delta F}$ w.c. (40 MHz)	R	--	±1	deg				--	
		$\frac{\Delta\phi}{\Delta F}$ w.c. (125 MHz)	R	--	±3	deg				--	
		Freq varied ± 63 MHz in region exhibiting greatest									
		phase deviation from linear									
		$\frac{\Delta\phi}{\Delta F}$ w.c. (40 MHz)	R	--	±1	deg				--	
		$\frac{\Delta\phi}{\Delta F}$ w.c. (125 MHz)	R	--	±3	deg				--	
		Center freq (w.c.)	R	7962	8337	MHz				--	

EDD 1045F—REV JULY74

HUGHES
HUGHES AIRCRAFT COMPANY
ELECTRON DYNAMICS DIVISION

PAR. 5.0 ENVIRONMENTAL TEST

DATA SHEET NO. DSB126546
REV.
SERIAL NO.

ACCEPTANCE TEST DATA SHEET

	PAR	TEST DESCRIPTION	R/C	MIN	MAX	UNIT	POST VIBRATION	POST BENCH HANDLING	POST TRANSIT DROP	ALTITUDE TEST	POST ALTITUDE
	4.3.4	Phase Linearity (Cont.)									
		Pi(rf) adj for Po between 200 mW and 20 watts which exhibits									
		greatest phase deviation from linear at F = 7962 MHz									
		F = 7900 to 8025 MHz									
		$\frac{\Delta\phi}{\Delta F}$ w.c. (40 MHz)	R	--	±1	deg				--	
		$\frac{\Delta\phi}{\Delta F}$ w.c. (125 MHz)	R	--	±3	deg				--	
		Po	R	0.2	20	W				--	
		Pi(rf) adj for Po between 200 mW and 20 watts which									
		exhibits greatest phase deviation from linear at									
		F = 8337 MHz F = 8275 to 8400 MHz									
		$\frac{\Delta\phi}{\Delta F}$ w.c. (40 MHz)	R	--	±1	deg				--	
		$\frac{\Delta\phi}{\Delta F}$ w.c. (125 MHz)	R	--	±3	deg				--	
		Po	R	0.2	20	W				--	

HUGHES ELECTRON DYNAMICS DIVISION
HUGHES AIRCRAFT COMPANY

PAR. 5.0 ENVIRONMENTAL TEST

DATA SHEET NO. DSB126546
REV.
SERIAL NO.

ACCEPTANCE TEST DATA SHEET

	PAR	TEST DESCRIPTION	R/C	MIN	MAX	UNIT	POST VIBRATION	POST BENCH HANDLING	POST TRANSIT DROP	ALTITUDE TEST	POST ALTITUDE
	4.3.4	Phase Linearity (Cont.)									
		Freq varied ± 63 MHz in region exhibiting greatest phase									
		deviation from linear									
		$\frac{\Delta\phi}{\Delta F}$ w.c. (40 MHz)	R	--	±1	deg				--	
		$\frac{\Delta\phi}{\Delta F}$ w.c. (125 MHz)	R	--	±3	deg				--	
		Po	R	0.2	20	W				--	
		Center freq (w.c.)	R	7962	8337	MHz				--	
		T amb	R	65	85	°F				--	
	4.3.9	Noise Figure									
		Calculate noise figure									
		N.F.	R	--	40	dB				--	
		T amb	R	65	85	°F				--	

HUGHES AIRCRAFT COMPANY — ELECTRON DYNAMICS DIVISION

PAR. 5.0 ENVIRONMENTAL TEST

DATA SHEET NO. DSB126546

REV. _____

SERIAL NO. _____

ACCEPTANCE TEST DATA SHEET

	PAR	TEST DESCRIPTION	R/C	MIN	MAX	UNIT	HIGH TEMP STEPS 3-4	HIGH TEMP STEPS 5-6	LOW TEMP STEPS 3-4	LOW TEMP STEPS 5-6
	4.3.1	Rated Output Power vs. Frequency								
		Steps 1-2 Ein (ac) = 120V ± 10%								
		F = 7.9 GHz; Po = 20W Pi(rf)	R	--	796	mW				
		F = 8.0 GHz; Po = 20W Pi(rf)	R	--	796	mW				
		F = 8.1 GHz; Po = 20W Pi(rf)	R	--	796	mW				
		F = 8.2 GHz; Po = 20W Pi(rf)	R	--	796	mW				
		F = 8.3 GHz; Po = 20W Pi(rf)	R	--	796	mW				
		F = 8.4 GHz; Po = 20W Pi(rf)	R	--	796	mW				
		Steps 3-4 Ein (ac) = 120V ± 10%								
		F = 7.9 GHz; Pi(rf) = 796 mW Po	R	20	--	W				
		F = 8.0 GHz; Pi(rf) = 796 mW Po	R	20	--	W				
		F = 8.1 GHz; Pi(rf) = 796 mW Po	R	20	--	W				
		F = 8.2 GHz; Pi(rf) = 796 mW Po	R	20	--	W				

HUGHES ELECTRON DYNAMICS DIVISION
HUGHES AIRCRAFT COMPANY

PAR 5.0 ENVIRONMENTAL TEST

DATA SHEET NO. DSB126546
REV. _____
SERIAL NO. _____

ACCEPTANCE TEST DATA SHEET

	PAR	TEST DESCRIPTION	R/C	MIN	MAX	UNIT	HIGH TEMP STEPS 3-4	HIGH TEMP STEPS 5-6	LOW TEMP STEPS 3-4	LOW TEMP STEPS 5-6
	4.3.1	Rated Output Power vs. Frequency (Cont.)								
		F = 8.3 GHz; Pi(rf) = 796 mW Po	R	20	--	W				
		F = 8.4 GHz; Pi(rf) = 796 mW Po	R	20	--	W				
		Step 5 T amb	R	65	85	°F				
	4.3.2	Gain vs. Frequency at Saturation								
		Calculate gain at rated Po G at F = 7.9 GHz	R	14	--	dB				
		F = 8.0 GHz	R	14	--	dB				
		F = 8.1 GHz	R	14	--	dB				
		F = 8.2 GHz	R	14	--	dB				
		F = 8.3 GHz	R	14	--	dB				
		F = 8.4 GHz	R	14	--	dB				

EDD 1045F-REV JULY74

HUGHES ELECTRON DYNAMICS DIVISION
HUGHES AIRCRAFT COMPANY

PAR. 5.0 ENVIRONMENTAL TEST

DATA SHEET NO. DSB126546
REV. _____
SERIAL NO. _____

ACCEPTANCE TEST DATA SHEET

	PAR	TEST DESCRIPTION	R/C	MIN	MAX	UNIT	HIGH TEMP STEPS 3-4	HIGH TEMP STEPS 5-6	LOW TEMP STEPS 3-4	LOW TEMP STEPS 5-6
	4.3.2	Gain vs. Frequency at Saturation (Cont.)								
		Calculate gain at max Pi(rf) G at F = 7.9 GHz	R	14	--	dB				
		F = 8.0 GHz	R	14	--	dB				
		F = 8.1 GHz	R	14	--	dB				
		F = 8.2 GHz	R	14	--	dB				
		F = 8.3 GHz	R	14	--	dB				
		F = 8.4 GHz	R	14	--	dB				
	4.3.3	Gain Variation								
		Ein (ac) = 120V ± 10% Pi(rf) adj for rated Po								
		Calculate max gain variation G(var) w.c. (40 MHz)	R	--	±0.15	dB				
		G(var) w.c. (125 MHz)	R	--	±0.25	dB				
		Center freq w.c.	R	7962	8337	MHz				

HUGHES AIRCRAFT COMPANY

HUGHES ELECTRON DYNAMICS DIVISION

PAR 5.0 ENVIRONMENTAL TEST

DATA SHEET NO. DSB126546

REV. _____

SERIAL NO. _____

ACCEPTANCE TEST DATA SHEET

	PAR	TEST DESCRIPTION	R/C	MIN	MAX	UNIT	HIGH TEMP STEPS 3-4	HIGH TEMP STEPS 5-6	LOW TEMP STEPS 3-4	LOW TEMP STEPS 5-6
	4.3.3	Gain Variation (Cont.)								
		Pi(rf) adj for Po = 200 mW Calculate max gain variations								
		G(var) w.c. (40 MHz)	R	--	±0.15	dB				
		G(var) w.c. (125 MHz)	R	--	±0.25	dB				
		Center freq w.c.	R	7962	8337	MHz				
		Pi(rf) adj for Po between 200 mW and 20 W which								
		exhibits greatest gain variation								
		Calculate max gain variation								
		G(var) w.c. (40 MHz)	R	--	±0.15	dB				
		G(var) w.c. (125 MHz)	R	--	±0.25	dB				
		Po	R	0.2	20	W				
		Center freq (w.c.)	R	7962	8337	MHz				
		T amb	R	65	85	^{o}F				

HUGHES ELECTRON DYNAMICS DIVISION
HUGHES AIRCRAFT COMPANY

PAR. 5.0 ENVIRONMENTAL TEST
PAR. 5.7 HUMIDITY TEST

DATA SHEET NO. DSB126546
REV. _____
SERIAL NO. _____

ACCEPTANCE TEST DATA SHEET

	PAR	TEST DESCRIPTION	R/C	MIN	MAX	UNIT	STEP 4	CYCLE 1 STEP 6	CYCLE 1 STEP 6	CYCLE 2 STEP 6	CYCLE 2 STEP 6
	4.3.1	Rated Output Power vs. Freq. Steps 1-2: Ein(ac) = 120V±10%									
		F = 7.9 GHz; Po = 20W Pi(rf)	R	--	796	mW					
		F = 8.0 GHz; Po = 20W Pi(rf)	R	--	796	mW					
		F = 8.1 GHz; Po = 20W Pi(rf)	R	--	796	mW					
		F = 8.2 GHz; Po = 20W Pi(rf)	R	--	796	mW					
		F = 8.3 GHz; Po = 20W Pi(rf)	R	--	796	mW					
		F = 8.4 GHz; Po = 20W Pi(rf)	R	--	796	mW					
		Steps 3-4: Ein(ac) = 120V±10% F=7.9GHz; Pi(rf)=796 mW Po	R	20	--	W					
		F = 8.0 GHz; Pi(rf) = 796 mW Po	R	20	--	W					
		F = 8.1 GHz; Pi(rf) = 796 mW Po	R	20	--	W					
		F = 8.2 GHz; Pi(rf) = 796 mW Po	R	20	--	W					
		F = 8.3 GHz; Pi(rf) = 796 mW Po	R	20	--	W					
		F = 8.4 GHz; Pi(rf) = 796 mW Po	R	20	--	W					
		Step 5 T amb	R	65	85	°F					

EDD 1045F-REV JULY74

HUGHES ELECTRON DYNAMICS DIVISION
HUGHES AIRCRAFT COMPANY

PAR. 5.0 ENVIRONMENTAL TEST
PAR. 5.7 HUMIDITY TEST

DATA SHEET NO. DSB126546
REV. _____
SERIAL NO. _____

ACCEPTANCE TEST DATA SHEET

	PAR	TEST DESCRIPTION	R/C	MIN	MAX	UNIT	CYCLE 3		CYCLE 4		CYCLE 5	
							STEP 6	STEP 6	STEP 6	STEP 6	STEP 6	STEP 6
	4.3.1	Rated Output Power vs. Freq. Steps 1-2: Ein(ac) =120V±10%										
		F = 7.9 GHz; Po = 20W Pi(rf)	R	--	796	mW						
		F = 8.0 GHz; Po = 20W Pi(rf)	R	--	796	mW						
		F = 8.1 GHz; Po = 20W Pi(rf)	R	--	796	mW						
		F = 8.2 GHz; Po = 20W Pi(rf)	R	--	796	mW						
		F = 8.3 GHz; Po = 20W Pi(rf)	R	--	796	mW						
		F = 8.4 GHz; Po = 20W Pi(rf)	R	--	796	mW						
		Steps 3-4: Pi(rf)=796 mW F = 7.9 GHz Po	R	20	--	W						
		F = 8.0 GHz; Pi(rf) = 796 mW Po	R	20	--	W						
		F = 8.1 GHz; Pi(rf) = 796 mW Po	R	20	--	W						
		F = 8.2 GHz; Pi(rf) = 796 mW Po	R	20	--	W						
		F = 8.3 GHz; Pi(rf) = 796 mW Po	R	20	--	W						
		F = 8.4 GHz; Pi(rf) = 796 mW Po	R	20	--	W						
		Step 5 T amb	R	65	85	°F						

EDD 1048F-REV JULY74

DATA SHEET NO. DSB126546
REV.
SERIAL NO.

ACCEPTANCE TEST DATA SHEET

CODE IDENT 73293

ITEM	SPEC. PAR. No.	TEST DESIGNATION	TEST CONDITION / DESCRIPTION	R/C	MIN.	DATA	MAX.	UNITS
	6.0		FINAL FUNCTIONAL TEST					
	4.3.1	Rated Output Power vs. Frequency	Steps 1-2:					
			Ein(ac) = 120V ± 10%					
			F = 7.9 GHz; Po = 20W Pi(rf)	R	--		796	mW
			F = 8.0 GHz; Po = 20W Pi(rf)	R	--		796	mW
			F = 8.1 GHz; Po = 20W Pi(rf)	R	--		796	mW
			F = 8.2 GHz; Po = 20W Pi(rf)	R	--		796	mW
			F = 8.3 GHz; Po = 20W Pi(rf)	R	--		796	mW
			F = 8.4 GHz; Po = 20W Pi(rf)	R	--		796	mW
			Steps 3-4:					
			Ein(ac) = 120V ± 10%					
			F = 7.9 GHz; Pi(rf) = 796 mW Po	R	20		--	W
			F = 8.0 GHz; Pi(rf) = 796 mW Po	R	20		--	W
			F = 8.1 GHz; Pi(rf) = 796 mW Po	R	20		--	W
			F = 8.2 GHz; Pi(rf) = 796 mW Po	R	20		--	W
			F = 8.3 GHz; Pi(rf) = 796 mW Po	R	20		--	W

DATA SHEET NO. DSB126546
REV.
SERIAL NO.

ACCEPTANCE TEST DATA SHEET

CODE IDENT 73293

ITEM	SPEC. PAR. No	TEST DESIGNATION	TEST CONDITION / DESCRIPTION	R/C	MIN.	DATA	MAX.	UNITS
	4.3.1	Rated Output Power vs. Frequency (Cont.)	Steps 3-4:					
			Ein(ac) = 120V ± 10%					
			F = 8.4 GHz; Pi(rf) = 796 mW					
			Po	R	20		--	W
			Step 5 T amb	R	65		85	°F
	4.3.2	Gain vs. Frequency at Saturation	Calculate gain at rated Po(20W)					
			G at F = 7.9 GHz	R	14		--	dB
			F = 8.0 GHz	R	14		--	dB
			F = 8.1 GHz	R	14		--	dB
			F = 8.2 GHz	R	14		--	dB
			F = 8.3 GHz	R	14		--	dB
			F = 8.4 GHz	R	14		--	dB
			Calculate gain at max Pi(rf)					
			G at F = 7.9 GHz	R	14		--	dB
			F = 8.0 GHz	R	14		--	dB
			F = 8.1 GHz	R	14		--	dB
			F = 8.2 GHz	R	14		--	dB
			F = 8.3 GHz	R	14		--	dB
			F = 8.4 GHz	R	14		--	dB

ACCEPTANCE TEST DATA SHEET

ITEM	SPEC. PAR. No.	TEST DESIGNATION	TEST CONDITION / DESCRIPTION	R/C	MIN.	DATA	MAX.	UNITS
	4.3.3	Gain Variation	Ein(ac) = 120V ± 10% Pi(rf) adj for rated Po at					
			F = 7962 MHz F = 7900 to 8025 MHz					
			G(var) w.c. (40 MHz)	R	--		±0.15	dB
			G(var) w.c. (125 MHz)	R	--		±0.25	dB
			Pi(rf) adj for rated Po at					
			F = 8337 MHz F = 8275 to 8400 MHz					
			G(var) w.c. (40 MHz)	R	--		±0.15	dB
			G(var) w.c. (125 MHz)	R	--		±0.25	dB
			Freq varied ± 63 MHz in region exhibiting greatest gain variation					
			G(var) w.c. (40 MHz)	R	--		±0.15	dB
			G(var) w.c. (125 MHz)	R	--		±0.25	dB
			Center freq w.c.	R	7962		8337	MHz
			Pi(rf) adj for Po = 200 mW at					
			F = 7962 MHz					
			F = 7900 to 8025 MHz					
			G(var) w.c. (40 MHz)	R	--		±0.15	dB
			G(var) w.c. (125 MHz)	R	--		±0.25	dB
			Pi(rf) adj for Po = 200 mW at F = 8337 MHz F = 8275 to 8400 MHz					
			G(var) w.c. (40 MHz)	R	--		±0.15	dB
			G(var) w.c. (125 MHz)	R	--		±0.25	dB

ACCEPTANCE TEST DATA SHEET

ITEM	SPEC. PAR. No.	TEST DESIGNATION	TEST CONDITION / DESCRIPTION	R/C	MIN.	DATA	MAX.	UNITS
	4.3.3	Gain Variation (Cont.)	Freq varied ± 63 MHz in region exhibiting greatest gain variation					
			G(var) w.c. (40 MHz)	R	--		±0.15	dB
			G(var) w.c. (125 MHz)	R	--		±0.25	dB
			Center freq w.c.	R	7962		8337	MHz
			Pi(rf) adj for Po between 200 mW and 20W which exhibits greatest gain variation at F = 7962 MHz F = 7900 to 8025 MHz					
			G(var) w.c. (40 MHz)	R	--		±0.15	dB
			G(var) w.c. (125 MHz)	R	--		±0.25	dB
			Po	R	0.2		20	W
			Pi(rf) adj for Po between 200 mW and 20W which exhibits greatest gain variation at F = 8337 MHz F = 8275 to 8400 MHz					
			G(var) w.c. (40 MHz)	R	--		±0.15	dB
			G(var) w.c. (125 MHz)	R	--		±0.25	dB
			Po	R	0.2		20	W
			Freq varied ± 63 MHz in region exhibiting greatest gain variation					
			G(var) w.c. (40 MHz)	R	--		±0.15	dB
			G(var) w.c. (125 MHz)	R	--		±0.25	dB
			Po	R	0.2		20	W
			Center Freq (w.c.)	R	7962		8337	MHz
			T amb	R	65		85	^{o}F

HUGHES ELECTRON DYNAMICS DIVISION
3100 West Lomita Boulevard, Torrance, California 90509 Tel (213) 534-2121

DATA SHEET NO. DSB126546
REV.
SERIAL NO.

ACCEPTANCE TEST DATA SHEET

CODE IDENT. 73293

ITEM	SPEC. PAR. No.	TEST DESIGNATION	TEST CONDITION / DESCRIPTION	R/C	MIN.	DATA	MAX.	UNITS
	4.3.4	Phase Linearity	Ein (ac) = 120V ± 10% Pi(rf) adj for rated Po at F = 7962 MHz F = 7900 to 8025 MHz					
			$\frac{\Delta\phi}{\Delta F}$ w.c. (40 MHz)	R	--		± 1	deg
			$\frac{\Delta\phi}{\Delta F}$ w.c. (125 MHz)	R	--		± 3	deg
			Pi(rf) adj for rated Po at F = 8337 MHz F = 8275 to 8400 MHz					
			$\frac{\Delta\phi}{\Delta F}$ w.c. (40 MHz)	R	--		± 1	deg
			$\frac{\Delta\phi}{\Delta F}$ w.c. (125 MHz)	R	--		± 3	deg
			Freq varied ± 63 MHz in region exhibiting greatest phase deviation from linear					
			$\frac{\Delta\phi}{\Delta F}$ w.c. (40 MHz)	R	--		± 1	deg
			$\frac{\Delta\phi}{\Delta F}$ w.c. (125 MHz)	R	--		± 3	deg
			Center freq (w.c.)	R	7962		8337	MHz
			Pi(rf) adj for Po = 200 mW at F = 7962 MHz F = 7900 to 8025 MHz					
			$\frac{\Delta\phi}{\Delta F}$ w.c. (40 MHz)	R	--		± 1	deg
			$\frac{\Delta\phi}{\Delta F}$ w.c. (125 MHz)	R	--		± 3	deg

DATA SHEET NO. DSB126546
REV.
SERIAL NO.

ACCEPTANCE TEST DATA SHEET

CODE IDENT 73293

ITEM	SPEC. PAR. No.	TEST DESIGNATION	TEST CONDITION / DESCRIPTION	R/C	MIN.	DATA	MAX.	UNITS
	4.3.4	Phase Linearity (Cont.)	Pi(rf) adj for Po = 200 mW at F = 8337 MHz F = 8275 to 8400 MHz					
			$\frac{\Delta\phi}{\Delta F}$ w.c. (40 MHz)	R	--		± 1	deg
			$\frac{\Delta\phi}{\Delta F}$ w.c. (125 MHz)	R	--		± 3	deg
			Freq varied ± 63 MHz in region exhibiting greatest phase deviation from linear					
			$\frac{\Delta\phi}{\Delta F}$ w.c. (40 MHz)	R	--		± 1	deg
			$\frac{\Delta\phi}{\Delta F}$ w.c. (125 MHz)	R	--		± 3	deg
			Center freq (w.c.)	R	7962		8337	MHz
			Pi(rf) adj for Po between 200 mW and 20 watts which exhibits greatest phase deviation from linear at F = 7962 MHz F = 7900 to 8025 MHz					
			$\frac{\Delta\phi}{\Delta F}$ w.c. (40 MHz)	R	--		± 1	deg
			$\frac{\Delta\phi}{\Delta F}$ w.c. (125 MHz)	R	--		± 3	deg
			Po	R	.2		20	W
			Pi(rf) adj for Po between 200 mW and 20 watts which exhibits greatest phase deviation from linear at F = 8337 MHz F = 8275 to 8400 MHz					
			$\frac{\Delta\phi}{\Delta F}$ w.c. (40 MHz)	R	--		±1	deg
			$\frac{\Delta\phi}{\Delta F}$ w.c. (125 MHz)	R	--		±3	deg
			Po	R	.2		20	W

HUGHES AIRCRAFT COMPANY

ELECTRON DYNAMICS DIVISION

3100 West Lomita Boulevard, Torrance, California 90509 Tel (213) 534-2121

DATA SHEET NO. DSB126546

REV. _____

SERIAL NO. _____

ACCEPTANCE TEST DATA SHEET

CODE IDENT 73293

ITEM	SPEC. PAR. No.	TEST DESIGNATION	TEST CONDITION / DESCRIPTION	R/C	MIN.	DATA	MAX.	UNITS
	4.3.4	Phase Linearity (Cont.)	Freq varied ±63 MHz in region exhibiting greatest phase deviation from linear					
			$\frac{\Delta\phi}{\Delta F}$ w.c. (40 MHz)	R	--		±1	deg
			$\frac{\Delta\phi}{\Delta F}$ w.c. (125 MHz)	R	--		±3	deg
			Po	R	.2		20	W
			Center freq (w.c.)	R	7962		8337	MHz
			T amb	R	65		85	^{o}F
	4.3.9	Noise Figure	Calculate noise figure N.F.	R	--		40	dB
			Tested by W.H. Lockyer					
			Date 23 Mar 76					
			TEST NONCONFORMANCES (ITR NO'S)					

TEST CONCURRENCE

DATE _____

QUALITY _____

DATE 2 April 76

P.S. Stevens

EDD 1045E REV JUN74

APPENDIX C

SUPPLEMENTARY DATA

APPENDIX C

DSB/EDTB 126546 M/P SUPPLEMENTARY DATA

1.0 POWER METER DATA REDUCTION

1.1 Output Power

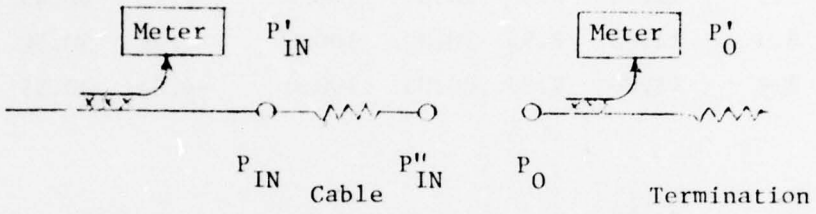

Calibration Factor: $C_O \equiv P_O - P'_O$ = Supplied by Calibration Lab.
(All readings in dBm)

1.2 Input Power

Connect input and output couplers directly:

$$P''_{IN} = P_O$$

Calibration Factor: $C_{IN} \equiv P''_{IN} - P'_{IN} = P_O - P'_{IN}$

$$= C_O + P'_O - P'_{IN}$$

$$= C_O + (P'_O - P'_{IN})$$

2.0 TESTS OF PARAGRAPH 4.3.1

f {DATA} (GHz)	P'_{IN} {DATA} (dBm)	C_{IN} (dB)	P''_{IN} (dBm)	(mw)	P'_O {DATA} (dBm)	C_O (dB)	P_O (dBm)	(W)
7.9	-13.67	8.85	-4.81	.33	1.36	30.40	31.76	1.5
8.0	-13.77	8.93	-4.84	.33	1.31	30.45	31.76	1.5
8.1	-7.57	8.90	1.33	1.36	1.31	30.45	31.76	1.5
8.2	10.0	8.90	18.90	77.6	-2.37	30.45	28.08	.643
8.3	10.0	8.95	18.95	78.5	-6.73	30.50	23.77	.238
8.4	10.0	9.00	19.00	79.5	-8.30	30.55	22.25	.168

f {DATA} (GHz)	P'_{IN} {DATA} (dBm)	C_{IN} (dB)	P''_{IN} (dBm)	(mw)	P'_O {DATA} (dBm)	C_O (dB)	P_O (dBm)	(W)
7.9	11.15	8.85	20.00	100.0	7.85	30.40	38.25	6.689
8.0	11.07	8.93	20.00	100.0	7.12	30.45	37.57	5.712
8.1	11.10	8.90	20.00	100.0	3.22	30.45	33.67	2.329
8.2	11.10	8.90	20.00	100.0	-2.40	30.45	28.05	.638
8.3	11.05	8.95	20.00	100.0	-6.36	30.50	24.14	.259
8.4	11.00	9.00	20.00	100.0	-6.04	30.55	24.51	.283

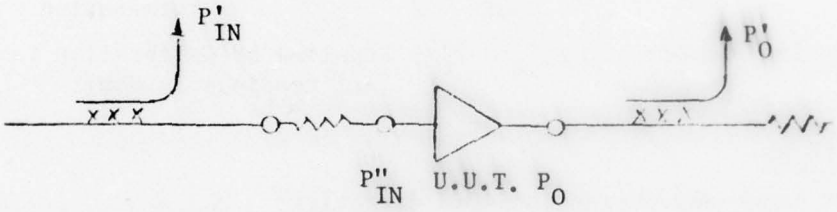

2.1 Gain Calculations; Paragraph 4.3.2:

$G = P_O(dBm) - P''_{IN}(dBm)$

f	P''_{IN}(dBm)	P_O(dBm)	G(dB)
7.9	-4.8	31.8	36.6
8.0	-4.8	31.8	36.6
8.1	1.3	31.8	30.4
8.2	18.9	28.1	9.2
8.3	19.0	23.8	4.8
8.4	19.0	22.2	3.3
7.9	20.0	38.2	18.3
8.0	20.0	37.6	17.6
8.1	20.0	33.7	13.7
8.2	20.0	28.0	8.0
8.3	20.0	24.1	4.1
8.4	20.0	24.5	4.5

3.0 GAIN VARIATION:

X-Y Plots attached for 1.5 W to 15 mW Output

3.1 Gain Response Near Saturation

X-Y Plots attached.

4.0 PHASE LINEARITY:

X-Y plots attached for inputs from -4.8 dBm to -24.8 dBm.

5.0 AM-PM CONVERSION:

Photographs of Network analyzer display attached.

1. Overall modulated phase response; 7.9-8.4 GHz, 10^{o}/div at 6 KHz modulation frequency.
2. Expanded scale photograph showing that a typical point in the band has an AM-PM conversion of 2^{o}/dB.
3. Overall phase response modulated at 5 Hz showing that the AM-PM increases to just 3^{o}/dB at this low frequency.

6.0 OUTPUT LOAD VSWR:

X-Y plots for 1.3:1 and 2:0:1 load VSWR's are attached. Terminated output plots were taken after the load VSWR plots to verify the unit was not damaged. The detector output voltage is plotted on a linear scale in order to emphasize small differences in output power.

7.0 INPUT/OUTPUT VSWR AND IMPEDANCE:

Photographs of network analyzer display are attached.

8.0 NOISE FIGURE:

Noise figure is calculated from the following small signal gain data:

f (GHz) {DATA}	P_{output} (P_{IN} = -24.9dBm) (dBm) {DATA}	Gain G (dB)	Gain g (Num. ratio)	Δf (MHz)	Curve Area $\frac{g_i+g_{i+1}}{2}x\Delta f$ (MHz)
7.80	-5.24	19.63	92		
				50	22,757
7.85	4.26	29.13	818		
				50	135,526
7.90	11.76	36.63	4603		
				50	297,428
7.95	13.76	38.63	7295		
				50	411,948
8.00	14.76	39.63	9183		
				50	459,166
8.05	14.76	39.63	9183		
				50	487,180
8.10	15.26	40.13	10,304		
				50	348,995
8.15	10.76	35.63	3656		
				50	127,785
8.20	6.76	31.63	1455		
				50	47,893
8.25	1.76	26.63	460		
				50	16,087
8.30	-2.24	22.63	183		
				50	6,206
8.35	-6.74	18.13	65		
				50	6,206
8.40	-2.24	22.63	183		
				50	4,945
8.45	-13.24	11.63	14		

The total area under the small signal gain curve, GBW, is the sum of the right hand column above.

$$GBW = \sum_{7.80}^{8.45} \text{curve area} = 2,372,123 \text{ MHz}$$

The thermal noise power is:

$$P_{no} = GBW \times 10^{-11.38}$$

$$= 9.889 \times 10^{-6} \text{ mW}$$

The measured noise output of the amplifier for zero RF input is:

$$P_o = .078 \text{ mW } \{data\}$$

The noise figure is then:

$$N.F. = 10 \log \left(\frac{P_o}{P_{no}} \right)$$

$$= 38.97 \text{ dB}$$

9.0 RESIDUAL AM MODULATION:

A photograph of the spectrum analyzer display of the carrier at 7.9 GHz showing residual AM modulation sidebands is attached.

10.0 HUM MODULATION:

The detected hum modulation voltage for 8.15 GHz is sketched below:

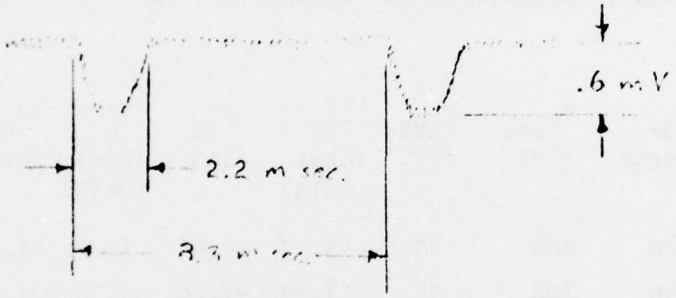

For integration purposes it is conservatively approximated by:

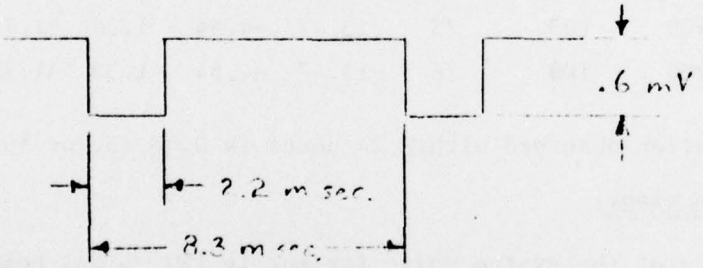

The rms hum modulation voltage, P_H, is calculated to be:

$$P_{H,rms} = \frac{\{ \int_0^{2.2} (.6mV)^2 \, dw \}^{1/2}}{\{ \int_0^{8.3} dw \}^{1/2}} = \frac{.6mV \sqrt{2.2}}{\sqrt{8.3}}$$

$$= .31 \text{ m Volt}$$

The detected carrier voltage, P_o, at this frequency is .37 Volt. The Hum Modulation level is calculated to be:

$$HM = 20 \log \{ \frac{P_o}{P_{H,rms}} \} = 20 \log \{ \frac{.37}{.31X10^{-3}} \}$$

$$= 61.5 \text{ dBc}$$

A summary of HM for three test frequencies follows:

f (GHz)	{DATA} P_H (mV)	$P_{H,rms}$ (mV)	{DATA} P_o (V)	HM (dBc)
7.9	2.2	1.14	0.46	52.1
8.15	0.6	0.31	0.37	61.5
8.4	1.4	0.72	0.15	46.3

11.0 GAIN STABILITY:

Gain stability data is summarized as follows, the carrier frequency is 8.0 GHz:

Date (1976)	Time (Hours)	T_{Case} (^oF)	T_{AMB} (^oF)	P'_{IN} (dBm) {DATA}	P''_{IN} (dBm)	P'_O (dBm) {DATA}	P_O (dBm)	Gain (dB)
22 Mar	0900	105	73	-13.57	-4.64	1.30	31.75	36.39
22 Mar	1700	108	76	-13.19	-4.26	1.30	31.75	36.01
23 Mar	0100	105	72	-13.67	-4.74	1.30	31.75	36.49
23 Mar	0900	107	75	-13.47	-4.54	1.30	31.75	36.29
23 Mar	1200	108	76	-13.47	-4.54	1.30	31.75	36.29

Total gain variation observed within 24 hours is 0.48 dB, or ±0.24 dB.

12.0 ADDITIONAL PHOTOGRAPHS:

Three photographs of the system noise (primarily TWT noise) being amplified by the small signal gain of the unit under test are attached. The three conditions shown are for an 8.15 GHz carrier, an 8.4 GHz carrier, and no carrier.

13.0 HIGH TEMPERATURE:

The amplifier was allowed to rise 20°C (36°F) in case temperature and its gain response recorded. X-Y plots taken during the test are attached. A linear (in detector voltage) scale was used to emphasize small differences in peak power output.

14.0 ATTACHMENTS:

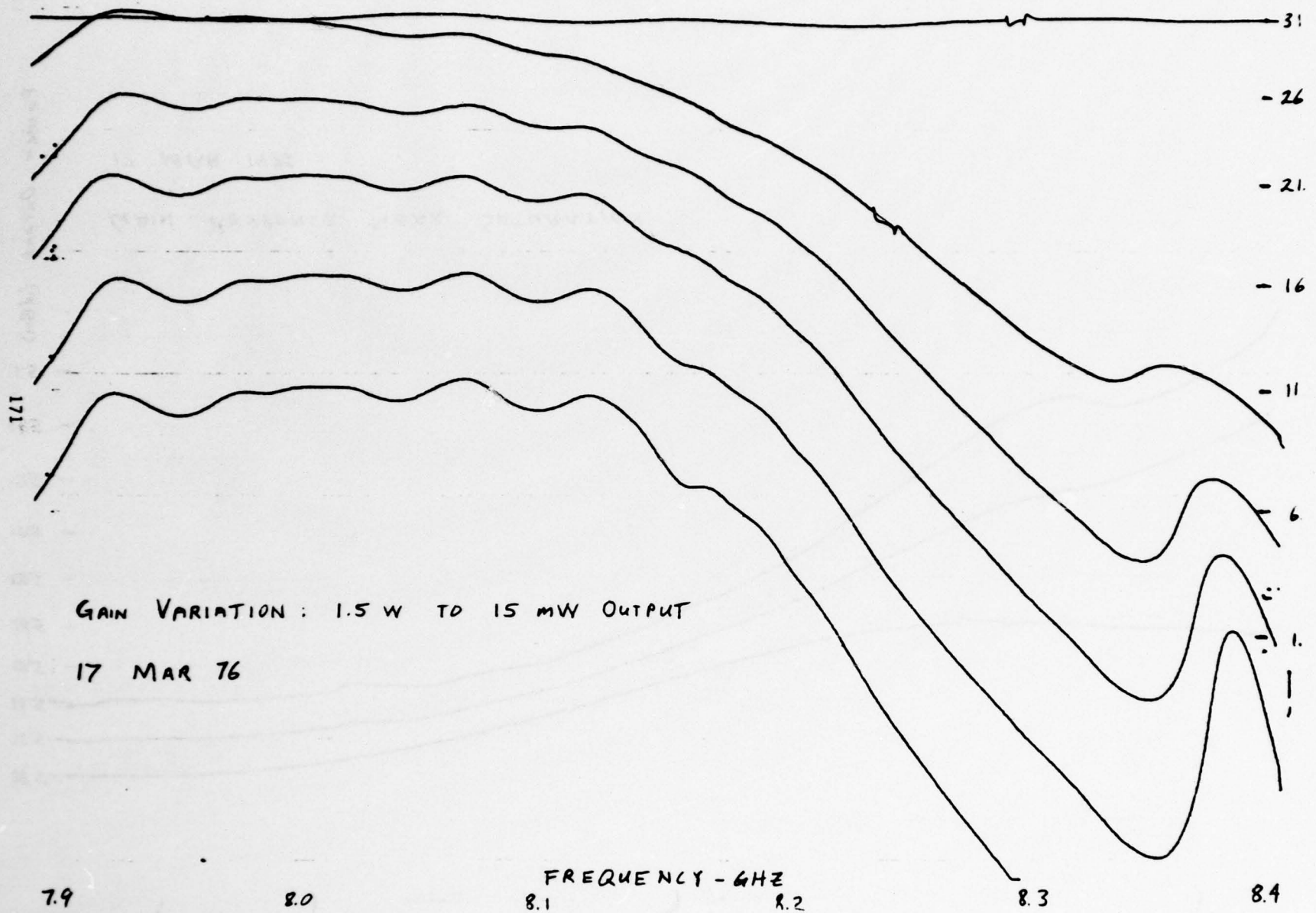

GAIN VARIATION : 1.5 W TO 15 mW OUTPUT

17 MAR 76

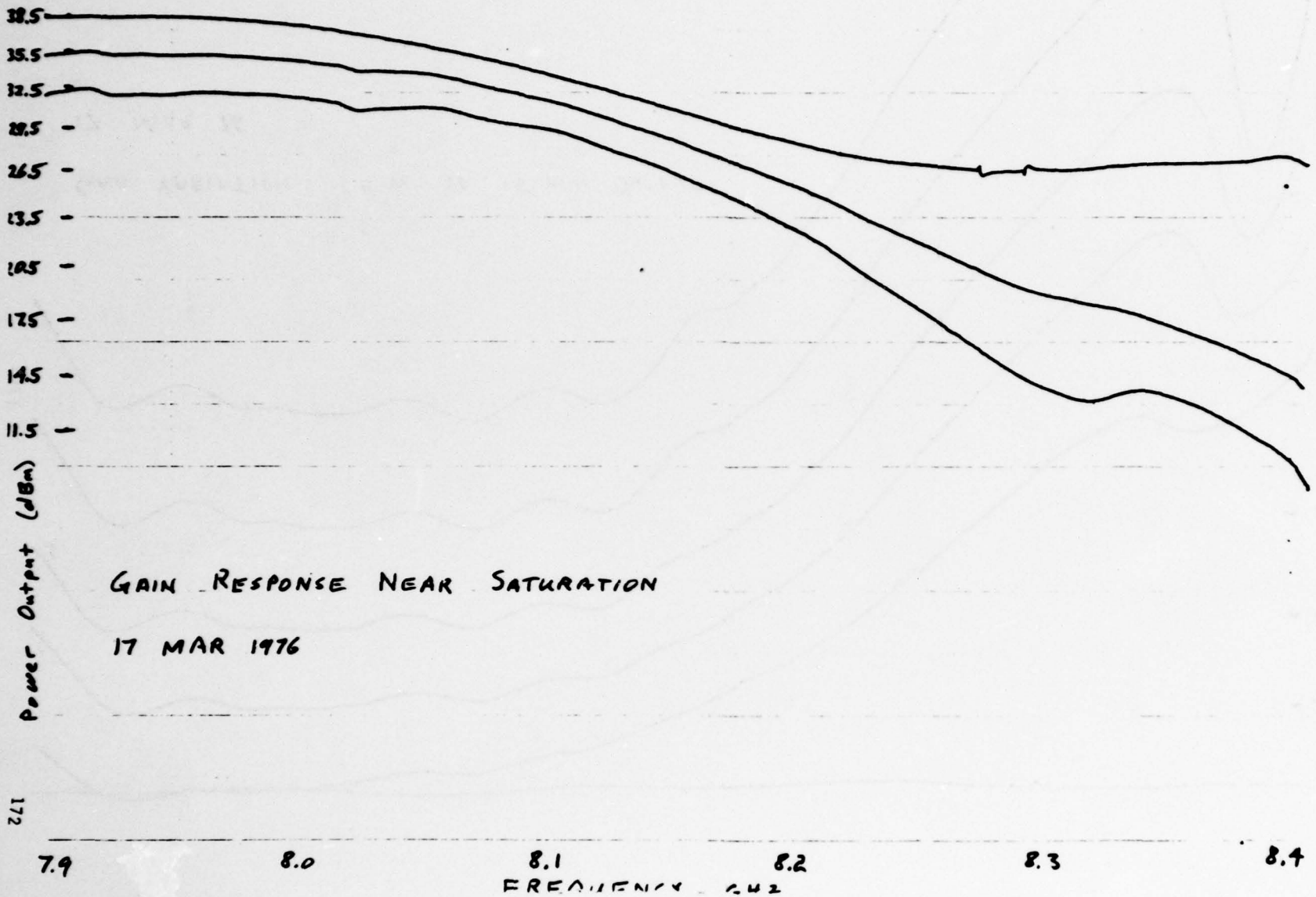

GAIN RESPONSE NEAR SATURATION

17 MAR 1976

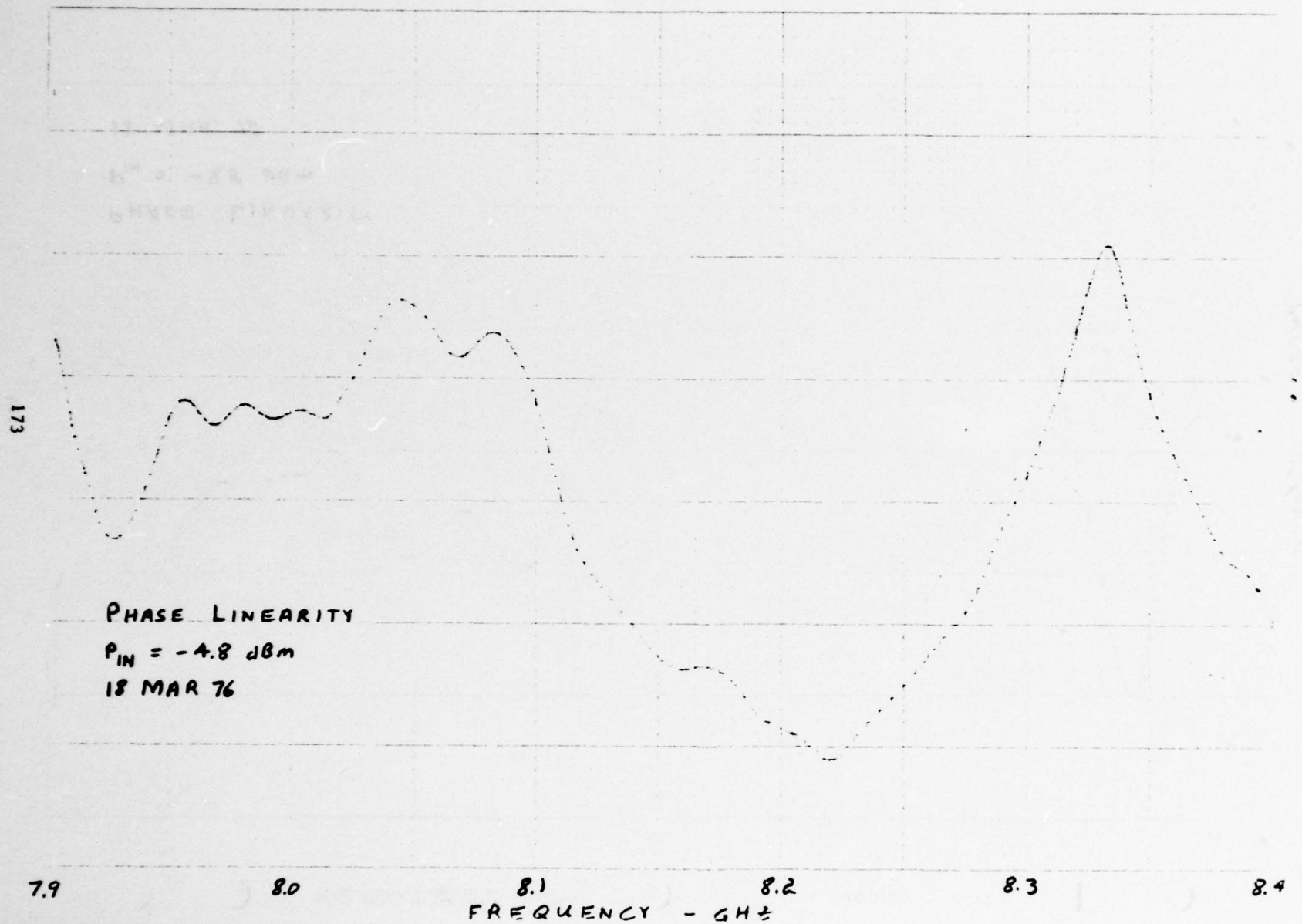
173
PHASE LINEARITY
P_{IN} = -4.8 dBm
18 MAR 76
7.9
8.0
8.1
8.2
8.3
8.4
FREQUENCY - GHz

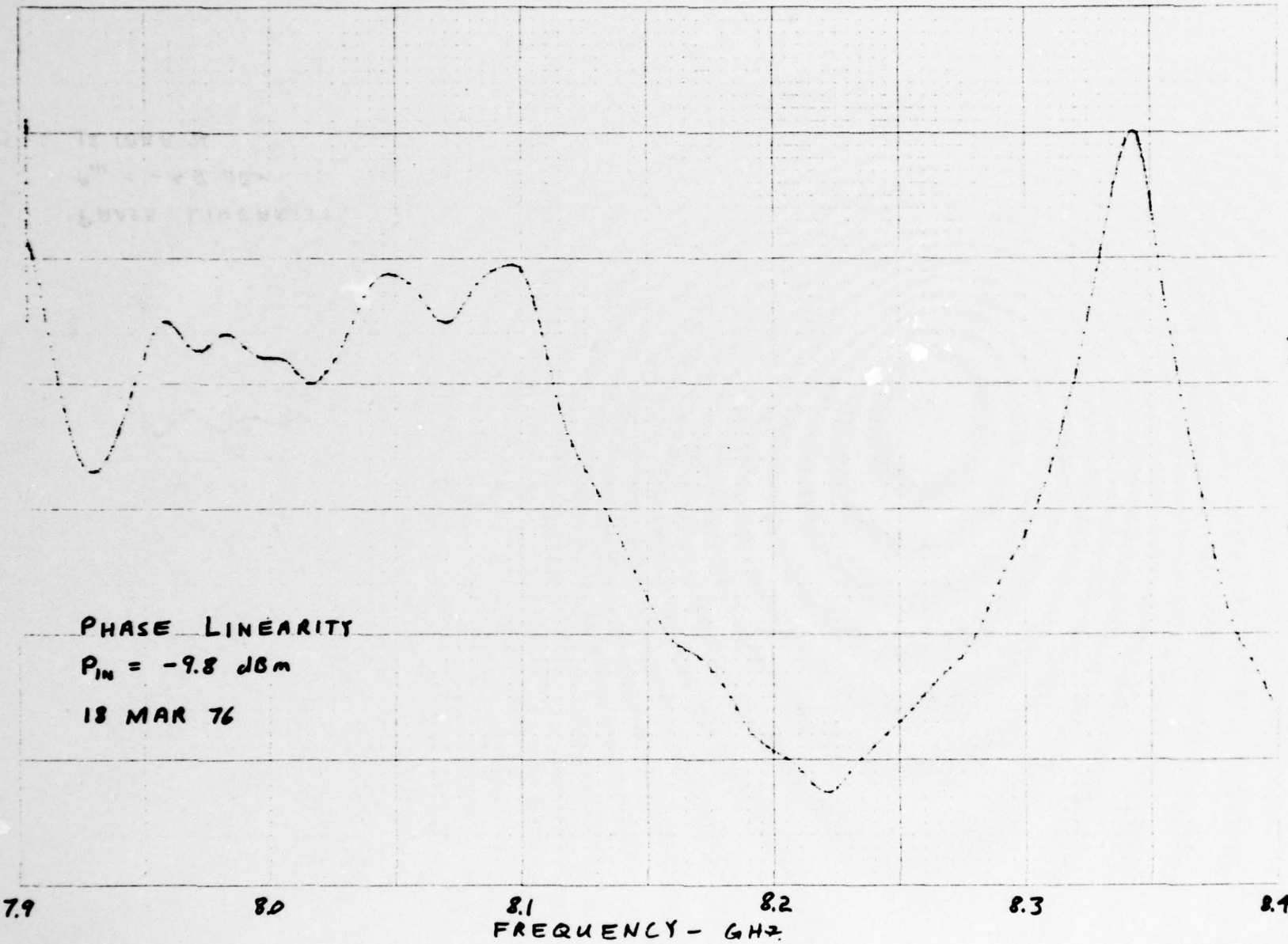

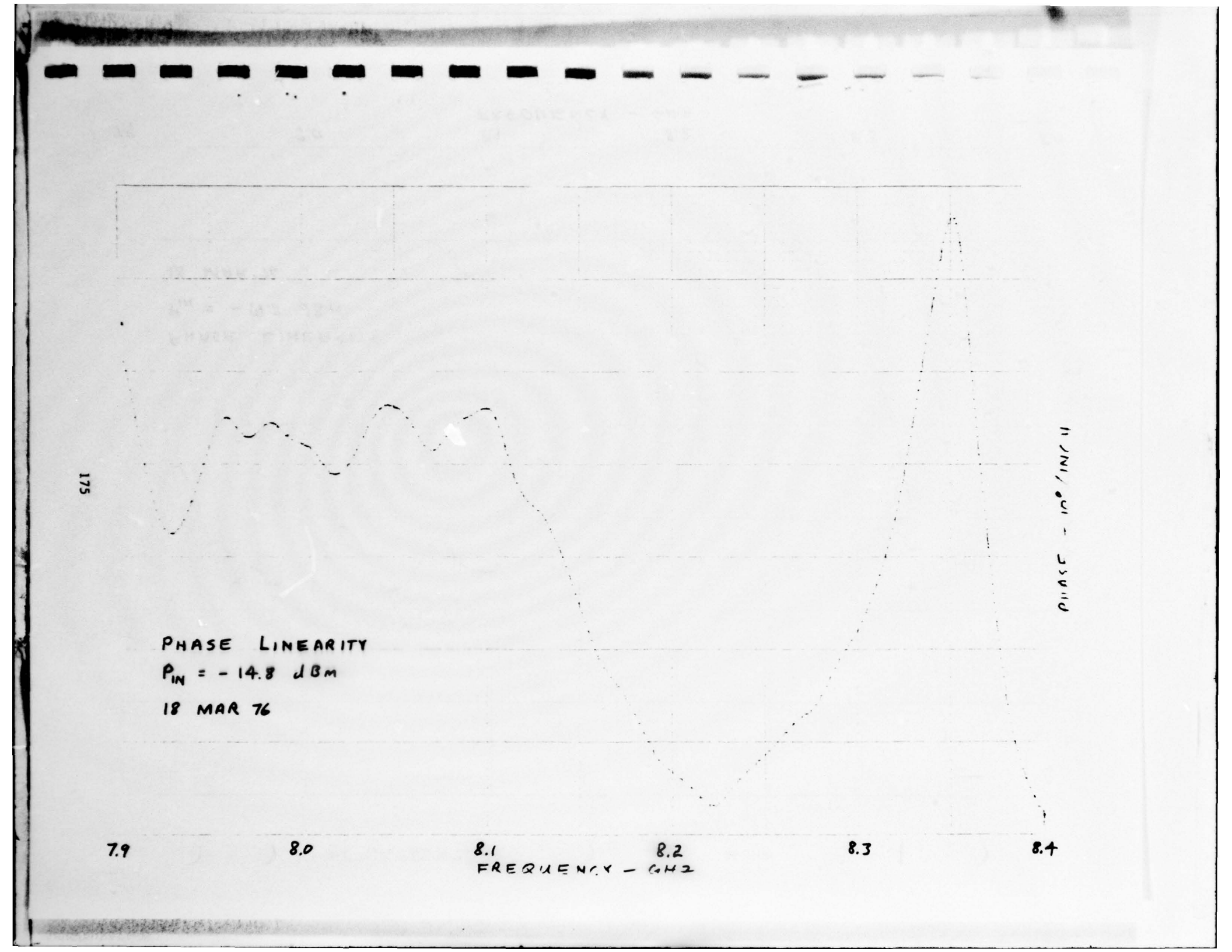
PHASE LINEARITY
P_{IN} = - 14.8 dBm
18 MAR 76
175
11 JAN / CM - 10° / DIV
7.9
8.0
8.1
8.2
8.3
8.4
FREQUENCY - GHz

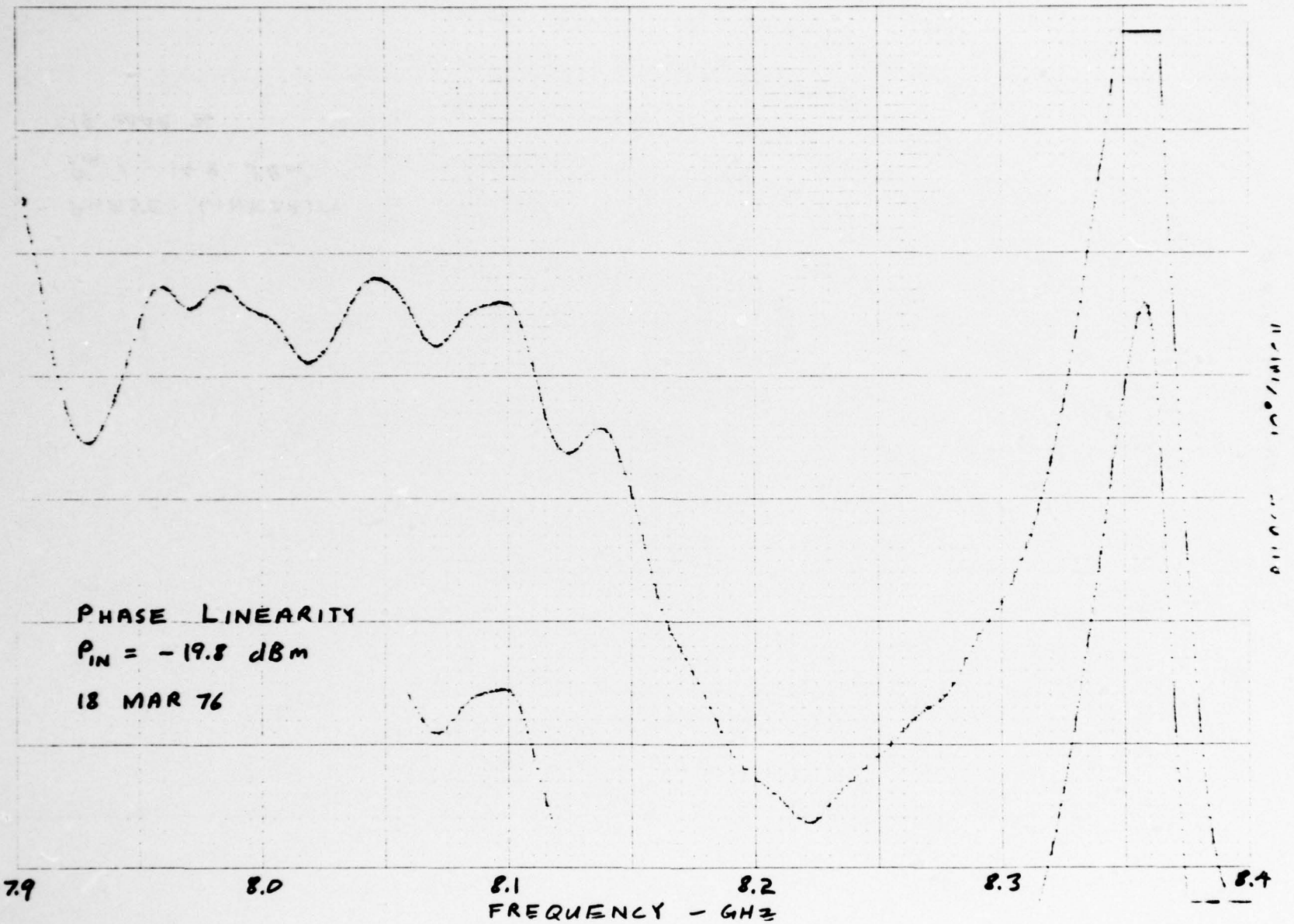

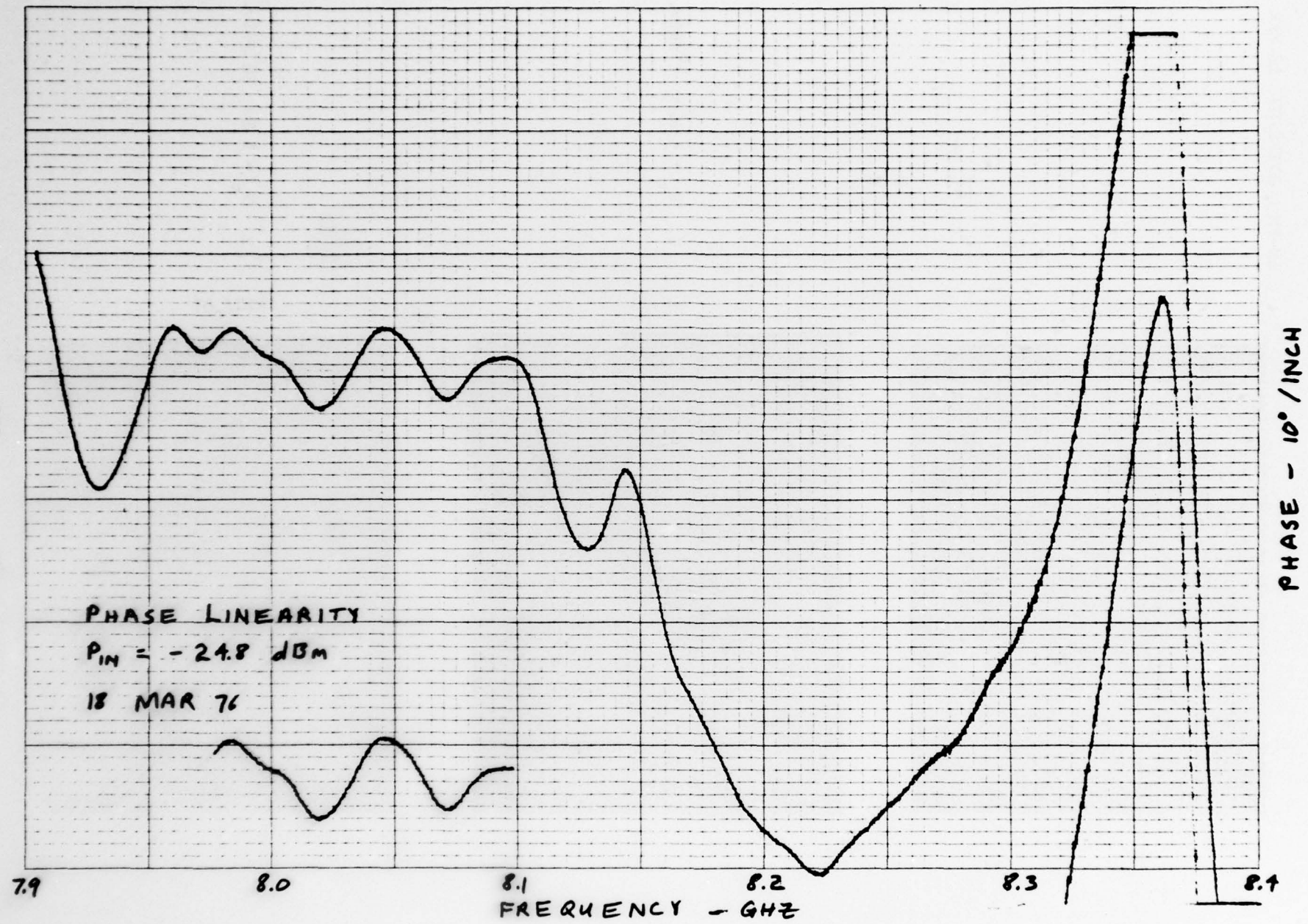

AM-PM CONVERSION 18 MAR 76

7.9 8.4

10^{o}/Div.

1. F_m = 6 kHz 10^{o}/Div.

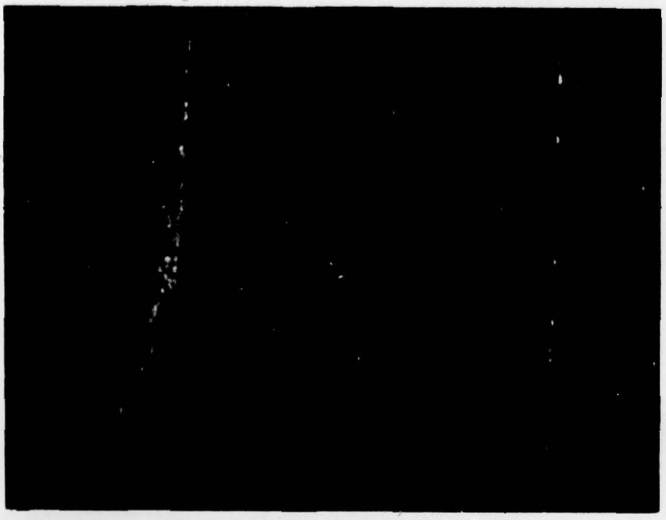

7.9 8.4

1^{o}/Div.

2. F_m = 6 kHz 1^{o}/Div.

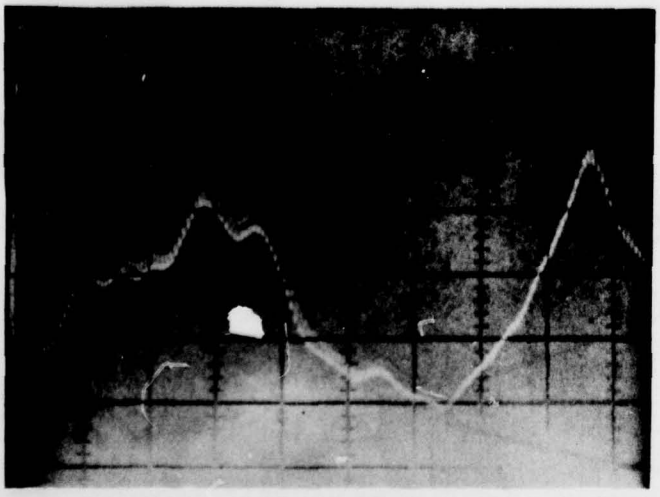

7.9 8.4

FREQUENCY - GHz

10^{o}/Div.

3. F_m = 5 Hz 10^{o}/Div.

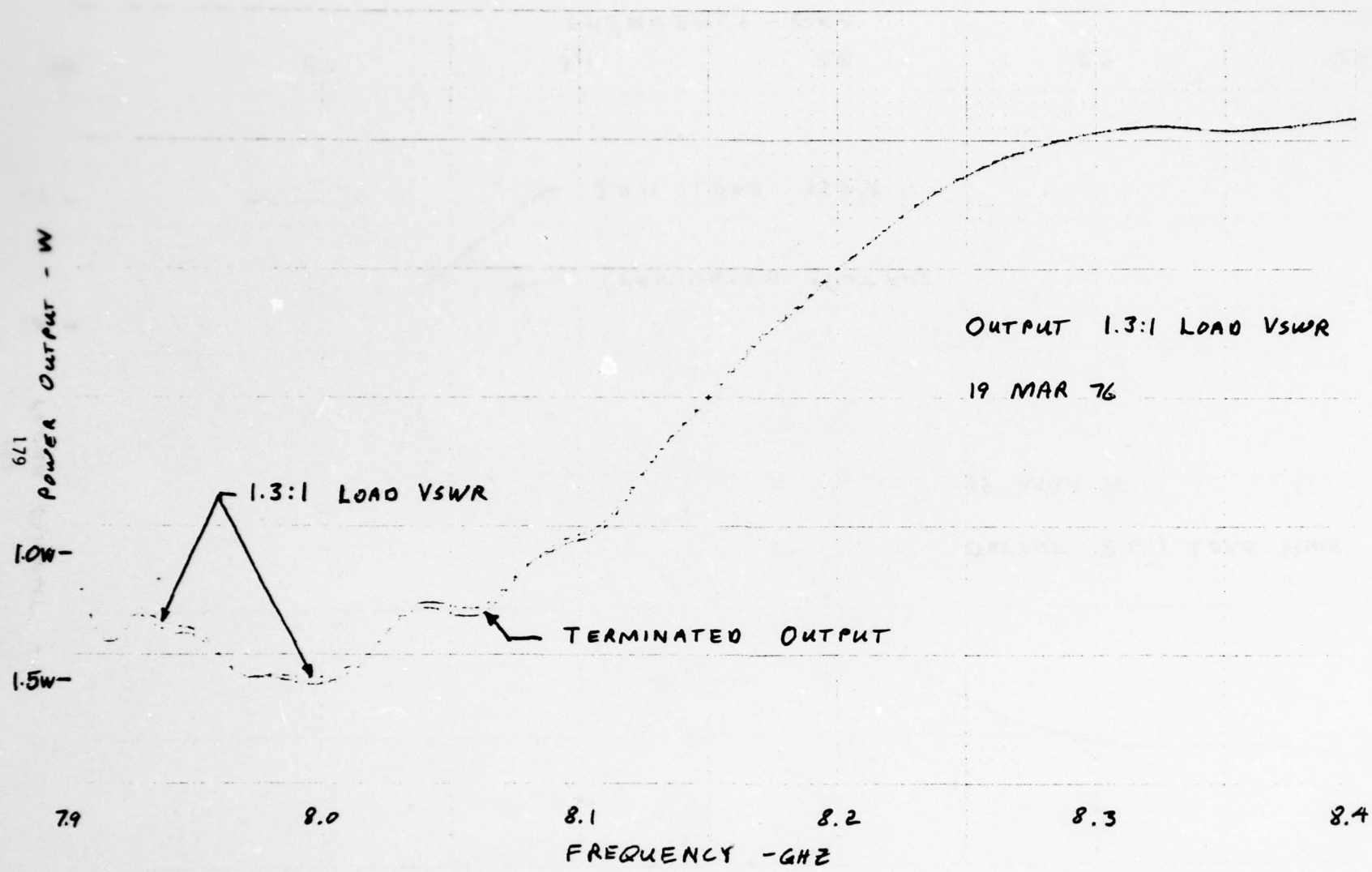
OUTPUT 1.3:1 LOAD VSWR
19 MAR 76
1.3:1 LOAD VSWR
TERMINATED OUTPUT
POWER OUTPUT - W
1.0W-
1.5W-
7.9
8.0
8.1
8.2
8.3
8.4
FREQUENCY -GHZ

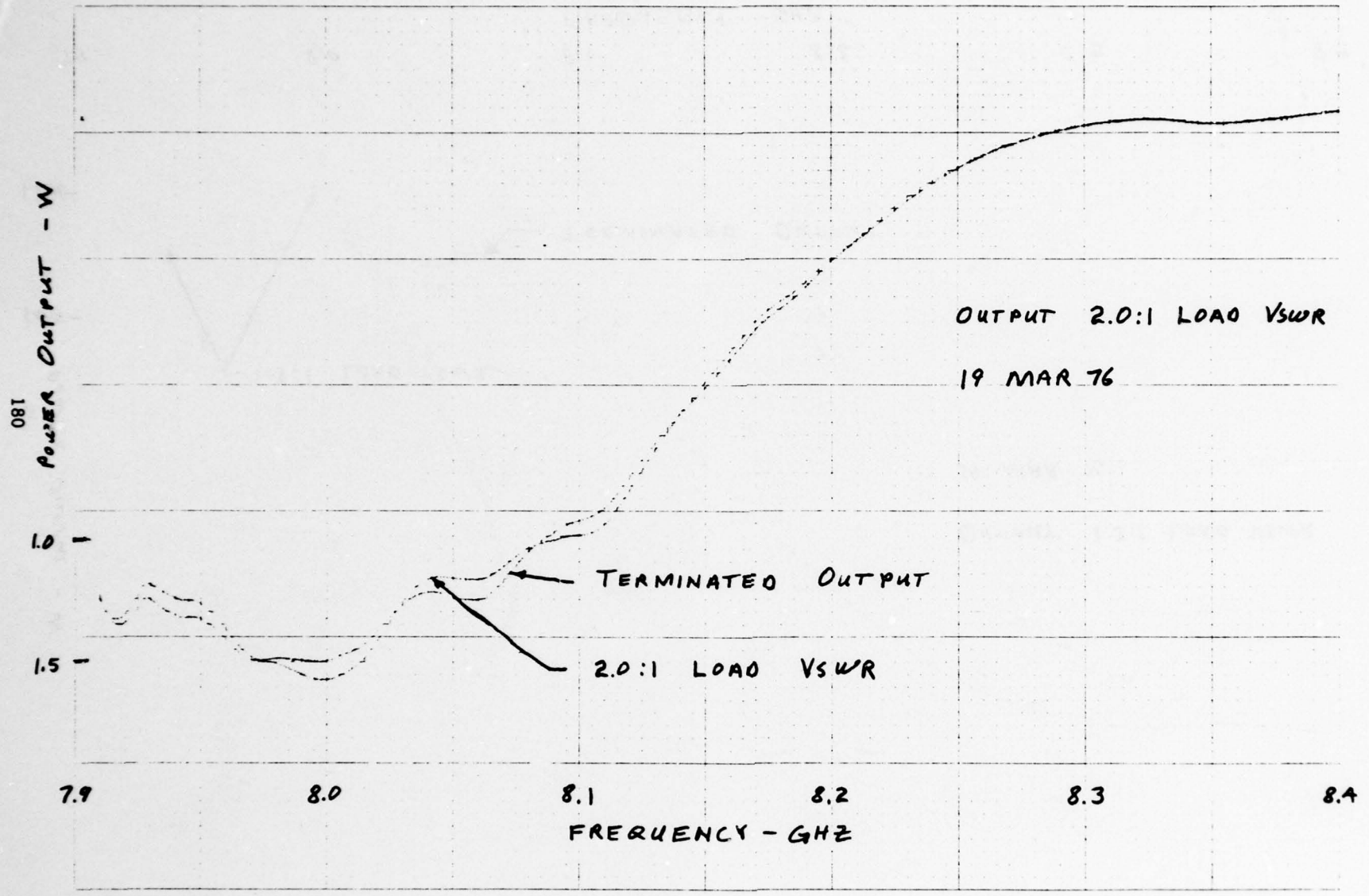

INPUT/OUTPUT VSWR

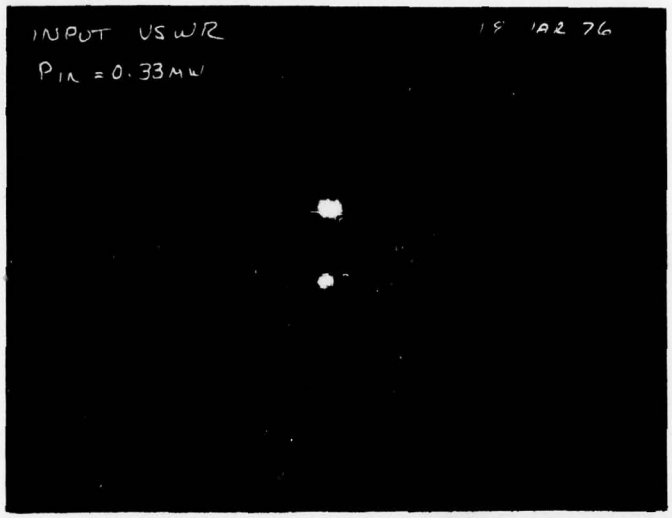

1. Input VSWR, operating expanded scale: Outer Circle = 1.5:1 VSWR

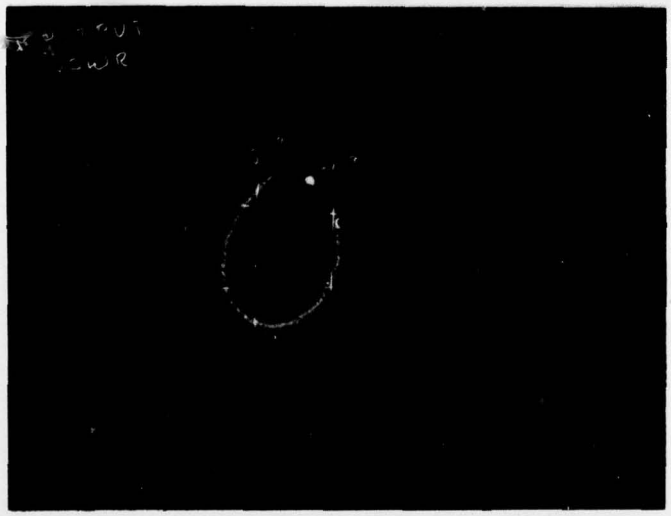

2. Output VSWR, operating expanded scale: Outer Circle = 1.5:1 VSWR

RESIDUAL AM MODULATION

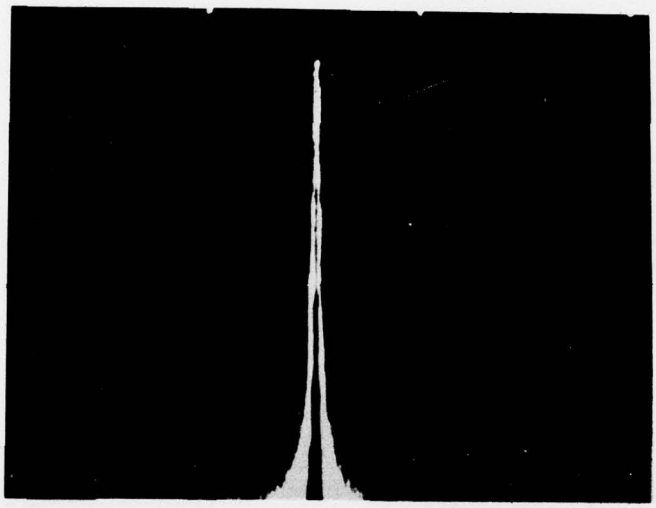

10 dB/Div.

F = 7.9 GHz

P_o = 1.5 W

0.5 MHz/Div.

SYSTEM NOISE AS AMPLIFIED
AMPLIFIED BY U.U.T.
(300 kHz MEAS. B.W.)

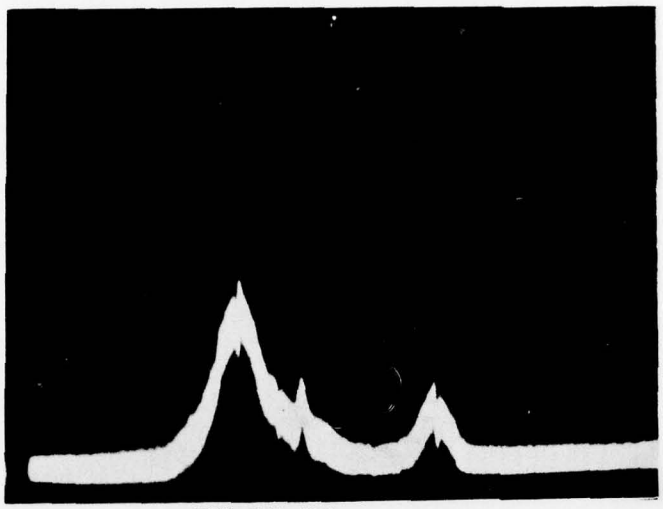

10 dB/Div.

200 MHz/Div.

1. Carrier at 8.15 GHz

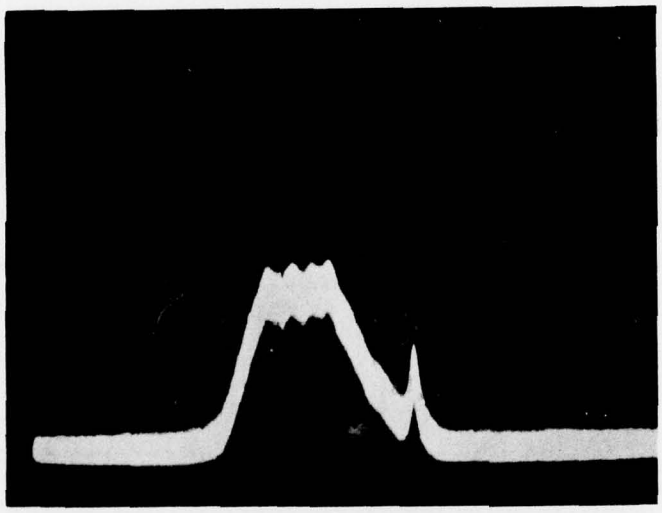

10 dB/Div.

200 MHz/Div.

2. No Carrier

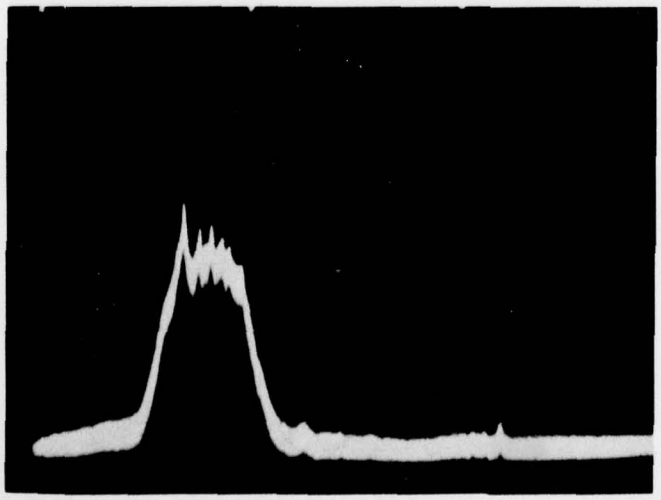

10 dB/Div.

500 MHz/Div.

3. Carrier at 8.4 GHz

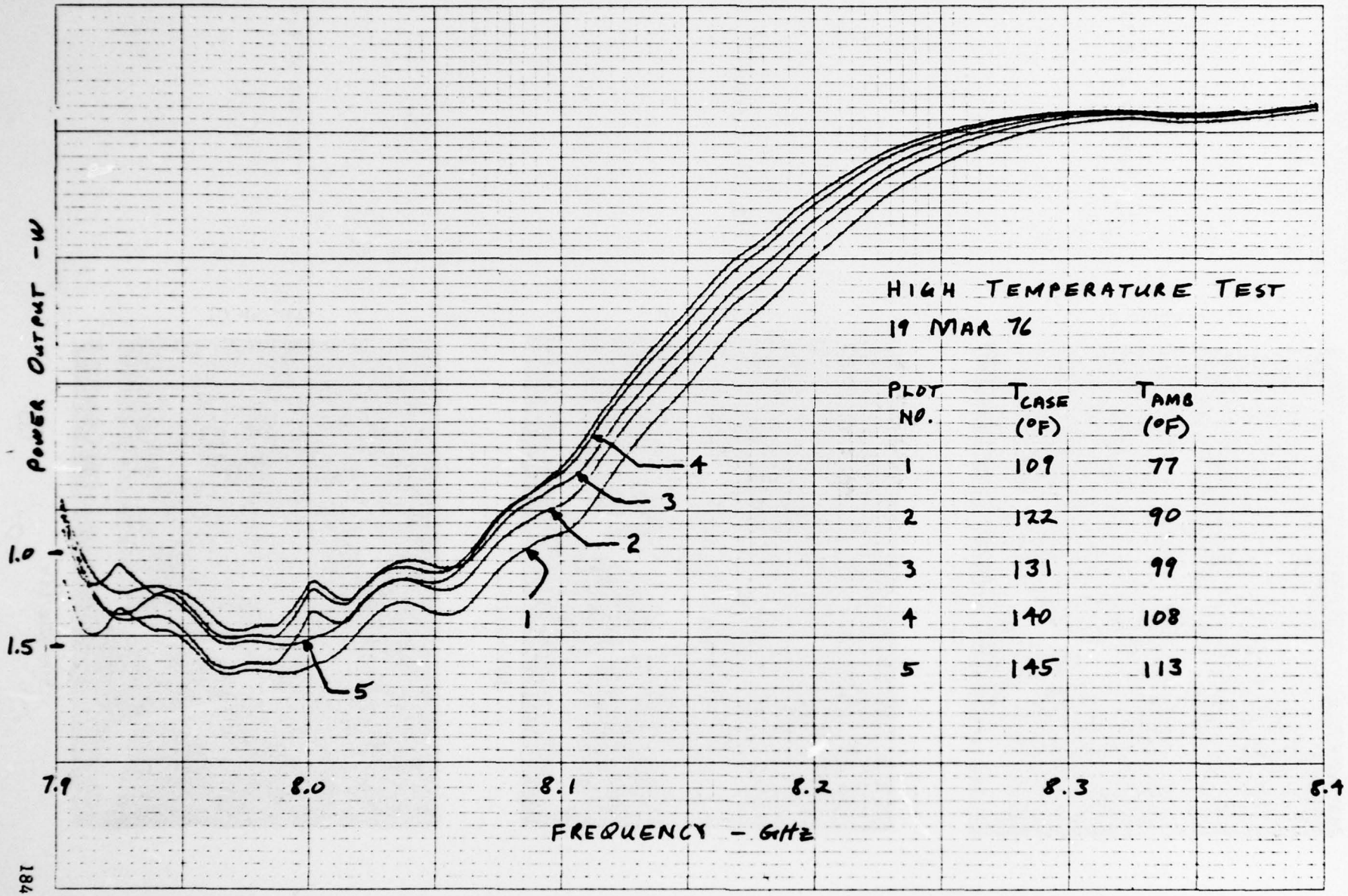
POWER OUTPUT - W
1.0
1.5
7.9
8.0
8.1
8.2
8.3
8.4
FREQUENCY - GHz
HIGH TEMPERATURE TEST
19 MAR 76
PLOT NO. | T CASE (°F) | T AMB (°F)
1 | 109 | 77
2 | 122 | 90
3 | 131 | 99
4 | 140 | 108
5 | 145 | 113
1
2
3
4
5
184